ADAPTIVE K-BEST SPHERE DECODER FOR DVB SYSTEMS AND COOPERATIVE NETWORKS

A THESIS

SUBMITTED TO THE GRADUATE SCHOOL OF
ELECTRONICS, COMMUNICATIONS AND COMPUTER ENGINEERING,
EGYPT-JAPAN UNIVERSITY OF SCIENCE AND TECHNOLOGY
(E-JUST)
IN PARTIAL FULFILLMENT OF THE REQUIREMENTS FOR THE DEGREE

OF

DOCTOR OF PHILOSOPHY DEGREE

IN

ELECTRONICS AND COMMUNICATIONS ENGINEERING (ECE)

BY

AHMED ABDELAZIZ BADAWI EL-BANNA

SEPTEMBER 2014

This page intentionally left blank.

ADAPTIVE K-BEST SPHERE DECODER FOR DVB SYSTEMS AND COOPERATIVE NETWORKS

Submitted by
Ahmed AbdelAziz Badawi El-Banna

For The Degree of

Doctor of Philosophy Degree

In
Electronics and Communications Engineering (ECE)

Supervisor Committee

Name, Title	Affiliation	Signature, Date
Adel Abdelrhman, Assoc. Prof.	E-JUST University - Egypt	……...
Maha Elsabrouty, Assoc. Prof.	E-JUST University - Egypt	……...
Mohammed Farag, Dr.	Alexandria University - Egypt	……...
Seiichi Sampei, Prof.	Osaka University - Japan	……...

Examination Committee

Name, Title	Affiliation	Approved, Date
Hosam Shalaby, Prof.	E-JUST University - Egypt	……...
Osamu Muta, Assoc. Prof.	Kyushu University - Japan	……...
Adel Abdelrhman, Assoc. Prof.	E-JUST University - Egypt	……...
Maha Elsabrouty, Assoc. Prof.	E-JUST University - Egypt	……...

Vice President for Education and Academic Affairs

Prof.: Ahmed Abo Ismail

ABSTRACT

MIMO communication is an appealing wireless communications technology. Using multiple antennas helped evolving several wireless communication systems i.e. the 4th generation cellular systems and digital terrestrial broadcast technology. Currently, virtual MIMO is a hot topic in cellular and cooperative networks.

In this thesis, we target the problem of frequency selectivity / time selectivity in space frequency / space time codes respectively. Generally, simple decoding of the space time / frequency codes relies on the assumption that the channel is constant over the consecutive symbols forming the diversity. However, in the case where this condition doesn't hold, i.e. varying channels, a more sophisticated decoding e.g. maximum likelihood or sphere decoding should be applied.

K-Best Sphere Decoder (KBSD) is a low complexity fixed throughput MIMO decoder. However, its performance is highly dependent on its K value which determines how many nodes will be visited while traversing the tree-based search. We propose employing several modifications to sphere decoder, to adapt the number of paths in the KBSD search. The developed algorithms adaptively estimate a suitable number of K-paths through an Adaptive Control Unit (ACU), depending on relevant criteria to the channel quality, namely, channel matrix analysis, channel quality estimation, and Signal-to-Noise power Ratio (SNR) estimation.

The good compromise between complexity and performance offered through adaptation makes the proposed KBSD more suitable for hardware implementations. This type of adaptation is performed over the horizontal level in the tree to achieve the best trade-off between performance and complexity. In cooperative networks, partial detection of selected group of symbols is possible leading to another dimension of adaptation over the vertical levels of the tree. The collective vertical and horizontal level adaptation can be utilized to reduce the overhead introduced in the MIMO relay. Therefore, we proposed a new 2-D AKBSD that makes use of the two vertical (number of traversed levels) and horizontal (number of visited nodes per level) dimensions of the adaptation process in the relay node to suit the dynamic conditions of the network. We also proposed a new hybrid partial and full detection protocol for multi-hop networks. Finally, as a step of the decoder implementation, we presented a hardware implementation and an Application Specific Instruction-Set Processor (ASIP) model for the ACU unit.

This page intentionally left blank.

ACKNOWLEDGMENT

First of all, great thanks to Allah the almighty for his grace to finish this work.

I would like to express my gratitude to my supervision committee, especially Dr. Maha Elsabrouty, for their kind guidance and continuous support.

I deeply thank my parents and all my family members for helping, guiding and encouraging me during all my life phases. I would like to also thank my colleagues and friends for being in my life and truthfully sharing me the good and bad moments.

I would like to express special thanks to Dr. Ehab Mahmoud for his valuable comments and his beautiful accompany during my study period in Japan.

I also appreciate Prof. Sampei and his lab members' efforts for their assistance and the kind hosting during my study period with them in Osaka University.

My sincere thanks to the Egyptian ministry of high education, the cultural affairs and missions sector for granting me a scholarship to complete my PhD through a fellowship program with E-JUST University.

Finally, I hope to successfully transfer the experience that I gained to my students in my future.

Ahmad El-Banna

Cairo, 2014

This page intentionally left blank.

TABLE OF CONTENTS

LIST OF TABLES

This page intentionally left blank.

LIST OF FIGURES

ABBREVIATIONS

ACU	Adaptive Control Unit
ADL	Architecture Description Language
AF	Amplify and Forward
AKBSD	Adaptive K-Best Sphere Decoder
ASIP	Application Specific Instruction Set Processor
AWGN	Additive White Gaussian Noise
BER	Bit Error Rate
BLAST	Bell laboratories layered space-time
BS	Base Station
BSP	Baseband Signaling Processing
CoMP	Coordinated MultiPoint
CQE	Channel Quality Estimation
CS	Combining Schemes
DF	Decode and Forward
DVB	Digital Video Broadcasting
EBU	European Broadcasting Union
EGC	Equal Gain Combining
ETSI	European Telecommunications Standards Institute
FDF	Full Detect and Forward
FEC	Forward Error Correction
FRFD	Full Rate Full Diversity
GP	Global Precoding
HPFD	Hybrid Partial and Full Detection
ICI	Inter Cell Interference
JT	Joint Transmission
JTC	Joint Technical Committee
KBSD	K-Best Sphere Decoder
KGE	Kilo Gate Equivalence
LDPC	Low Density Parity Check
LLR	Log-Likelihood Ratios

LP	Local Precoding
LST	Layered Space-Time
LTE	Long-Term Evolution
LUT	Look Up Tables
MIMO	Multiple Input Multiple Output
MISO	Multi Input Single Output
ML	Maximum Likelihood
MLSE	Maximum Likelihood Sequence Estimator
MMSE	Minimum Mean Square Error
MRC	Maximum Ratio Combining
MRT	Maximum Ratio Transmission
MS	Mobile Station
PD	Partial Detection
PLP	Physical Layer Pipes
QAM	Quadrature Amplitude Modulation
QoS	Quality of Service
RAC	Relay Assisted Communication
RR	Register and Register
RRE	Remote Radio Equipment
RTL	Register To Logic
SC	Selection combining
SD	Sphere Decoding
SFBC	Space Frequency Block Codes
SINR	Signal-to-Interference-plus-Noise Ratio
SNR	Signal-to-Noise Ratio
SP	Scattered Pilot
STBC	Space-Time Block Codes
STC	Space-Time Coding
STTC	Space-Time Trellis Codes
VHDL	VHSIC Hardware Description Language
VN	Visited Nodes
ZF	Zero-Forcing

CHAPTER: 1

INTRODUCTION

Wireless communications technology is developing rapidly to utilize the maximum available channel capacity and to achieve the best Quality of Service (QoS) to follow the increased demand of high definition applications. Multiple antenna techniques, cooperative communications, cognitive radios, millimeter wave communication, heterogeneous wireless/cellular networks, radio access technologies, transmission technologies, femto cell technologies, management and security of wireless and 4G mobile networks and beyond are examples of recent trends in wireless communication research. This chapter is intended to provide an overview of some new technologies of several wireless communication applications that utilize Multiple Input Multiple Output (MIMO) communication then state the problem that we work on and finally show the thesis objectives and organization.

1.1 Wireless Communications Technology Trends

Various trends evolved to assist in the development of high performance and bandwidth-efficient wireless transmission. A major technology in this direction is *multiple antenna techniques*, employing Multiple Input and/or Multiple Output antenna (MIMO). Generally, MIMO techniques can be divided into two main categories spatial diversity, and spatial multiplexing [1][2].

MIMO technology has found its way rapidly in several wireless communication standards. One wireless communication standard that employs MIMO is the *Digital Video Broadcasting (DVB)* technology. DVB system made a paradigm shift in the video transmission over the different media. DVB standards dominate the market satellite, cable,

terrestrial and IP-based television transmission services. The European Telecommunications Standards Institute (ETSI), the Centre for Electro-technical Standards (CENELEC) and the European Broadcasting Union (EBU) have formed a Joint Technical Committee (JTC) to handle the DVB family of standards to cover all these TV services serving mainly, Europe, Africa, central Asia and the middle-east [3].

Coordinated Multipoint (CoMP) transmission is another rising technology for current and future cellular systems that is built on virtual MIMO. It is a technique used to improve the coverage area by changing the Inter Cell Interference (ICI) problem occurring at the cell-edge into a useful cooperation between the different cells [4]-[6]. The CoMP idea is to establish cooperation between various Base Stations (BSs) for collective signal processing in both up and downlinks [7], where each transmitting node sends its data based on scheduling information sent to it by a centralized Baseband Signaling Processing (BSP) unit [4].

Another technology that is based on the idea of virtual MIMO is *relaying and cooperative communication.* Relaying can be described, in easy terms, as introducing helping nodes between the source and destination to act as extra antenna for the transmission, especially when the direct link between the source and destination node experience sever fading. As a result, cooperative relaying extends the coverage area, increases the diversity and code rates, and reduces the transmit power [8].

1.2 Problem Statement

Wireless communication systems can employ multiple antennas to achieve diversity and/or multiplexing gains. In real world, current application of MIMO system diversity is the dominant objective of several communication systems e.g. Long Term

Evolution (LTE) and DVB utilizing space coding algorithms. Decoding space time/ space frequency codes relies on a basic assumption that the channel is constant over the block of transmitted symbols in time or frequency respectively. This assumption enables the application of linear complexity zero forcing decoding. However, with the increase in the applications bit rate and the increasing demand of mobility, the problem of frequency selectivity and time varying channels arises. In this case more complex decoding algorithms are required to obtain an acceptable performance.

Exhaustive search, or Maximum Likelihood (ML) decoding, is the optimum decoding method in selective channels case. However, it is plagued with exponential decoding complexity making it impractical for implementation. Another decoding method that gives a near performance to ML with low complexity is Sphere Decoding (SD). K-Best Sphere Decoder (KBSD) is a low complexity fixed throughput MIMO decoder. However, its performance is highly dependent on its K-parameter value, which determines how many nodes will be visited while traversing the tree-based search. Therefore, selecting the K value is a challenge. Increasing the value of K increases the decoder performance but also increases the complexity and vice versa. Using fixed value of the K that used in the KBSD is not always suitable for all the system operating conditions. Therefore, a further challenge is finding a suitable K that gives the best performance-complexity trade-off for every system condition. We propose an Adaptive K-Best Sphere Decoder (AKBSD) that changes the number of K-paths (number of visited nodes per level) to accommodate the varying environment conditions according to some criteria such as: Channel Quality Estimation (CQE) (e.g. channel selectivity measurement), channel matrix analysis (matrix norm and column norm calculations) and Signal-to-Noise power Ratio (SNR) estimation. We propose to add tiny pre-processes before the regular KBSD without changing the internal construction of the algorithm. We also propose a 2-D AKBSD that makes use of the two

vertical (number of traversed levels) and horizontal (number of visited nodes per level) dimensions of the adaptation process in the relay node to accommodate the dynamic conditions of cooperative networks.

1.3 Thesis Objectives and Organization

The main contributions of this thesis can be listed in the following:

- Propose multiple AKBSD methods and apply them in DVB and cellular systems.
- Propose a novel 2-D AKBSD and apply it in relay-assisted networks.
- Propose a Hybrid Partial and Full Detection (HPFD) protocol for multi-hop networks.
- Verify the AKBSD by implementing the Adaptive Control Unit (ACU) via Field Programmable Gate Array (FPGA) and Application Specific Instruction-Set Processors (ASIP) platforms.

The rest of the thesis is organized as follows: Chapter 2 gives an overview of the current MIMO techniques, then reviews the different MIMO decoding algorithms such as linear, ML and SD algorithms, and finally proposes the K-Best SD. Chapter 3, illustrates the various methods applied on the KBSD to change the K-value adaptively, then it shows how we can employ the AKBSD in the DVB systems including DVB-T2 and DVB-NGH. Chapter 4 illustrates the application of the AKBSD in cooperative and relay networks such as CoMP and proposes the 2-D AKBSD that makes partial detection in the relay nodes and finally it proposes the HPFD protocol to be utilized in multi-hop networks. Chapter 5 is dedicated to present the hardware implementation of the ACU unit via the FPGA and ASIP platforms. Finally, chapter 6 concludes this thesis and shows some future work that can be used to extend this work.

CHAPTER: 2

REVIEW ON MIMO DETECTION TECHNIQUES

MIMO Techniques are widely employed in modern wireless communication systems. Several setups and diverse antenna modes are developed to enable achieving diversity or multiplexing. However, the decoding task in the receiver side is highly dependent on the assumptions regarding the coding technique and the channel knowledge. In this chapter, we give an overview of the different MIMO techniques. An introduction to the most widely used MIMO decoding algorithms such as linear, ML and Sphere Decoding (SD) algorithms is presented. Finally, we move to the main focus of the thesis work namely, the K-Best SD algorithm.

2.1 Introduction to MIMO Techniques

Multiple antennas can be exploited at the transmitter and/or the receiver. Consequently, a number of different MIMO configurations can be used. Depending on the number of antennas at the transmitter/receiver, multiple antennas can be categorized as Single Input Single Output (SISO), Single Input Multiple Output (SIMO), Multiple Input Single Output (MISO) and MIMO. These different MIMO topologies offer different advantages and disadvantages that balance between hardware feasibility and coding design to provide the optimum solution for any given application [9].

Generally, multiple antennas, i.e. MIMO, systems introduce three type of antenna gains: diversity, multiplexing and beam-forming gains. These gains can be achieved through investigating variety of multiple antennas schemes. The three kinds of diversity

schemes: Combining Schemes (CS), Space-Time Coding (STC), and Maximum Ratio Transmission (MRT), are mainly used to overcome channel fading and to improve the signal quality with or without channel knowledge at the transmitter or receiver. The spatial multiplexing is used to increase the data rate by transmitting multiple data streams together without increasing neither the bandwidth nor the transmission power. While Antenna beam-forming techniques are used to increase Signal-to-Interference-plus-Noise Ratio (SINR) by collecting the signals with different phase and amplitude coherently at the transmitter or the receiver. Another advantage of using beam-forming is to ease multiuser accesses in spatial domain and to control multiuser interference in an effective way [10]. Figure 2.1 shows a schematic of the different multiple antenna techniques.

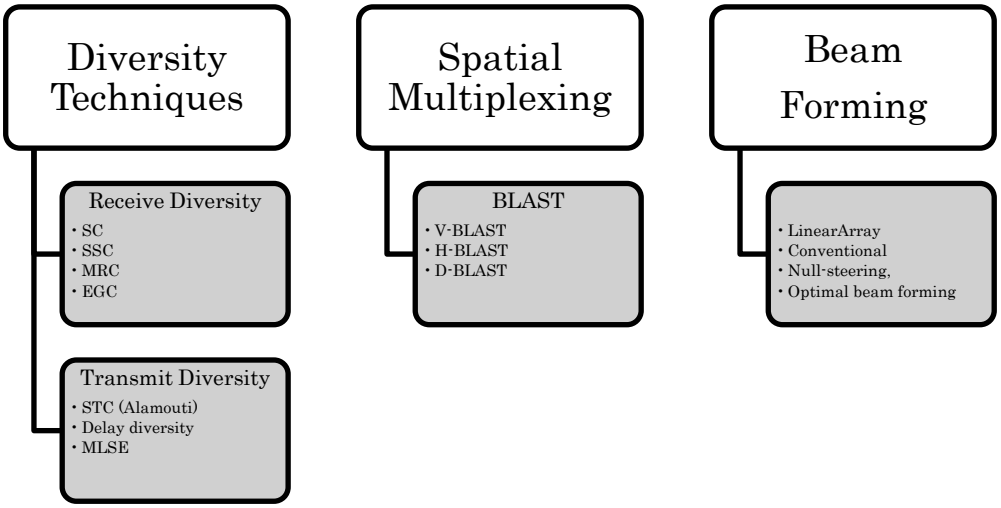

Figure 2.1: Multiple Antenna Techniques.

The performance of the receive diversity does not only depend on the number of antennas but also on the combining methods used at the receiver side. There are four types of combining techniques that differ in the implementation complexity in the receiver which are:

- *Selection combining (SC)*: In this setup, the antenna branch with the largest instantaneous SNR is selected to receive signals at every symbol period. Since it is

difficult to measure the SNR, the SC scheme can be implemented by accumulating and averaging the received signal power, consisting of both signal and noise power, for all antenna branches, and selecting the branch with the highest output signal power.

- *Switch (or Switch and Stay)combining (SSC)*: In this setup, the receiver scans all the antenna branches and selects a certain branches with the SNR values higher than a preset threshold to receive signals. When the SNR of the selected antenna drops below the given threshold due to fading, the receiver restarts scanning all branches again and switches to other antenna branches with better SNR.
- *Maximum Ratio Combining (MRC)*: In this setup, multiple received replicas at all antenna branches are individually weighted and summed up as an output signal. Since the multiple replicas experience different channel fading gains, the combining scheme can provide diversity gains.
- *Equal Gain Combining (EGC)*: In this setup, instead of requiring both the amplitude and phase knowledge of Channel State Information (CSI), EGC simply needs phase information for each individual channels, and set the amplitude of the weighting factor on each individual antenna branch to be unity.

On the other hand, transmit diversity techniques are developed to avoid the difficulty of utilizing receive diversity such as the limited antenna space available in a small size devices, the increased power consumption, and the implementation cost as a function of the required multiple components. First attempt was a delay diversity scheme, in which replicas of the same symbol are transmitted through multiple antennas at different time slots to create a virtual multipath [11]. A Maximum Likelihood Sequence Estimator (MLSE) or a MMSE equalizer may be employed to obtain spatial diversity gains. The STC is another

approach and is divided into Space-Time Trellis Codes (STTCs) [12] and Space Time Block Codes (STBCs) [13].

Space time coding schemes make use of both the channel code design and multiple transmit antennas configurations. The encoded data is divided into N_t simultaneous streams transmitted using N_t transmit antennas while the received data is a linear combination of these streams mixed by channel effects. Space time decoders at the receiver utilize both diversity advantages and coding gain [10],[14]. In the STTC scheme, symbols are transmitted simultaneously through different antennas and then decoded using a ML decoder to take the advantages of the coding and diversity gains. The complexity of this scheme grows exponentially with the decoded streams making it impractical for real applications. Alamouti's STC [15] is the first STBC to offer transmit diversity gains for a two transmit antennas communication system. It has been adopted in a number of wireless standards, e.g., 3GPP LTE [16] and IEEE 802.16e [17] standards because of its simplicity and remarkable performance. It should be noted that sending the symbols replicas over different subcarriers yields a Space Frequency Block Codes (SFBC) instead of STBC. Another common scheme is the MRT scheme which used to achieve transmit and receive diversity gains besides maximizing the post-output SNR.

In spatial multiplexing-based MIMO (SM-MIMO) systems, to achieve high data rate transmission, multiple data streams are simultaneously transmitted through multiple antennas. However, the detection at the receiver is a difficult task. The ML decoder achieves the best performance, but its complexity increases exponentially as the number of data stream and the number of transmit antennas increase. Layered Space-Time (LST) or Bell Laboratories Layered Space-Time (BLAST) architecture [18] is proposed to allow for processing multi-dimensional received signals in spatial domain. Multiple data streams are encoded and distributed over multiple antennas then the received signals are separated and

decoded by combining interference suppression or cancellation techniques with decoding algorithms. This gives a much lower computation complexity than the ML decoding. Various BLAST architectures, depending on whether error control coding is adopted or not, have been investigated, e.g. Horizontal BLAST (H-BLAST) [19], Diagonal BLAST (D-BLAST) [20], and Vertical BLAST (V-BLAST) [21].

Finally, Beam-forming is used to control the directions for transmitting or receiving signals in spatial-angular domain. By adjusting the beam-forming weights, the setting can direct the transmission or the reception of desired signals at a particular spatial angle or remove unwanted interference signals from other spatial angles [10]. The main categories are linear [22], conventional [23], null-steering, and optimal beam forming [10].

2.2 MIMO Detection

Using antenna diversity techniques gives reliability to the system and increases the spectral efficiency but with a challenge in the signal detection. Signal detection techniques for MIMO systems include the simple ZF and MMSE linear signal detections and the exhaustive search, i.e. ML detection, and in between there are various techniques such as Ordered Successive Interference Cancellation (OSIC), SD and others [12].

2.2.1 Linear Signal Detection

In linear signal detection, interference signals from other transmit antennas are minimized or set to zero in order to enable the detection of the desired signal from the target transmit antenna. This is done by inverting the effect of the channel (H) i.e. multiplying the received symbols (Y) by some weighted matrix (W) that cancels the channel effects introduced to the transmitted symbols. ZF and MMSE are the two methods of the standard linear signal detection.

1) ZF Signal Detection

The ZF technique nullifies the interference by a weight matrix:

$$W_{ZF} = (H^H H)^{-1} H^H \tag{2.1}$$

where $(.)^H$ denotes the Hermitian transpose operation and the estimated symbols are found by:

$$\hat{\mathrm{X}} = \mathrm{W_{ZF}Y} = \mathrm{X} + (\mathrm{H^H H})^{-1}\mathrm{H^H N} \tag{2.2}$$

where N is the noise term added to the transmitted signal.

2) MMSE Signal Detection

The MMSE method maximizes the post-detection SINR, by using a weight matrix:

$$\mathrm{W_{MMSE}} = (\mathrm{H^H H} + \alpha^2 \mathrm{I})^{-1}\mathrm{H^H} \tag{2.3}$$

The MMSE receiver requires the knowledge of the statistical information of the noise α^2. The estimated symbols are found by:

$$\hat{\mathrm{X}} = \mathrm{W_{MMSE}Y} = \mathrm{X} + (\mathrm{H^H H} + \alpha^2 \mathrm{I})^{-1}\mathrm{H^H N} \tag{2.4}$$

2.2.2 ML Signal Detection

Maximum Likelihood detection calculates the Euclidean distance between the received signal vector and all possible transmitted signal vectors with the given channel H. By selecting the possible symbol corresponding to the minimum distance, the most probable sent signal is obtained. For a $\mathbb{C}$ set of signal constellation symbol points and N_t transmitting antennas, the estimate of the transmitted signal vector X using ML method is:

$$\hat{X} = \arg\min_{\mathrm{X} \in \mathbb{C}} \|\mathrm{Y} - \mathbf{H}\mathrm{X}\|^2 \tag{2.5}$$

where $\|Y - \boldsymbol{H}X\|^2$ corresponds the ML metric. The ML method achieves the optimal performance as the Maximum A Posteriori (MAP) detection when all the transmitted vectors are equally likely. However, due to the exhaustive search of all possible points, the

complexity of the ML method increases exponentially as the modulation order and/or the number of transmit antennas increases.

2.2.3 Sphere Detection

Sphere Detection/Decoding searches for the ML solution over a smaller constellation set around the received vector to reduce the computational complexity of the exhaustive search. This area takes the hyper sphere shape. However, the sphere radius defines the SD complexity order. If the chosen radius is large enough to contain more the constellation points then SD tends to the original ML solution achieving good performance at increased complexity penalty and vice versa.

Considering an $N \times M$ MIMO system, the received signal is given by $Y = \boldsymbol{H}X + N$ where $Y \in \mathbb{C}^M$ is the received M-dimensional complex vector, $X \in \mathbb{C}^N$ is the transmitted N-dimensional complex vector with elements having integer real and imaginary parts, $\boldsymbol{H} \in \mathbb{C}^{M \times N}$ is the MIMO channel matrix and $N \in \mathbb{C}^M$ is the Additive White Gaussian Noise (AWGN) vector. The ML decoding defined in (2.5) is an exhaustive search which is impractical in most of the systems. On the other hand, the SD considers only the vectors inside a sphere with radius R_{SD} with upper limit of [12]:

$$\arg\min_{\mathrm{X} \in \mathbb{C}} \|\mathrm{Y} - \mathbf{H}\mathrm{X}\|^2 \leq \mathrm{R_{SD}}^2 \tag{2.6}$$

SD converts the underlying complex system into an equivalent real one as:

$$\begin{bmatrix}\mathrm{Re}\{\mathrm{Y}\} \\ \mathrm{Im}\{\mathrm{Y}\}\end{bmatrix} = \begin{bmatrix}\mathrm{Re}\{\mathbf{H}\} & -\mathrm{Im}\{\mathbf{H}\} \\ \mathrm{Im}\{\mathbf{H}\} & \mathrm{Re}\{\mathbf{H}\}\end{bmatrix}\begin{bmatrix}\mathrm{Re}\{\mathrm{X}\} \\ \mathrm{Im}\{\mathrm{X}\}\end{bmatrix} + \begin{bmatrix}\mathrm{Re}\{\mathrm{N}\} \\ \mathrm{Im}\{\mathrm{N}\}\end{bmatrix} \tag{2.7}$$

where Re{.}, Im{.} represents the real and imaginary parts respectively. The equivalent system is written as $\bar{Y} = \bar{\boldsymbol{H}}\bar{X} + \bar{N}$.

Using QR decomposition, $\bar{\boldsymbol{H}} = \boldsymbol{QR}$, where **R** is an upper triangle matrix with positive diagonal elements, **Q** is an orthogonal matrix and $\tilde{Y} = \boldsymbol{Q}^H \bar{Y}$. The system can now be written as:

$$\arg\min_{\bar{\mathrm{X}} \in \mathbb{C}} \left\| \tilde{\mathrm{Y}} - \mathbf{R}\bar{\mathrm{X}} \right\|^2 \leq \mathrm{R_{SD}}^2 \tag{2.8}$$

and

$$\left\| \tilde{\mathrm{Y}} - \mathbf{R}\bar{\mathrm{X}} \right\|^2 = \sum_{\mathrm{i}=1}^{2\mathrm{N_t}} \mathrm{d}\left(\bar{\mathrm{X}}_{\mathrm{i}}^{2\mathrm{N_t}}\right) \leq \mathrm{R_{SD}}^2 \tag{2.9}$$

where $d(\bar{X}_i^{2Nt})$ is the squared Partial Euclidian Distance (PED) of $\bar{X}_i^{2N_t}$ (symbols ordered from i to $2N_t$) and is calculated recursively by [12]:

$$\mathrm{d}\left(\bar{\mathrm{X}}_{\mathrm{i}}^{2\mathrm{N_t}}\right) = \mathrm{d}\left(\bar{\mathrm{X}}_{\mathrm{i+1}}^{2\mathrm{N_t}}\right) + \left| \tilde{\mathrm{Y}}_{\mathrm{i}} - \sum_{\mathrm{k=i}}^{2\mathrm{N_t}} \mathrm{R_{ik}} \bar{\mathrm{X}}_{\mathrm{k}} \right|^2 \tag{2.10}$$

where R_{ik} is the $(i,k)^{\text{th}}$ element of **R** and $i = 2N_t, \ldots, 1$

For a 2×1 complex MISO system using square Quadrature Amplitude Modulation (QAM) and applying SFBC, the equivalent channel takes the form:

$$\mathbf{H} = \begin{bmatrix} H_{11} & -H_{21} \\ H_{22}^* & H_{12}^* \end{bmatrix}. \tag{2.11}$$

The complex system model is represented as:

$$\begin{bmatrix} Y_{1R} + jY_{1I} \\ Y_{2R}^* + jY_{2I}^* \end{bmatrix} = \begin{bmatrix} H_{11R} + jH_{11I} & -H_{21R} - jH_{21I} \\ H_{22R}^* + jH_{22I}^* & H_{12R}^* + jH_{12I}^* \end{bmatrix} \begin{bmatrix} X_{1R} + jX_{1I} \\ X_{2R}^* + jX_{2I}^* \end{bmatrix} + \begin{bmatrix} N_{1R} + jN_{1I} \\ N_{2R}^* + jN_{2I}^* \end{bmatrix} \tag{2.12}$$

The underlying complex system in (2.12) is converted into an equivalent real one presented in (2.7) as:

$$\begin{bmatrix} Y_{1R} \\ Y_{2R}^* \\ Y_{1I} \\ Y_{2I}^* \end{bmatrix} = \begin{bmatrix} H_{11R} & -H_{21R} & -H_{11I} & H_{21I} \\ H_{22R}^* & H_{12R}^* & -H_{22I}^* & -H_{12I}^* \\ H_{11I} & -H_{21I} & H_{11R} & -H_{21R} \\ H_{22I}^* & H_{12I}^* & H_{22R}^* & H_{12R}^* \end{bmatrix} \begin{bmatrix} X_{1R} \\ X_{2R}^* \\ X_{1I} \\ X_{2I}^* \end{bmatrix} + \begin{bmatrix} N_{1R} \\ N_{2R}^* \\ N_{1I} \\ N_{2I}^* \end{bmatrix} \tag{2.13}$$

with the equivalent system $\bar{Y} = \bar{\boldsymbol{H}}\bar{X} + \bar{N}$. The SD considers only the vectors inside a

sphere with radius R_{SD} with upper limit of (2.6). Simplifying (2.6) by performing QR decomposition of the complex channel ***H=QR***, we get [12]:

$$\left\| R(\bar{X} - \hat{\bar{X}}) \right\|^2 \leq {R_{\mathrm{SD}}}^2 \tag{2.14}$$

where $\hat{\bar{X}}$ represents the ZF solution and the constraint becomes:

$$\left\| R\left(\bar{X} - \hat{\bar{X}}\right) \right\|^2 = \left\| \begin{bmatrix} R_{11} & R_{12}R_{13} & R_{14} \\ 0 & R_{22}R_{23} & R_{24} \\ 0 & 0\,R_{33} & R_{34} \\ 0 & 0 \quad 0 & R_{44} \end{bmatrix} \begin{bmatrix} \bar{X}_1 - \hat{\bar{X}}_1 \\ \bar{X}_2 - \hat{\bar{X}}_2 \\ \bar{X}_3 - \hat{\bar{X}}_3 \\ \bar{X}_4 - \hat{\bar{X}}_4 \end{bmatrix} \right\|^2$$

$$= \left| R_{44}\left(\bar{X}_4 - \hat{\bar{X}}_4\right) \right|^2 + \left| R_{33}\left(\bar{X}_3 - \hat{\bar{X}}_3\right) + R_{34}\left(\bar{X}_4 - \hat{\bar{X}}_4\right) \right|^2$$

$$+ \left| R_{22}\left(\bar{X}_2 - \hat{\bar{X}}_2\right) + R_{23}\left(\bar{X}_3 - \hat{\bar{X}}_3\right) + R_{24}\left(\bar{X}_4 - \hat{\bar{X}}_4\right) \right|^2$$

$$+ \left| R_{11}\left(\bar{X}_1 - \hat{\bar{X}}_1\right) + R_{12}\left(\bar{X}_2 - \hat{\bar{X}}_2\right) + R_{13}\left(\bar{X}_3 - \hat{\bar{X}}_3\right) + R_{14}\left(\bar{X}_4 - \hat{\bar{X}}_4\right)) \right|^2 \leq {R_{\mathrm{SD}}}^2 \tag{2.15}$$

Solving the upper triangular matrix from bottom to top, we can find the candidate selections for $\hat{\bar{X}}_i$, $i = 4 - s + 1$ in four repetitive steps s =1,2,3 and 4.

SD search method is generally represented as a tree search. Two main commonly used search strategies are used. The first is Fincke–Pohst (FP) [24] is based on breadth first search in the forward direction only. On the other hand, Scnorr-Euchner (SE) [25] is a depth first algorithm permitting forward and backward search [26].

2.3 K-Best Sphere Decoder

The K-Best SD [26] is based on the FP method that processes the tree search in the forward direction only. The K-Best SD follows the steps in Fig. 2.2 in the decoding

process. The main advantage of the K-Best SD is its fixed throughput which enables parallel and pipelined implementation [25].

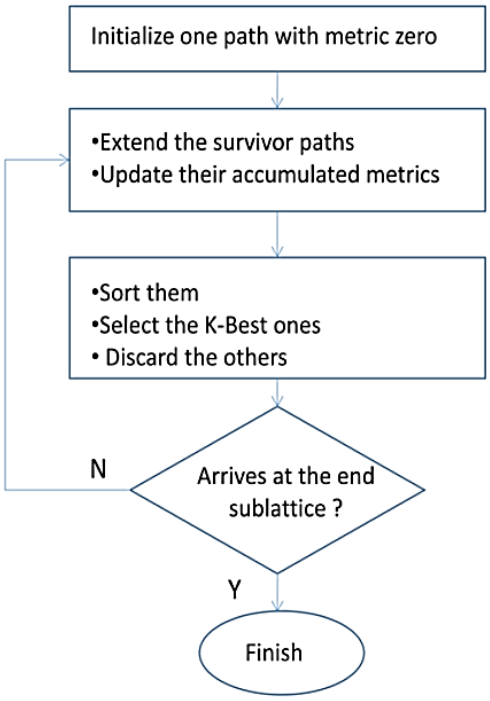

Figure 2.2: K-Best SD decoding steps.

The most effective step in the KBSD decoding process is selecting the K-Best paths while traversing the tree. Choosing the best K value is a challenge as increasing the K value means processing more tree branches and although this gives better performance, it consumes more computations and hence increases the complexity. On the other hand, selecting a small value of K gives lower computations and results in lower complexity decoding but in the price of degradation of the decoder performance. Moreover, selecting a fixed K value is not the optimum solution as there are many parameters that change in the communication system specially channel variations, and a fixed value is not the appropriate one for all the conditions. This leads to the importance of emerging various ways to adapt the K value depending on some criteria that affect the communication system. The most important criteria are the channel variations and received SNR levels.

Most of the K value adaptation in previous work e.g. [27]-[33] changes the number of K-Best paths during the entire tree search i.e. while calculating the PEDs of each visited node. Other adaptations were performed using some kinds of channel matrix analysis e.g. [34].

In this thesis, We address the case of varying channel conditions which renders the simple zero-forcing receiver for the Alamouti based transmission or the golden code transmission suboptimal. We propose employing a modified sphere decoder that relies on adapting the number of paths in the search of the KBSD. We offer to adaptively estimate a suitable number of K-paths depending on the channel state and to search only this number of branches to save more processing operations while traversing the tree. The achieved reduction in the complexity of the decoder makes it more suitable for hardware implementations. We propose an AKBSD that changes the number of K-paths according to the criteria of channel quality estimation, channel matrix analysis and SNR estimation.

2.4 Summary

This chapter is dedicated to present an overview of the different MIMO techniques through reviewing the three main categories diversity, spatial multiplexing and beam forming. Following this, the different MIMO decoding algorithms such as the linear ZF and MMSE, the ML and the SD algorithms are reviewed. We have focused on the Sphere decoding detailed operation, more specifically the K-Best sphere decoder. The effects of the K branch search are reviewed. This inherent effect of the choice of the K values provided us with the idea for adapting the number of different branches visited according to the channel conditions. In the next chapter, we illustrate the various methods applied on the KBSD then show how we can utilize the AKBSD in DVB systems.

This page intentionally left blank.

CHAPTER: 3

ADAPTIVE K-BEST SPHERE DECODER AND ITS APPLICATION IN DVB SYSTEMS

Changing the number of the K paths that the KBSD processes while detecting the transmitted symbols has a considerable effect on the decoder complexity. This change should be done adaptively depending on the current situation of the communication system i.e. modulation scheme, data rate, channel quality … etc. Most of the communication system parameters are fixed over long blocks of data transmission. However, major changes occur rapidly and randomly in the wireless channel. Therefore, estimating the channel quality is the criteria that should be taken into consideration while adapting the K paths while processing the tree search of the KBSD. In this chapter, we propose various methods to estimate the channel quality and apply them on the regular KBSD then we show how the AKBSD can be employed in DVB systems.

3.1 Adaptive K-Best Sphere Decoder

To provide a good trade-off between the performance and complexity, the proposed AKBSD methods determine the value of the feasible number of branches K by defining sub-optimum K value for different channel states.

3.1.1 Matrix Norm method (M1)

Assuming a known CSI at the receiver, we calculate the channel matrix norm as:

$$m_i = \|\mathbf{H}_i\|_2, i = 1,2, \dots Nc/2 \quad (3.1)$$

where $\mathbf{H_i}$ is the channel matrix corresponding to the i^{th} pair of the payload cells N_c. If the channel is ideal in the 2×1 SFBC case, i.e. $\mathbf{H}=\begin{bmatrix}1 & -1\\ 1 & 1\end{bmatrix}$ (see (2.11)), its norm equals $m_{ideal} = \left\|\begin{bmatrix}1 & -1\\ 1 & 1\end{bmatrix}\right\|_2 = 1.4142$, then we take this value as a reference and calculate the deviation of the calculated channel matrix norm m_i to indicate the state of the current channel, and if m_i lies between a threshold value (δ) around the ideal value (e.g. 0.4 below and above m_{ideal} i.e. m_{th1} = 1.0142 and m_{th2} = 1.8142), we assign a small value K_1 and if it lies outside the defined threshold region, a higher K_2 value is assigned and passed to the K-Best SD as illustrated in Fig. 3.1 (a). The threshold value was empirically defined based on a numerical analysis to select the optimum trade-off between the complexity and performance as shown in Fig. 3.2. Normalized values of average number of visited nodes during the tree search as a measure of complexity were plotted against SNR values for a system target BER of 6.3×10^{-5}.

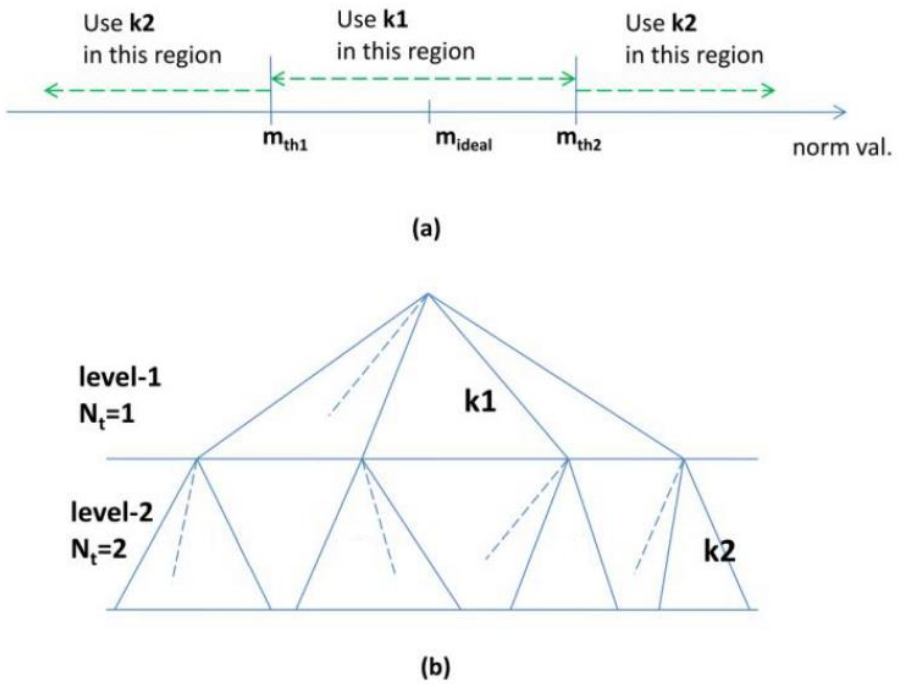

Figure 3.1: Assigning K-values for (a) Matrix Norm method and (b) Column Norm method.

We assume hard decoding in our system, i.e. no channel coding was implemented in this stage, as a measure of the system performance at different δ values, the superior value of δ is 0.4 which gives the best trade-off between the complexity and performance with a loss of performance of only 1×10^{-4}.

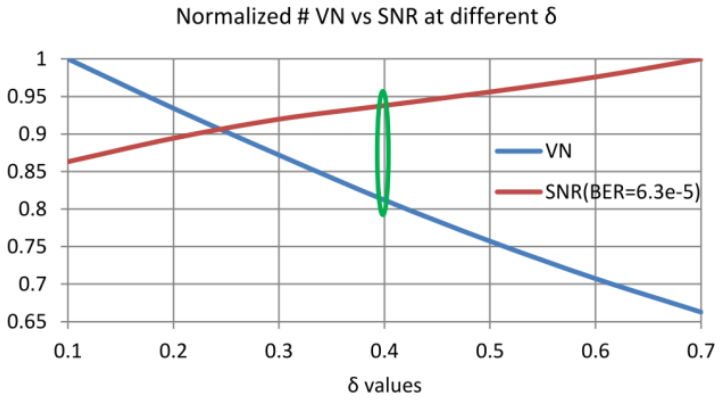

Figure 3.2: Complexity-Performance analysis at different threshold δ values to select the best δ which gives the best trade-off between the complexity and performance.

3.1.2 Column Norm method (M2)

In this method, instead of using the channel matrix norm, we employ the columns norm:

$$m_j = \left\|H_j\right\|_2, j = 1,2,..N_t \tag{3.2}$$

where H_j is the j^{th} column vector of the channel $\mathbf{H_i}$ and N_t is the number of transmitting antennas. Using the column norm enables us to adapt the K-value over the two transmitted symbols (in case of 2×1 MISO) within the pair of the payload cells rather than a fixed K over each pair of cells based on the fact that H_j column vector affects only the corresponding X_j transmitted symbol. Therefore, it provides an extra degree of adaptation. The two column norms m_1 and m_2 are used as indicators of the strength of their equivalent received signals X_1 and X_2 and hence the channel state affecting them and therefore can be used to define a suitable K value for the current tree level (as shown in Fig. 3.1 (b)) by the

same way described above where a m_j value within the threshold region gives a small K because of small deviation from the ideal norm value and vice versa. It is worth noting that other publications addressed the usage of the column norm such as in [34]. However, the method in [34] rearrange the channel used in the decoding process and modifies the complete decoding of the K-Best method by determining the signals detection order according to the distribution of the used number of points per level. On the other hand, the proposed method does not change the internal structure of the decoder, we introduce a preprocessing operation that involves calculating only the two norms and according to their values we define a sub-optimum K that gives a lower complexity with good performance in an adaptive way.

3.1.3 CQE based method (M3)

In this third proposed modified K-Best method, a possible selection criterion is chosen based on the channel quality. Assuming a known CSI at the receiver, and performing a CQE by making use of the Channel Response (CR) [35], we can measure the selectivity of the channel as follows:

- For two consecutive channel coefficients H_1 and H_2 in the frequency domain, we measure the channel selectivity by defining C parameter as the ratio between the two coefficients $\frac{|H_1|^2}{|H_2|^2}$.
- If $C >$ threshold value Γ, the channel is most likely a high frequency selective channel and if $C < \Gamma$, the channel is somehow a frequency selective while if $|H_1|^2 = |H_2|^2$ the channel is non-frequency selective.
- If $C > \Gamma$, we can enter Mode 1 of adaptation by defining small value of K and vice versa at $C < \Gamma$ where Mode 2 that defines a higher K is activated.

For the 2×1 varying channel matrix in SFBC MISO environment, as defined in (2.11), we have two varying channels for the two transmitting antennas therefore we have two *C* parameters and to enclose the *C* values within the range [0,1], the two *C* parameters are calculated as:

$$C_1 = \frac{min\,(H_{1,j}\ ,\ H_{1,j+1})}{max\,(H_{1,j}\ ,\ H_{1,j+1})}\ \&\ C_2 = \frac{min\,(H_{2,j}\ ,\ H_{2,j+1})}{max\,(H_{2,j}\ ,\ H_{2,j+1})} \tag{3.3}$$

where $H_{i,j}$ is the channel coefficient for the i^{th} transmit antenna at the j^{th} payload cell. Therefore, we have four different modes as described in table 3.1. Modes 2 and 3 are merged together and use one value of K_2 as they have similar effect, meaning that one C parameters is greater than Γ and the other is lower.

Table 3.1: Different Adaptation Modes of operation

Mode #	Conditions	Actual K
Mode 1	$C_1 > \Gamma$ & $C_2 > \Gamma$	K_1
Mode 2	$C_1 < \Gamma$ & $C_2 > \Gamma$	K_2
Mode 3	$C_1 > \Gamma$ & $C_2 < \Gamma$	
Mode 4	$C_1 < \Gamma$ & $C_2 < \Gamma$	K_3

For example, Mode 1 uses small values of K, i.e. K_1, to search the tree using it and is activated when the two C parameters are greater than Γ. Noting that Γ value is chosen based on a numerical analysis such that done for the δ value in Fig. 3.2 to select the superior value that gives the best trade-off between the complexity and the performance. Meaning that Mode 1 is activated if the difference between two adjacent coefficients H_j, H_{j+1} in the two channels are very small or even they are with equal values meaning that both channels are facing a very small or even no frequency selectivity. While if there is big difference between H_j, H_{j+1} in one channel, then this channel is somehow a frequency

selective one and Mode 2 or Mode 3 is activated where an intermediate value of K (K_2) is chosen for the tree search process and so on.

3.1.4 Estimated SNR method (M4)

In this method, the K-value is assigned according to the SNR value calculated by:

$$\text{SNR}= \frac{E_S}{\sigma^2 \left\| \boldsymbol{W_{zf}} \right\|^2} \tag{3.4}$$

where σ^2 is the statistical information of noise and $\boldsymbol{W}_{zf} = (\boldsymbol{H}^H\boldsymbol{H})^{-1}\boldsymbol{H}^H$ and E_s is the transmitted signal energy. We divide the SNR asymptote into regions and each region uses a suitable K that passed to the KBSD to work on as shown in Fig. 3.3. In low SNR, KBSD with different K-values (i.e. 2,6,16,85) have a near BER values and so we need only small value of K to save the excessive complexity while in high SNR we need higher K-values to approach ML performance as lower K-values (2,6,16) BER is far from the ML BER value.

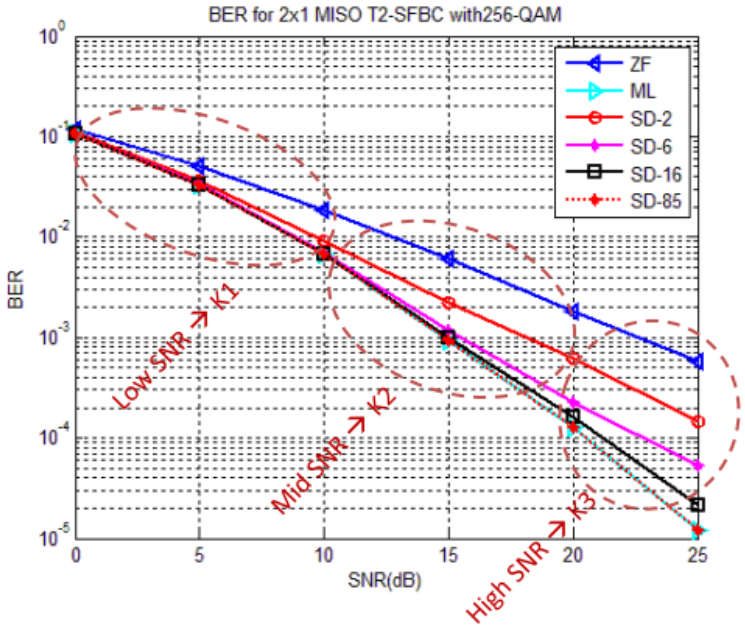

Figure 3.3: Assigning different K-values for SNR Regions.

For instance, in the low SNR region in Fig. 3.3, the best selected K-value is K=2

which provides the lowest complexity among all tested K-values while exhibiting a loss in the BER performance of less than 2×10^{-3} at the higher bound of this region (which extends till SNR= 10 dB), while in the mid SNR region (SNR= 10 to 20 dB), the best K-value is 6 and so on. In this method we need the knowledge of the statistical information of the noise to include its effect in the adaptation process as shown in (3.4). Also calculating the weight $\mathbf{W}_{zf}$ is required, however if these data are available, a low complexity decoding is obtained.

One advantage of the proposed methods (M_1-M_4) is the flexibility to switch between different values of K and giving the option of employing the original K-Best algorithm if the computational resources are available in the decoder. Thus, the proposed methods are suitable for implementation on flexible engines like the ASIP platform.

3.2 DVB-T2 Application

DVB-T2, the second-generation terrestrial transmission system for digital television broadcasting, builds on some technologies used in the previous generation DVB-T. DVB-T2 extends most of the parameters ranges of DVB-T and reduces the overhead to achieve better transmission capacity than its predecessor providing a capacity increase of at least 30% over the existing standard and enable a flexible and configurable robustness for each transmitted service [36]-[39].

To increase the system performance, five key technologies were used in the DVB-T2 as [40]:

1- *Error Protection Coding:* Combining LDPC codes with BCH codes to achieve high performance with a target BER in the order of 10^{-10} for a 5 Mbps service.

2- *Scheduling:* In order to offer service-specific robustness and optimize time-interleaving memory requirements, the DVB-T2 system can be described as a set of fully transparent

Physical Layer Pipes (PLPs), each one performing independent mode adaptation, Forward Error Correction (FEC) encoding, bitmapping onto constellation points (cells), and time interleaving.

3- *Modulation Techniques:*

- Extend the range for payload data to 256-QAM which offers increased throughput compared to a maximum of 64-QAM in DVB-T.
- Including rotated constellation as an optional feature.

4- *Synchronization and Channel Estimation:* Including particular design solutions to ease the time and frequency synchronization of the receiver such as P1 and P2 symbols [36],[37] and defining conventional Scattered Pilot (SP) sequences that modulate a set of equally spaced subcarriers. One novelty introduced by DVB-T2 is that it supports eight different SP patterns with pilot reference sequence.

5- *Multiple-Antenna Techniques:* Providing efficient means to exploit the presence of multiple transmitters i.e. obtain a distributed MISO system where the data on the two transmitters are not identical but closely related, avoiding destructive interference.

MISO Processing in DVB-T2

MISO processing is defined in the DVB-T2 standard [37] as an optional part of the OFDM generation block in the generic DVB-T2 system model as shown in Fig. 3.4. It is introduced to enhance the diversity by generating a second set of the transmitted signal to be sent over the second antenna element. MISO encoding process is done on pairs of OFDM payload cells[1]by taking the input data cells and produce two similar/correlated sets of data cells at the output to be directed to the two groups of transmitters as shown in Fig. 3.5.

[1] *Payload cells or data cells are the data symbols needed to be transmitted and are known as payload cells as they can carry any combination of video, audio and other data services.*

A modified Alamouti encoding, with a codeword equals the transpose of the original Alamouti codeword (for backwards compatibility) is used to produce the two sets of data cells as:

$$\mathbf{X} = \begin{bmatrix} X_1 & X_2 \\ -X_2{}^* & X_1{}^* \end{bmatrix} \tag{3.5}$$

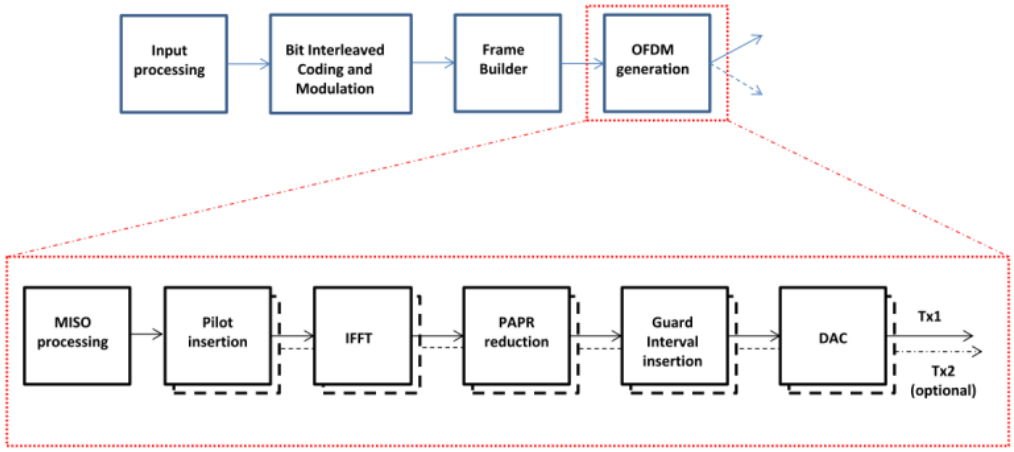

Figure 3.4: Generic DVB-T2 block diagram (top) including MISO processing block in the OFDM generation part (bottom) [37].

The rows represent the data carriers not the time intervals as in STBC. The transmitter in MISO group 1 remains unmodified regarding frequency order or arithmetic operations, while the transmitter group 2 performs pairwise modification according to the above codeword [36].

The received pair of cells is given by:

$$\mathrm{Y_1} = \mathrm{H_{11}X_1} - \mathrm{H_{21}X_2^*} + \mathrm{N_1}$$

and

$$\mathrm{Y_2} = \mathrm{H_{12}X_2} + \mathrm{H_{22}X_1^*} + \mathrm{N_2} \tag{3.6}$$

where N_1 and N_2 are AWGN noise and H_{ij} is the channel coefficient for i^{th} transmit antenna at the j^{th} payload cell. Simplifying the above equation by taking the complex conjugate of the second received signal and putting it in a matrix form ($Y = \boldsymbol{H}\, X + N$), we have:

$$\begin{bmatrix} Y_1 \\ Y_2^* \end{bmatrix} = \begin{bmatrix} H_{11} & -H_{21} \\ H_{22}^* & H_{12}^* \end{bmatrix} \begin{bmatrix} X_1 \\ X_2^* \end{bmatrix} + \begin{bmatrix} N_1 \\ N_2^* \end{bmatrix} \tag{3.7}$$

The various methods (M1-M4) of the AKBSD can be used to detect the transmitted symbols.

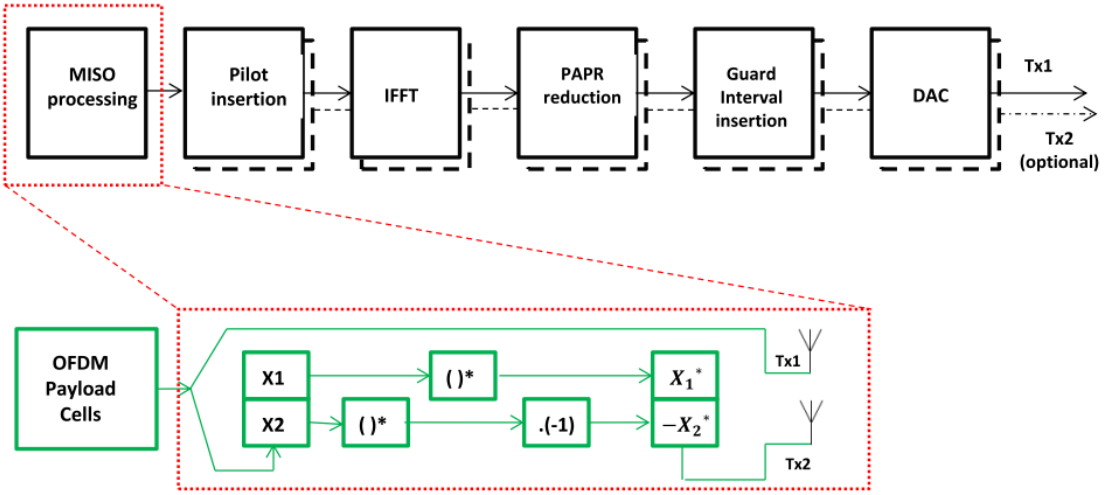

Figure 3.5: MISO Encoding Processing [37].

AKBSD in DVB-T2 system

Monte Carlo simulations were run for the 2×1 SFBC MISO system using 256-QAM modulation scheme that the DVB-T2 included recently over a frequency selective Rayleigh fading channel with perfect CSI at the receiver. BER curves, normalized execution time and number of Visited Nodes (VN), for different K-values (K=4 and 64) were plotted against the ZF, ML and the AKBSD decoding methods (M_1, M_2, M_3 and M_4) to measure the performance and the complexity of each system.

It is important to note that the node computation complexity increases by going from one level to a bottom one during the tree traversal [41], as can be deduced from (2.14) due to the existence of the upper triangle matrix **R**, but the adaptation methods above (M_1-M_4) makes changes in a preprocess stage to select an instantaneous suitable K-value to the current system conditions and this value become fixed while processing the

tree levels as same as the fixed K-value KBSD, so we can use the average number of VN as a measure of complexity.

Applying the AKBSD methods (with threshold values $\delta = 0.4$ for M_1 and M_2 and $\Gamma=0.82$ for M_3 and SNR regions bounds of 12, 24 dB for M_4) shows performance enhancement over the ZF linear method and approaching the higher K-value KBSD and the ML BER as shown in Fig. 3.6 with acceptable increase in complexity over the ZF and significant complexity reduction below ML as shown in Figs. 3.7 and 3.8.

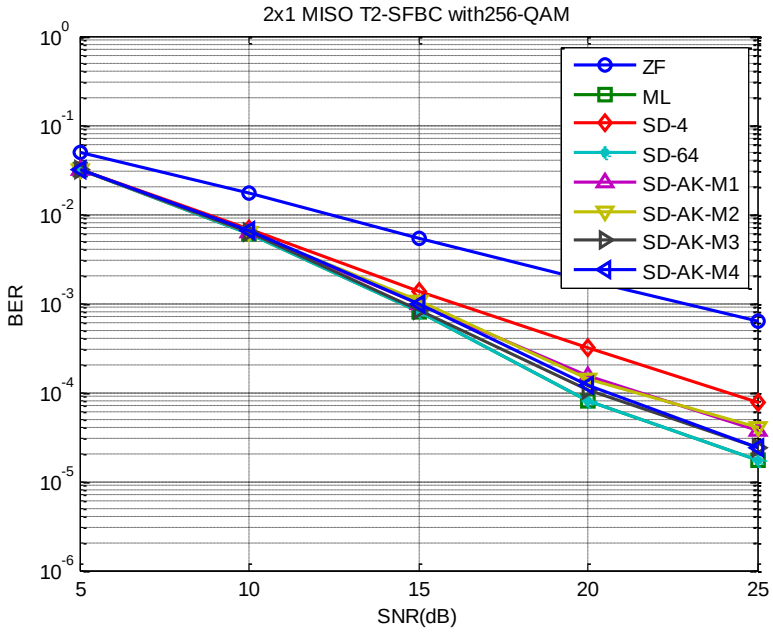

Figure 3.6: BER simulation results of different AKBSD methods over 2×1 MISO-SFBC with 256-QAM modulation scheme.

Figure 3.7 shows the curves for complexity measurement in the terms of the execution times of ZF, KBSD with fixed K-values and the AKBSD methods normalized to the ML execution time (which takes the value of one and not shown in Fig. 3.7). The average number of VN is another complexity measurement and is shown in Fig. 3.8. Exhaustive search, i.e. ML, visits 17092 nodes during decoding while the numbers of VN for the AKBSD methods are much smaller as can be seen from Fig. 3.8. The various

AKBSD methods M_1, M_2 and M_3 give a complexity reduction between 19% and 31% over regular KBSD that uses K=64 while M_4 gives a varying complexity reduction between 9% and 70% depending on the SNR region.

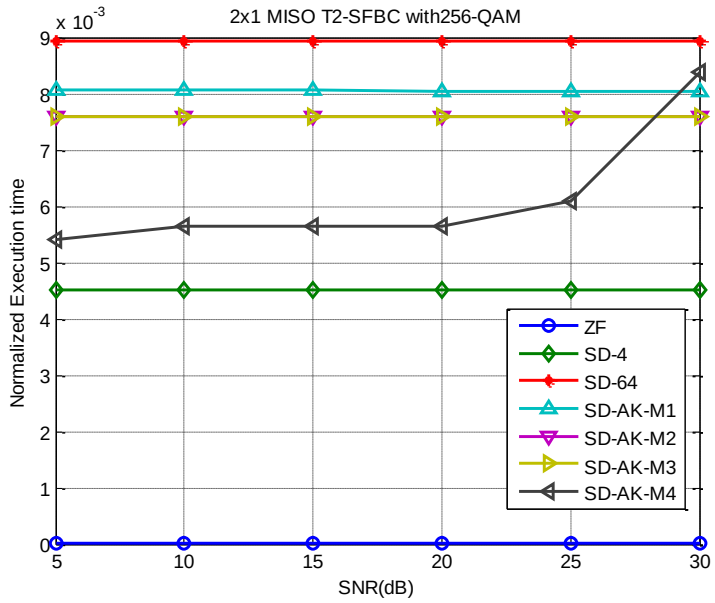

Figure 3.7: Complexity measurement in terms of normalized execution time (to ML time) for AKBSD methods versus ZF and different K-SD decoding methods.

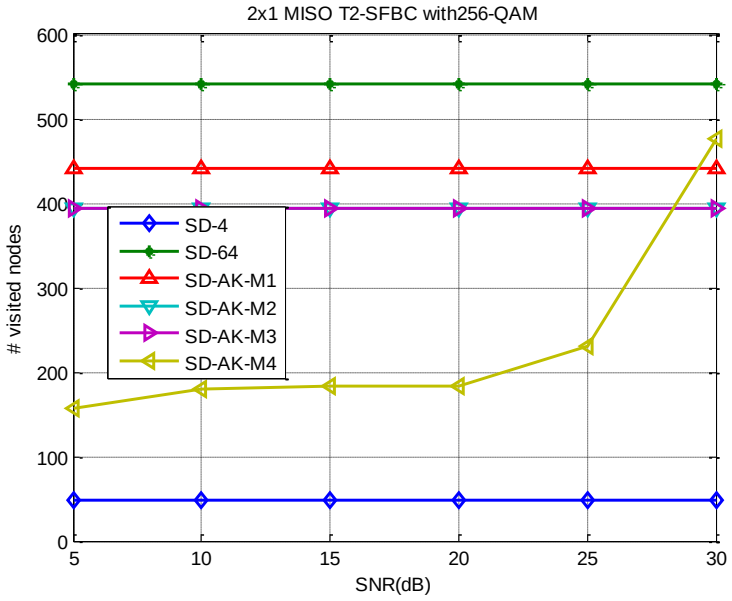

Figure 3.8: Complexity measurement in terms of number of visited nodes for AKBSD methods versus different K-SD decoding methods.

To fairly compare the four proposed AKBSD methods M_1-M_4, we need to define:

1. A working SNR.
2. A proposed comparison parameter called reliability η which gives the best performance-complexity trade-off (i.e. minimize both BER and VN) as:

$$\eta = 1/(\mathrm{BER} * \mathrm{VN}) \tag{3.8}$$

The comparison is done over four SNR values of 12, 20, 28 and 36 dB as shown in Fig. 3.9; noting that all values are normalized to M_1 corresponding values. We can conclude that comparison as:

- M_1 reliability is higher than M_2 but both still lower than M_3 and M_4.
- M_3 has the superior performance (i.e. lower BER) ever, which mean it is the best method that approaches the ML performance.
- M_4 has very low complexity in lower SNR regions (12, 20 dB) but the highest complexity in higher SNR ones (28, 36 dB); noting that increasing the K in low SNR does not increase the performance gain with a big value as shown in Fig. 3.6. Then a good way to reduce the complexity is using the lowest K in small SNR and that is exactly what M_4 does making use of the knowledge of SNR.
- M_3 and M_4 reliabilities are alternating in lower and higher SNR because of the lower complexity of M_4 in lower SNR; however the M_3 performance is always the better.

Using the information provided by the defined reliability parameter, we can conclude that M_3 and M_4 are the most feasible methods. The reliability values obtained from M_3, i.e. $\eta_{(M3)}$, increase proportionally with SNR increase while $\eta_{(M4)}$ is inversely proportional with SNR and they have an equal η at SNR of about 26 dB, and hence M_3 is preferable at working SNR greater than 26 dB while M_4 is preferable at working SNR lower than 26 dB. Moreover, the receiver can select M_3 or M_4 as a decoding method depending on the system target SNR.

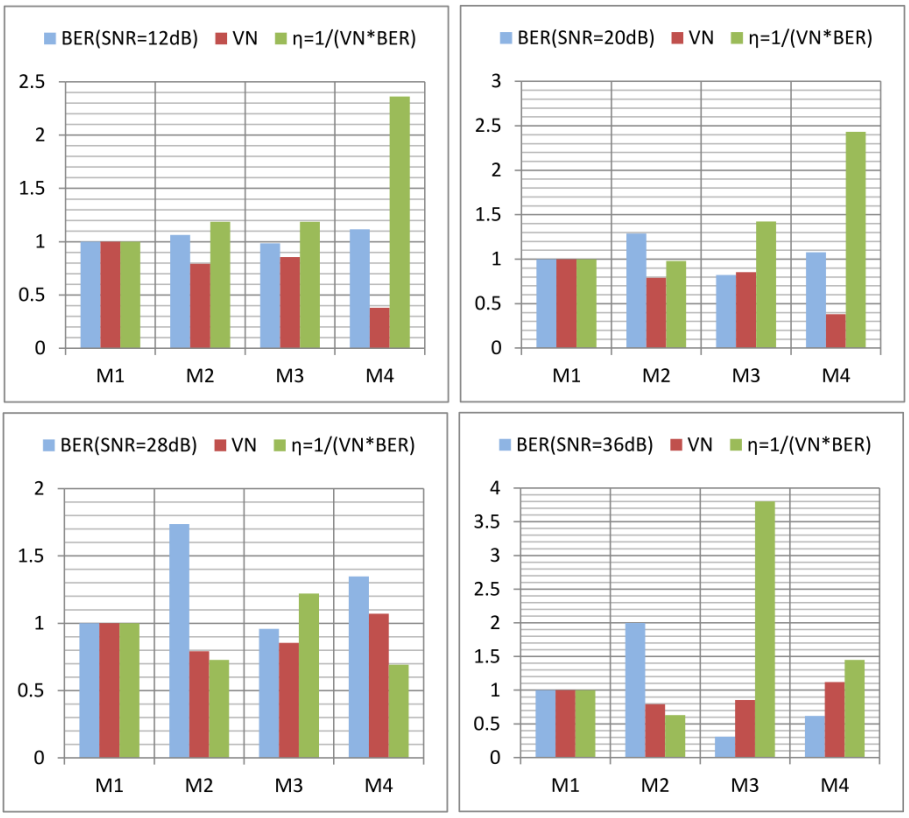

Figure 3.9: AKBSD methods comparison at target SNRs of 12, 20, 28 and 36 dB.

3.3 Adaptive K-Best List Sphere Decoder

To be applicable in iterative receivers, we applied the proposed adaptive methods (M_1-M_4) on the soft version of the KBSD which is known as K-Best List Sphere Decoder (KB-LSD) that exchanges its soft output values with the Low Density Parity Check (LDPC) decoder as shown in Fig. 3.10 to reach near optimal soft output MAP detection with reduced complexity. The ACU is the unit that performs one of the methods (M_1-M_4) and adapts the number of K-paths chosen by the KB-LSD as well as the iterations number of the LDPC decoder and the iterations number of the outer-loop of the iterative receiver as well. Adapting iterations number prevents excessive computations and reduces the iterative receiver complexity.

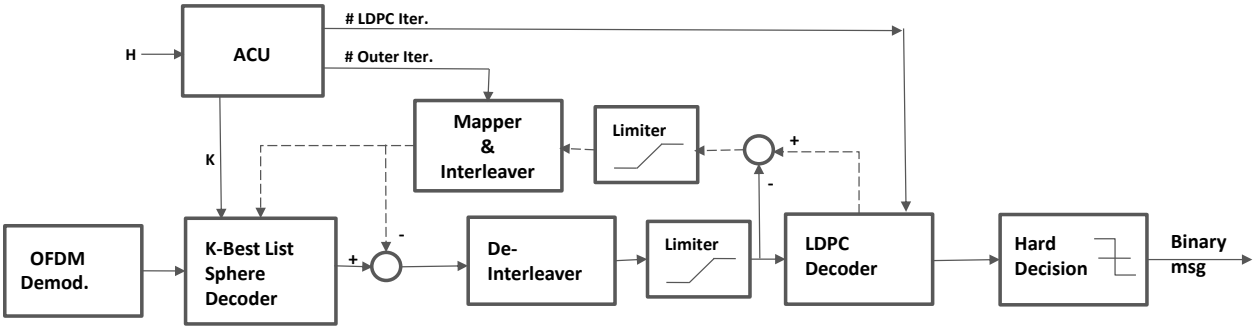

Figure 3.10: MISO-BICM iterative receiver.

The block diagram of the KB-LSD is shown in Fig. 3.11 where four main functions are performed, the first is the QR decomposition of the channel matrix, then the tree search is performed to output a list of the candidates symbols that contains the solution within it, then these symbols are demodulated to get their equivalent individual bits and finally these bits are used to get the Log-Likelihood Ratios (LLR) values that exchanged with the LDPC decoder. Using the KB-LSD algorithm in [42] and modifying it to use the MAP of each transmitted symbol as a cost function of each child in the tree.

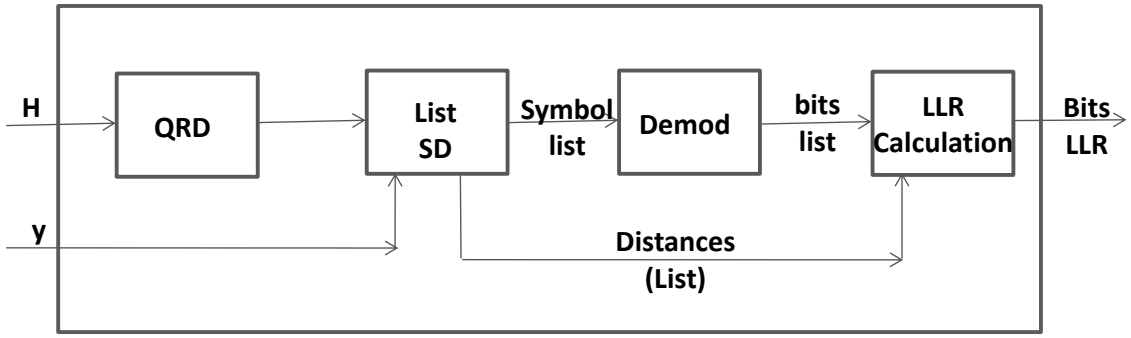

Figure 3.11: KB-LSD structure.

The modified algorithm can be described as follows:

Preprocessing:

Input: Q, R,$\bar{y}$, R_{SD}, K,M(modulation used, M-QAM)

Calculate: $\tilde{y}$

Algorithm:

1.Start point: Root level is the start point, the initial candidate set is empty.

2.Creating new partial Candidate set: Progressing from layer i+1 to layer i, and denoting the partial candidate set at parent layer as $\bar{x}_{i+1}^{2Nt}$ *:*

2.1 Select child nodes $\bar{x}_i$ *with given* $R_{SD.}$

2.2Calculate the corresponding PEDs $d(\bar{x}_i^{2Nt})$

2.3. Store the new partial candidates and their PEDs to a temporary stack memory.

3.Calculate the LLR of the transmitted bits over symbol $\bar{x}_i$.

4.The new partial Euclidean distance PED_i^{new} *is used to sort the partial candidates in ascending order.*

5.Store the first K candidates and their bits' LLR to the final list stack memory.

6.Iteration: Iterate steps 2-5. If the iterations reach the leaf nodes partial candidate set, stop the algorithm and output the LLR values.

The KB-LSD LLR output of the k^{th} transmitted bit is calculated as:

$$L(u_k) = \min_{\bar{x}\in\mathcal{L}_{k,-1}} \{PED_i^{new}\} - \min_{\bar{x}\in\mathcal{L}_{k,+1}} \{PED_i^{new}\} \tag{3.9}$$

where the k bit is carried by the i^{th} symbol. PED_i^{new} is the PED of the vector contains all symbols from i to $2N_t$ and it is calculated at the i^{th} tree level.

MAP-based KB-LSD

The LLR of k^{th} coded bit u_k using MAP detection of LSD with Max-Log approximation is calculated by [43]:

$$L(u_k) = \max_{\bar{x}\in\mathcal{L}_{k,+1}} \left\{-\frac{1}{2\sigma^2}\|\tilde{y} - R\bar{x}\|^2 + 0.5\bar{u}^T\bar{L}_A\right\}$$
$$- max_{\bar{x}\in\mathcal{L}_{k,-1}}\{-\tfrac{1}{2\sigma^2}\|\tilde{y} - R\bar{x}\|^2 + 0.5\bar{u}^T\bar{L}_A\} \tag{3.10}$$

where $\bar{u}$ is a vector contains the bits transmitted at this time slot, $\bar{L}_A$ is the vector contains a prior LLR of this time slot's bits (calculated using LDPC output in the previous iteration), $\mathcal{L}_{k,\pm1}$ is the set of possible transmitted vectors contain ±1 at the k^{th} position. A new PED is

used to increase the confidence of including the maximization process into the list.

Equation (3.10) can be modified by adding $0.5\mathbf{1}^T\bar{L}_A$ to both maximization functions as:

$$L(u_k) = \max_{\bar{x}\in\mathcal{L}_{k,+1}}\left\{-\frac{1}{2\sigma^2}\|\tilde{y} - R\bar{x}\|^2 + 0.5\bar{u}^T\bar{L}_A + 0.5\mathbf{1}^T\bar{L}_A\right\}$$
$$- max_{\bar{x}\in\mathcal{L}_{k,-1}}\{-\tfrac{1}{2\sigma^2}\|\tilde{y} - R\bar{x}\|^2 + 0.5\bar{u}^T\bar{L}_A + 0.5\mathbf{1}^T\bar{L}_A\} \quad (3.11)$$

The term $0.5\bar{u}^T\bar{L}_A + 0.5\mathbf{1}^T\bar{L}_A$ is equivalent to $\boldsymbol{\gamma}^T\bar{L}_A$ where $\boldsymbol{\gamma}_{\bar{x}} = 0.5(\bar{u} + 1)$, in other words $\boldsymbol{\gamma}_{\bar{x}}(k) = 1$ where $\boldsymbol{u_k} = 1$ and zero otherwise.

$$L(u_k) = \max_{\bar{x}\in\mathcal{L}_{k,+1}}\left\{-\frac{1}{2\sigma^2}\|\tilde{y} - R\bar{x}\|^2 + \boldsymbol{\gamma}_{\bar{x}}{}^T\bar{L}_A\right\}$$
$$- max_{\bar{x}\in\mathcal{L}_{k,-1}}\{-\tfrac{1}{2\sigma^2}\|\tilde{y} - R\bar{x}\|^2 + \boldsymbol{\gamma}_{\bar{x}}{}^T\bar{L}_A\} \quad (3.12)$$

By replacing $max(-a)$ with $-min(a)$, we can rewrite (3.12) as:

$$L(u_k) = min_{\bar{x}\in\mathcal{L}_{k,-1}}\{\tfrac{1}{2\sigma^2}\|\tilde{y} - R\bar{x}\|^2 - \boldsymbol{\gamma}_{\bar{x}}{}^T\bar{L}_A\} - min_{\bar{x}\in\mathcal{L}_{k,+1}}\{\tfrac{1}{2\sigma^2}\|\tilde{y} - R\bar{x}\|^2 - \boldsymbol{\gamma}_{\bar{x}}{}^T\bar{L}_A\} \quad (3.13)$$

By defining the modified PED of each leaf child as:

$$PED_1^{new} = \tfrac{1}{2\sigma^2}\|\tilde{y} - R\bar{x}\|^2 - \boldsymbol{\gamma}_{\bar{x}}{}^T\bar{L}_A \quad (3.14)$$

and we can rewrite (3.13) as:

$$L(u_k) = \min_{\bar{x}\in\mathcal{L}_{k,-1}}\{PED_1^{new}\} - \min_{\bar{x}\in\mathcal{L}_{k,+1}}\{PED_1^{new}\} \quad (3.15)$$

and

$$PED_1^{new} = \sum_{i=1}^{2Nt}\left[\tfrac{1}{2\sigma^2}\left|\tilde{y}_i - \sum_{g=i}^{2Nt} r_{ig}\bar{x}_g\right|^2 - \sum_{l\epsilon\, v_{i,1}} L_A(u_l)\right] \quad (3.16)$$

where $v_{i,1}$ is the set of ones' indices into symbol $\bar{x}_i$. PED_1^{new} can be calculated sequentially at each child in level *i* (like PED) as:

$$PED_i^{new} = PED_{i+1}^{new} + \tfrac{1}{2\sigma^2}\left|\tilde{y}_i - \sum_{j=i}^{2Nt} r_{ij}\bar{x}_j\right|^2 - \sum_{l\epsilon\, v_{i,1}} L_A(u_l) \quad (3.17)$$

We can approximate (3.14) to (3.9) to avoid storing all visited nodes (step 3 in the

algorithm); simulation results gives nearly no error with this approximation. $L(u_k)$ is the output of *LSD* which is used to calculate the a prior LLR of the LDPC decoder or present iteration (this forms the outer iteration).

The SFBC MISO-BICM system shown in Fig. 3.10 is simulated using the following DVB-T2 parameters:

- 2×1 MISO system
- LDPC block Length: 64800 bits
- K_1, K_2, K_3 = 2, 6, 12
- Constellation size: 16, 64-QAM
- LDPC code rate =1/2
- I_1, I_2, I_3 = 10, 30, 45

The simulations have been carried over a Rayleigh channel with perfect CSI at the receiver. Figure 3.12 shows the BER of different number of K-Best values and the adaptive K-best LSD (*AK1*, *AK2* and *AK3*) plotted after fixed four outer iterations between the MISO detector and the LDPC decoder.

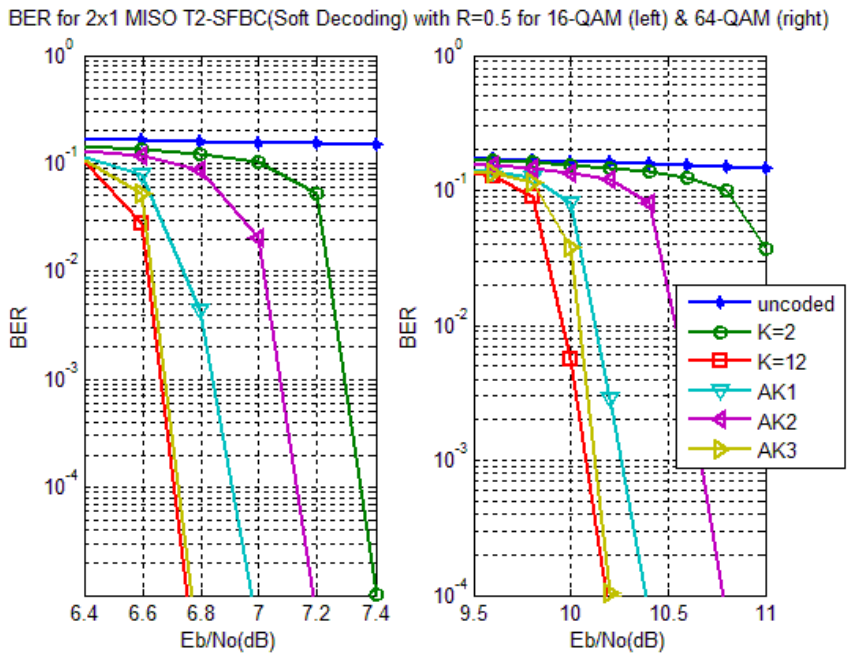

Figure 3.12: BER of adaptive KB-LSD after 16-QAM (left) and 64-QAM (right) modulation scheme.

The results show that the three adaptive KB-LSD gives different performance that approaches the highest K value (*K*=12) in both 16-QAM and 64-QAM modulation schemes.

The complexity of the system is measured in terms of the number of visited nodes. Table 3.2 shows that the three adaptive KB-LSD visits less nodes than the KB-LSD with *K*=12 and hence it gives a lower complexity with good performance. The third adaptive KB-LSD (*AK3*) for example gives a complexity reduction of 14.3% and 18.5% over the *K*=12 KB-LSD in the 16-QAM and the 64-QAM respectively.

TABLE 3.2: NUMBER OF VISITED NODES

KB-LSD	***16-QAM***	***64-QAM***
K=2	103	224
K=12	287	1056
AK1	330	967
AK2	239	688
AK3	256	862

3.4 DVB-NGH Application

The DVB-NGH specifies a transmission system which is designed for carrying transport streams feeding linear and non-linear applications such as television, radio and data services. It is the DVB standard specially proposed for the second generation mobile broadcasting standard. DVB-NGH uses rate 2 MIMO transmission to improve robustness of the transmitted signal (by spatial diversity) and to achieve increased data rates (by spatial multiplexing). It identifies MIMO techniques as one of its key technologies

which include 2×2 preferred antenna solution and Golden Codes as a STBC. Golden Codes [44] are Full Rate Full Diversity (FRFD) codes but has a main drawback of large decoding complexity. DVB-NGH standard proposes four different structures of the transmitter networks namely as *Base profile* which includes terrestrial transmission with single and multi-antenna structures that requires only one antenna and tuner at the receiver side. The second is *MIMO profile* which includes terrestrial transmission with multi-antenna structures at both ends where the terminals need to include two tuners to be suitable for this profile. The third is *Hybrid profile* which includes a collection of terrestrial and satellite transmissions that requires only a single tuner at the receiver side. Finally, the *Hybrid MIMO profile* which includes a collection of terrestrial and satellite transmissions that requires double antenna and tuners at the receiver side [45]. In this section, we focus on the *MIMO profile* with double antennas at both the base station and the receiver side i.e. 2×2 MIMO system using Golden codes as the SFBC transmit diversity technique employed in the transmission chain of the DVB-NGH system. We propose to use the AKBSD in the decoding process to cover the *MIMO profile* in the DVB-NGH as well as the *Base Profile* which is similar to the DVB-T2 in the previous sections.

Golden Codes

The Golden code first appeared in [44], provides FRFD property for 2×2 MIMO systems. Using the Golden code for SFBC ($N_t = N_r = 2$), four symbols (X_1, X_2, X_3, X_4) are transmitted over two subcarriers ($N_c = 2$) with a codeword defined as [44]:

$$\boldsymbol{S} = \frac{1}{\sqrt{5}}\begin{bmatrix} \alpha(X_1 + X_2\theta) & \alpha(X_3 + X_4\theta) \\ i\bar{\alpha}(X_3 + X_4\bar{\theta}) & \bar{\alpha}(X_1 + X_2\bar{\theta}) \end{bmatrix} \tag{3.18}$$

where $\theta = \frac{1+\sqrt{5}}{2}$ & $\bar{\theta} = \frac{1-\sqrt{5}}{2}$ and $\alpha = 1 + i(1-\theta)$ & $\bar{\alpha} = 1 + i(1-\bar{\theta})$.

To work with the real lattice representation, the codeword matrix is transformed to a

vector form by stacking the **S** matrix column wise and the real and imaginary parts are then separated to get the real $(2N_tN_c \times 2N_tN_c) = (8 \times 8)$ real matrix **G** and **S** is now:

$$\boldsymbol{S} = \boldsymbol{G}X = \frac{1}{\sqrt{5}}\begin{bmatrix} 1 & -\bar{\theta} & \theta & 1 & 0 & 0 & 0 & 0 \\ \bar{\theta} & 1 & -1 & \theta & 0 & 0 & 0 & 0 \\ 0 & 0 & 0 & 0 & -\theta & -1 & 1 & -\bar{\theta} \\ 0 & 0 & 0 & 0 & 1 & -\theta & \bar{\theta} & 1 \\ 0 & 0 & 0 & 0 & 1 & -\bar{\theta} & \theta & 1 \\ 0 & 0 & 0 & 0 & \bar{\theta} & 1 & -1 & \theta \\ 1 & -\theta & \bar{\theta} & 1 & 0 & 0 & 0 & 0 \\ \theta & 1 & -1 & \bar{\theta} & 0 & 0 & 0 & 0 \end{bmatrix}\begin{bmatrix} X_{1\mathrm{R}} \\ X_{1\mathrm{I}} \\ X_{2\mathrm{R}} \\ X_{2\mathrm{I}} \\ X_{3\mathrm{R}} \\ X_{3\mathrm{I}} \\ X_{4\mathrm{R}} \\ X_{4\mathrm{I}} \end{bmatrix} \tag{31}$$

The received signal is:

$$\mathrm{Y} = \mathbf{HS} + \mathrm{N} = \mathbf{HG}\mathrm{X} + \mathrm{N} \tag{32}$$

where $\boldsymbol{H} = \begin{bmatrix} \boldsymbol{H'} & \mathbf{0} \\ \mathbf{0} & \boldsymbol{H'} \end{bmatrix}$ and $\boldsymbol{H'} = \begin{bmatrix} H_{11\mathrm{R}} & -H_{11\mathrm{I}} & H_{12\mathrm{R}} & -H_{12\mathrm{I}} \\ H_{11\mathrm{I}} & H_{11\mathrm{R}} & H_{12\mathrm{I}} & H_{12\mathrm{R}} \\ H_{21\mathrm{R}} & -H_{21\mathrm{I}} & H_{22\mathrm{R}} & -H_{22\mathrm{I}} \\ H_{21\mathrm{I}} & H_{21\mathrm{R}} & H_{22\mathrm{I}} & H_{22\mathrm{R}} \end{bmatrix}$.

The methods M_1-M_4 can be directly extended here. For example, applying the third method of the AKBSD (M3), for the 2×2 varying channel matrix in SFBC MIMO system yields four varying channels between the two transmitting and the two receiving antennas and therefore we have four *C* parameters as:

$$C_1 = \frac{min\,(H_{11}^k\ ,\ H_{11}^{k+1})}{max\,(H_{11}^k\ ,\ H_{11}^{k+1})}\ \&\ C_2 = \frac{min\,(H_{12}^k\ ,\ H_{12}^{k+1})}{max\,(H_{12}^k\ ,\ H_{12}^{k+1})}$$

$$C_3 = \frac{min\,(H_{21}^k\ ,\ H_{21}^{k+1})}{max\,(H_{21}^k\ ,\ H_{21}^{k+1})}\ \&\ C_4 = \frac{min\,(H_{22}^k\ ,\ H_{22}^{k+1})}{max\,(H_{22}^k\ ,\ H_{22}^{k+1})} \tag{3.19}$$

where H_{ij}^k is the channel coefficient between the i^{th} transmit antenna and the j^{th} receive antenna at the k^{th} payload cell and therefore we have eight different modes and for simplicity we combine similar combinations of operation to get only four modes that represent the state of the channel as described in table 3.3. The four modes Mode1 to 4

define four different values of K_1, K_2, K_3 and K_4 that the KBSD can work on according to the estimated channel selectivity.

TABLE 3.3: 2×2 MIMO ADAPTATION MODES OF OPERATION

Mode #	Conditions	Actual K
Mode 1	$C_1 > \Gamma$ & $C_2 > \Gamma$ & $C_3 > \Gamma$ & $C_4 > \Gamma$	K_1
Mode 2	*Any three* $C < \Gamma$	K_2
Mode 3	*Any two* $C < \Gamma$	K_3
Mode 4	*Any single* $C < \Gamma$	K_4

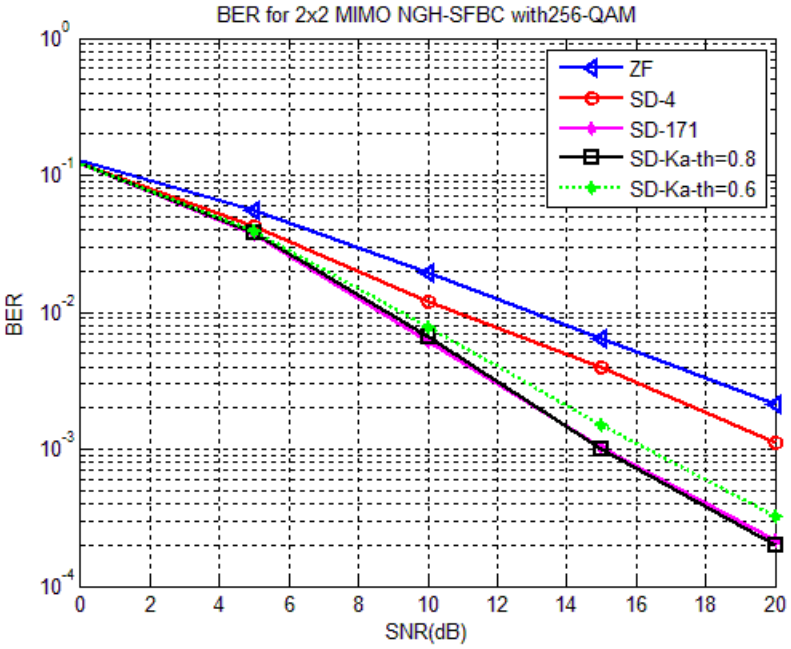

Figure 3.13: BER Performance for AKBSD versus different K-SD under 2x2 MIMO system with Γ=0.6 and Γ=0.8.

The simulation results of the Golden codes as SFBCs for a 2×2 MIMO system using 256-QAM modulation scheme and AKBSD-M3 with different K-values (K_1, K_2, K_3, K_4 equal 4, 32, 128, 171 respectively) selected to be passed to the KBSD according to the

channel selectivity as shown in table 3.3 are shown in Figs. 3.13 and 3.14. The lower fixed K-values were selected for comparison as they give the lower complexity while the upper were selected as they give almost the ML performance and any increase in K-value after them is just an increase in complexity without any noticeable performance gain i.e. any value more than K_4=171 is just an increase the complexity with a limited performance enhancement. The simulations have been carried over a frequency selective Rayleigh channel with perfect CSI at the receiver. Applying the AKBSD method with different threshold values Γ=0.6 and 0.8 shows performance enhancement over the ZF linear method and coincide the higher K-value (K=171) BER as shown in in Fig. 3.13 with a lower complexity measured in terms of the execution time and normalized to the higher K-value execution time as shown in Fig. 3.14.

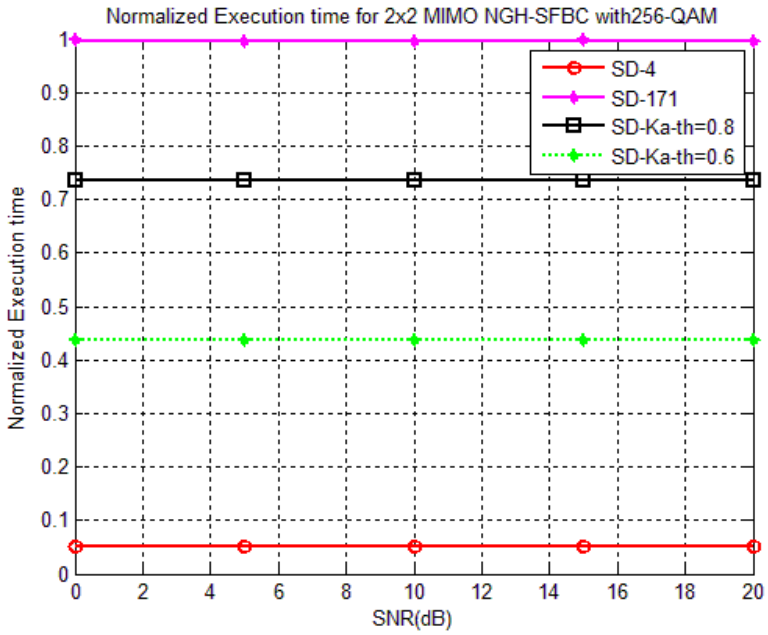

Figure 3.14: Complexity in terms of normalized execution time for AKBSD versus different K-SD under 2×2 MIMO system with Γ=0.6 and Γ=0.8.

Regarding the power consumption, the AKBSD alternates between different K-values for the KBSD and subsequently it consumes different powers with average power

value below than that of the KBSD using the K_4=171 value as shown in in Fig. 3.14 and hence a power saving is tacitly obtained by using the AKBSD. The AKBSD achieves a complexity reduction versus the K_4 KBSD of about 27% and 56% for Γ=0.8 and 0.6 respectively, noting that different Γ means different performance. This complexity reduction can be directly transformed into execution time reduction which means that the device is idle for longer periods than the ordinary KBSD corresponding to the value of K_4. Therefore, a roughly obtained power reduction for the M_3 method is in the range of 27-56% for different threshold values 0.8 and 0.6 respectively.

3.5 Summary

In this chapter, we illustrated the various methods applied on the KBSD to change the K-value adaptively, we used the channel quality estimation, channel matrix analysis and SNR estimation criteria to indicate the channel quality and then select the most suitable K value that should be used in these channel conditions. We also showed how we can employ the AKBSD in the DVB systems including DVB-T2 and DVB-NGH. Using a KB-LST as a soft decoder in the MISO-BICM chain was also illustrated. In the next chapter, we propose 2-D AKBSD and its application in cooperative and relay networks e.g. CoMP and also propose a hybrid partial and full detection protocol to be utilized in multi-hop networks.

CHAPTER: 4

2-D ADAPTIVE K-BEST SPHERE DECODER AND ITS APPLICATION IN COOPERATIVE NETWORKS

Cooperative communication is one major trend that assists in the vast development of wireless communication technology e.g. modern wireless and mobile communication networks. It enhances the performance of the system and increases the transmission data rate. It also removes the need for installing multiple antennas at the network nodes which is, in many cases, impractical due to size, hardware complexity and/or power limitations [4]-[6]. Moreover, it also reduces the transmission power and extends the coverage area of the network. In this chapter, we discuss the application of the AKBSD in Coordinated MultiPoint (CoMP) transmission and propose a 2-D AKBSD that can be applied in cooperative relay networks and finally propose a Hybrid Partial and Full Detection protocol, HPFD, protocol to be used in multi-hop networks.

4.1 CoMP Application

CoMP transmission has been considered in the 3GPP LTE Release 9 [46] then standardized in LTE-Advanced [47] as one technique used to improve the coverage area by changing the Inter Cell Interference (ICI) problem occurring at the cell-edge into a useful cooperation between the different cells [4]-[6]. The CoMP establishes cooperation between the various BSs for collective signal processing in both up and downlinks [7]. The main categories of the downlink CoMP (DL-CoMP) are summarized in Fig. 4.1 [4]-[6].

In Coordinated Scheduling / Beamforming (CoMP-CBF), each Base Station (BS)

(or Remote Radio Equipment (RRE)) transmits beamformed signal for the cell-edge user in its serving cell only. This results in reduced ICI. In Joint Processing/Transmission (CoMP-JP), eNodeB controls the transmission of the cell-edge user data symbols transmitted from all RREs at the same time, and then this data is received and jointly processed across the RREs. CoMP-JP is further divided into two categories. The first category is Joint Transmission (JT) where the same data is transmitted from multiple serving cells (coordinated cells) as well as non-serving cells [5]. In JT, one transmission scheme is Local Precoding (LP) in which multiple BSs transmit the same cell-edge user signal that is separately precoded by each BS. Another scheme is Global Precoding (GP) where the channel matrices for the multiple BSs are aggregated as $\mathbf{H_{global}} = [\mathbf{H_1}\ \mathbf{H_2}..\ ]$ where $\mathbf{H_i}$ is the channel matrix associated with BS_i. The GP scheme is considered as a generalization of single-cell multi-antenna transmission to antenna ports of more than one cell [6]. The second category is Dynamic Cell Selection (D-CS), where a dynamic fast scheduling at the central BS is responsible for selecting one base station to transmit the data block.

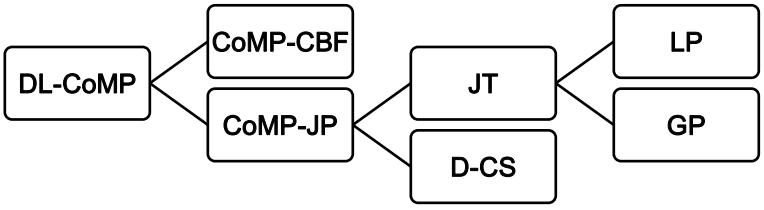

Figure 4.1: Downlink CoMP categories.

Another technique used to improve the reliability in large wireless networks, e.g. Relay-Assisted Communication (RAC), is Distributed STBC/SFBC (DSTBC/DSFBC). RAC is introduced to cellular systems to improve the performance of cell-edge users and is recommended in modern wireless standards [48] e.g. 3GPP LTE-Advanced. In DSFBC multiple transmission nodes are used together in a distributed way to transmit a SFBC

codeword to the cell-edge user, this redundancy in space and frequency increases the reliability of the communication in OFDM systems by increasing the diversity gain.

In high mobility cell-edge user scenario, the channels between the BSs and the Mobile Station (MS) are time varying. Moreover, sending high data rates and the existence of different delayed paths of the signal give rise to frequency selective channels. In this section, we use the DSFBC as a transmit diversity technique which distributes the SFBC codeword among different transmission BSs in an open-loop CoMP scheme. The scenario we consider is the realistic case of two time varying frequency selective channels, in which case the simple linear decoder basic assumption of static channel over two frequency symbols no longer holds. We propose to decode the combined received signal by the AKBSD as it modifies the K-paths of the traditional KBSD in an adaptive way depending on the channel quality of each transmission link. The selectivity of each channel and the received signal strength are measured and a suitable K-value is assigned for different equivalent tree levels to search among them separately. This gives lower complexity decoding processing which maintains the power in a cell-edge user. Using the AKBSD decoder helps to reduce the large computational processing associated with the CoMP technique at the MS. Therefore, it encourages the CoMP operation in varying channels.

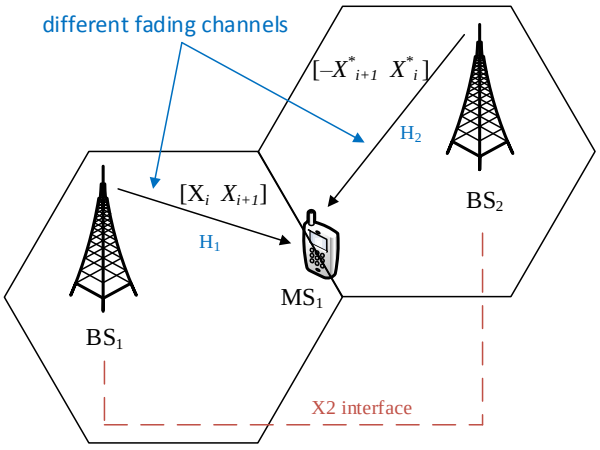

Figure 4.2: CoMP System model.

The system model that we work on is shown in Fig. 4.2. BS_1 and BS_2 are two base stations covering two coordinated serving cells and MS_1 is a cell-edge mobile user. The general communication between the two base stations and the mobile MS_1 can be viewed as 2×1 MISO system. Data symbols $X_1, X_2, \ldots, X_i, \ldots, X_{Nc}$ from the constellation set $\mathbb{C}$ are sent over subcarriers $1, 2, \ldots, i, \ldots, N_c$ respectively of an OFDM system and N_c is the number of used subcarriers. A distributed Alamouti codeword [15] is spread between the BSs as shown in Fig. 4.2 where one BS transmits the symbols $[X_i \quad X_{i+1}]$ and the other transmits $[-X_{i+1}^* \quad X_i^*]$ over two different frequency selective fading channels.

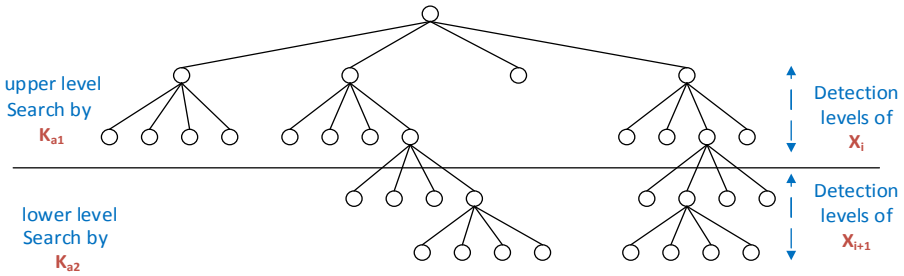

Figure 4.3: Different K-values are assigned for different levels of the tree.

The AKBSD algorithm estimates the selectivity of the two channels together and combines it with the estimated received signal strength to select one suitable K-value to be passed to the KBSD. This combined decision takes into consideration the effect of the two channels on the multiple versions of the same symbol which are transmitted from the two BSs according to the Alamouti codeword and then select an appropriate K-value to search the equivalent levels of the tree which related to that transmitted symbol and therefore two values of K (ka_1 and ka_2) are used while exploring the tree as shown in Fig. 4.3, where the upper levels represent the detection levels of the symbol X_i while the lower levels represent those of X_{i+1}.

The steps used in the decoding process are as follows:

for each pair of cells, do:

Preprocess:

define $m_{ideal} = \|[1\ 1]^T\| = \|[-1\ 1]^T\| = 1.4142$

define $m_{th1} = m_{ideal} + \delta$ *and* $m_{th2} = m_{ideal} - \delta$

calculate $m_i = \|\boldsymbol{H}(:,i)\|$ *and* $C_i = \frac{min\,(H_{i,j}\ ,\ H_{i,j+1})}{max\,(H_{i,j}\ ,\ H_{i,j+1})}$ $\forall i=1,2$; $j=1:N_c-1$

using $k_{i+1} > k_i$

if $C_i > \Gamma$ *and* $m_{th1} < m_i < m_{th2}$

$k_{ai}=k_1$;

else if $(C_i > \Gamma$ *and* $(m_{th1} > m_i \| m_i > m_{th2})) \| (C_i < \Gamma$ *and* $m_{th1} < m_i < m_{th2})$

$k_{ai}=k_2$;

else

$k_{ai}=k_3$;

end if

Search the tree:

start from root level

initialize a zero metric path between the root and the first tree level nodes

loop:

extend the survivor paths and update their PEDs

if upper level

set $k=k_{a1}$;

end if

if lower level

set $k=k_{a2}$;

end if

sort and select the K-Best PEDs and discard the others

if leaves level is reached

exit;

else

go back to loop;

end if

end

For the first pair of cells, the two C parameters are calculated as

$$C_1 = \frac{min\,(H_{1,k}\ ,\ H_{1,k+1})}{max\,(H_{1,k}\ ,\ H_{1,k+1})}\ \&\ C_2 = \frac{min\,(H_{2,k}\ ,\ H_{2,k+1})}{max\,(H_{2,k}\ ,\ H_{2,k+1})}$$

where $H_{j,k}$ is the channel coefficient for j^{th} BS at the k^{th} subcarrier i.e. $C_1 = \frac{min\,(H_{11}\ ,\ H_{12})}{max\,(H_{11}\ ,\ H_{12})}\ \&\ C_2 = \frac{min\,(H_{21}\ ,\ H_{22})}{max\,(H_{21}\ ,\ H_{22})}$.

The two columns norms are calculated as

$$m_1 = \|\boldsymbol{H}(:,1)\| = \|[H_{11}\ H_{22}^*]^T\|,$$

$$m_2 = \|\boldsymbol{H}(:,2)\| = \|[-H_{21}\ H_{12}^*]^T\|.$$

Using the ideal channel $\mathbf{H}_{\text{ideal}} = \begin{bmatrix} 1 & -1 \\ 1 & 1 \end{bmatrix}$, we can calculate its ideal column norm $m_{ideal} = \|[1\ 1]^T\| = \|[-1\ 1]^T\| = 1.4142$ and use it with the defined threshold value δ to estimate the strength of the received symbol by defining two boundaries $m_{th1} = m_{\,ideal} + \delta$ and $m_{th2} = m_{\,ideal} - \delta$, and if m_1 or m_2 lies in-between these boundaries, the current signal strength is near the transmitted one and hence the channel has a small effect on it i.e. the channel is in good quality state, and if m_1 or m_2 lies outside these boundaries, the channel is in bad quality state and has significant effect on the transmitted signals. Therefore, if C_1 is greater than threshold Γ and $m_{th1} < m_i < m_{th2}$ then we search the upper level of the tree with a small K-value as the channel is most likely non-frequency selective or facing a small fading conditions and the symbol strength is high as well and if $C_1 < \Gamma$ and $m_{th1} < m_i < m_{th2}$ then the channel is somehow frequency selective but symbol strength is still high and hence an intermediate K-value is needed. Otherwise, a high K-value is required to compensate for the high selectivity of the channel and the symbol weakness. The same is done for the lower level of the tree search depending on the value of C_2.

The system model in Fig. 4.2 is simulated using16-QAM and 64-QAM modulation schemes under frequency selective fading channels between the BSs and the MS_1. The

model assumes perfect CSI at MS_1. Increasing the K-value passed to the KBSD increases its performance as shown in Fig. 4.4 in which different K-values are passed to the KBSD for the 16-QAM and 64-QAM modulation schemes and each higher K-value gives lower BER at the same SNR. The ML optimum detector was plotted as well. To clarify the performance-complexity trade-off, two BER values (at SNR = 15 dB and 21 dB) are plotted against the average number of visited nodes, i.e. VN, at different K-values for 16-QAM as shown in Fig. 4.5, where increasing the number of K-values increases the performance (decreases the BER curve) but increases the complexity (increases the average number of VN curve).

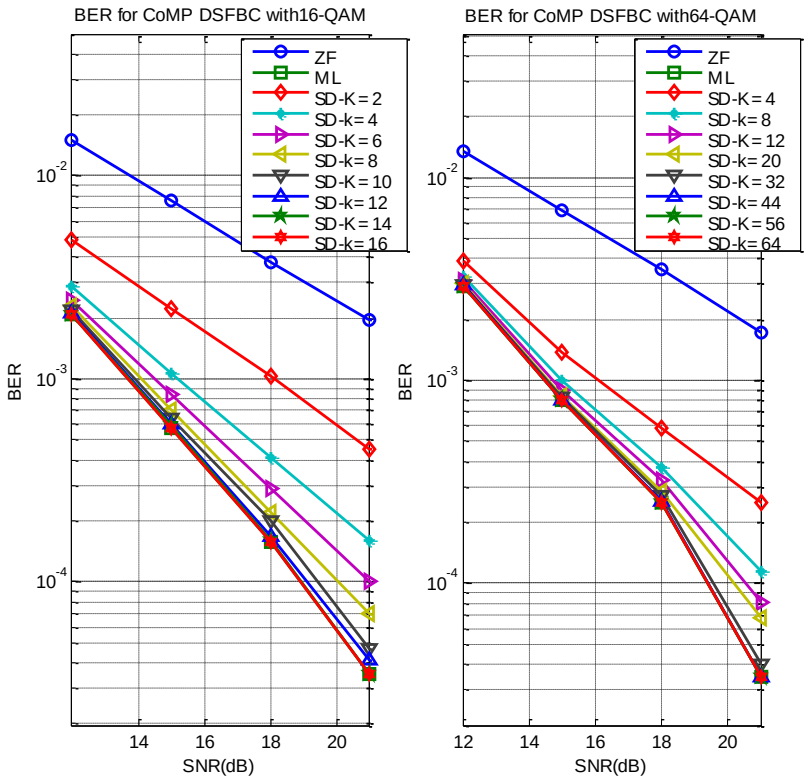

Figure 4.4: BER performance for different K-values of KBSD.

Using Γ=0.82 as a threshold value in the AKBSD and δ= 0.3, a comparison between the performance of two fixed K-values KBSD (with K=2, 16 for 16-QAM and K=4, 44 for 64-QAM) and the AKBSD is done as shown in Fig. 4.6. The lower and upper fixed K-values

are selected for comparison because they give the lower complexity and almost the ML performance respectively. The AKBSD gives a performance that is very near to the higher K-value KBSD in both the 16-QAM and 64-QAM modulation schemes. Measuring the complexity using the average number of VN in the tree during the search process of the various decoding algorithms and its results are summarized in table 4.1.

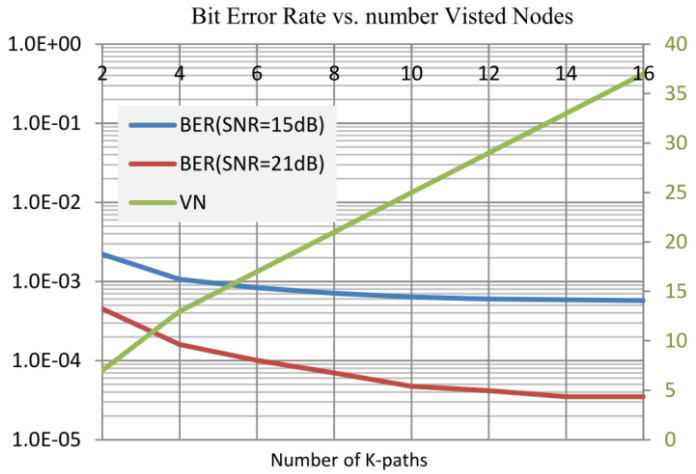

Figure 4.5: The trade-off between the performance (BER) and complexity (in terms of the number visited nodes) for 16-QAM.

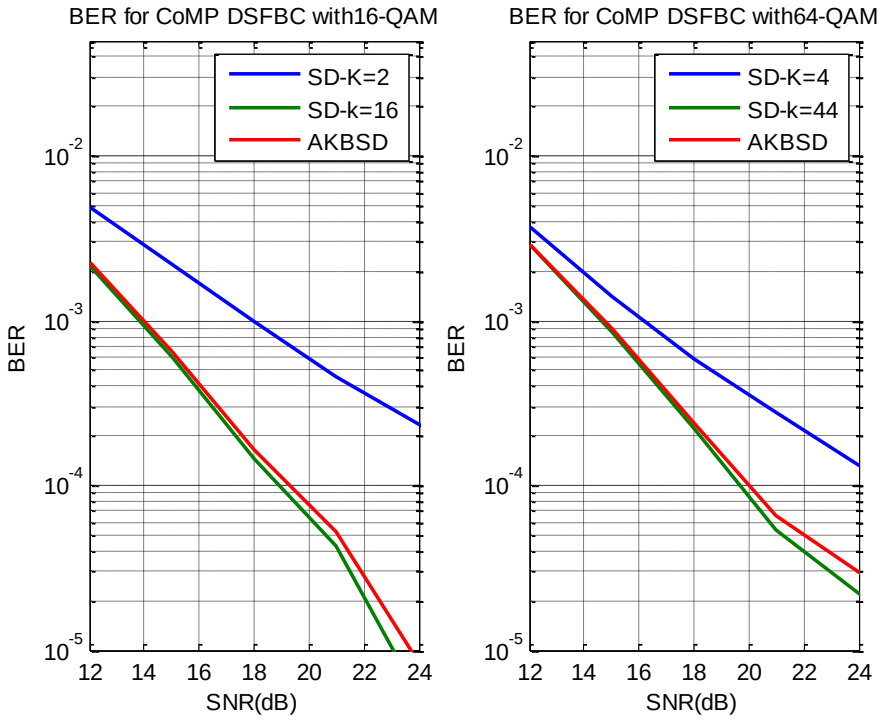

Figure 4.6: BER performance of AKBSD in CoMP system.

As shown in Fig. 4. 6 and table 4.1, the AKBSD requires much lower number of VN than ML and a considerable lower number than the higher K-value KBSD (K=16 for 16-QAM and K=44 for 64-QAM scheme) e.g. at a target BER of 10^{-4}, about 33.5 % reduction for the 64-QAM scheme and 18.9% for the 16-QAM scheme obtained with loss of performance of only 0.37 dB and 0.4 dB respectively. Therefore, the AKBSD in such a scenario can be used to offer coverage to the cell-edge user with lower complexity decoding which in its turn reduce the power consumption. This is especially valuable for handheld battery-based devices.

Table 4.1: Average Number of Visited Nodes

Decoding method	**# visited nodes**	
	16-QAM	**64-QAM**
KBSD(K_1)	(K_1=2) 7	(K_1=4) 26
KBSD(K_2)	(K_2=16) 37	(K_2=44)194
ML	85	1170
AKBSD(Γ=0.82)	30	129

4.2 Relay Assisted Networks

Cooperative networks play a major role in the current modern wireless and mobile cellular networks. By introducing a relay node between the two communicating points, i.e. the source and destination, they enhance the performance of the system by increasing the transmission data rate. This is achieved by making use of the cooperative diversity property, which removes the need for installing multiple antennas at the network nodes [49]-[54]. Cooperative networks can also be used to extend the network coverage area and reduce the transmit power [8]. This helps the nodes to communicate anywhere and anytime.

To utilize the cooperative network merits, cooperation protocols need to be

employed. Two main protocols have been widely adopted. The first is Amplify and Forward (AF) in which the received signal is amplified at the relay and then forwarded to the destination. The second relaying protocol is Detect or Decode and Forward (DF) in which the received signal is detected and then decoded and forwarded to the destination. DF gives better performance than the simpler AF scheme, a property that made DF the favorable relaying protocol for multi-hop system suffering from incremental loss of performance per hop [8]. However, DF requires more processing and consumes considerable resources at the relay. Hence, the relay consumed power is increased causing a problem in many cases, e.g. an idle mobile MIMO user may not choose to operate as a relay in DF mode due to its limited battery power.

4.2.1 Partial Detection

Partial Detection (PD) at the relay is a strategy that can reduce the complexity of the decoding process by detecting only part of the received signal then forwarding it. There are various parameters that determine the amount of the detected part e.g. received signal strength, available resources at the relay node… etc. Thereafter, the destination combines both the source signal and the partial relay signal to recover the transmitted signal [41].The PD has a major advantage when employing a mobile multi-antenna user as MIMO relays that can assist the current active links through their idle times. This saves much of the relay processing and transmit power while enhancing the performance compared to the non-relay case. Otherwise, PD performance is poor when the number of the detected symbols at the relay is small [8], [41]. The PD in [41] modifies the tree search of the tree-based sphere detector depending on the relay available resources to include only some levels of the tree instead of all tree levels in the case of Full Detect and Forward (FDF); we name this a change in the number of vertical levels in a tree search.

The partial sphere detection scheme proposed in [41] was employed for the spatial multiplexing transmission technique in a MIMO wireless communication. In this work, we utilize it for transmit antenna diversity techniques by employing the Alamouti and the Golden codewords in a time varying environment.

In this part, we propose a new idea that allows a change in the two dimensions of the tree during the tree traversal to give more complexity reduction at the relay node. The first dimension is the horizontal dimension, in which we change the number of the visited nodes per level depending on some criteria e.g. the channel quality. The second dimension is the vertical dimension in which the number of the explored tree levels is chosen depending on the source-relay link capacity, besides this change is adaptive depending on the current state of the network environment specifically the channel and link qualities in the network. The proposed detector, namely 2-D AKBSD, gives a considerable complexity reduction in the relay and also the destination nodes.

We consider the simple 3 nodes wireless network with one Source node (S) that cooperate with one Relay node (R) assisting in data transmission to one Destination node (D). The distance between the S and D nodes is denoted as d_{sd} while d_{sr} and d_{rd} define the distances between the S-R and R-D nodes respectively. Each node is equipped with N_t and N_r transmitting and receiving antennas respectively. Combinations of different numbers of N_t and N_r are studied to cover the SISO, MISO and MIMO transmission scenarios. However, the maximum number is chosen to be two for analysis simplicity and to meet the practical limitation of installing antennas in the network devices. The transmission is assumed to be executed over two phases T_1 and T_2. We assume half-duplex communication i.e. nodes can only transmit or receive at the same instance, and consider a Rayleigh time-varying fading channel, a case where linear decoding is no more the optimum decoding method as in the quasi-static channel case and more sophisticated decoding algorithms are required to obtain

a near optimum performance. We refer to the channels between S and D, S and R and R and D as $\mathbf{H_{sd}}$, $\mathbf{H_{sr}}$ and $\mathbf{H_{rd}}$ respectively and it is assumed that these channels are known in their corresponding receiving nodes while the SNRs at the nodes receiving antennas are defined as [41]:

$$SNR_{sd} = \frac{\mu p}{(d_{sd})^{\alpha}}, SNR_{sr} = \frac{\mu p}{(d_{sr})^{\alpha}}, SNR_{rd} = \frac{(1-\mu)p}{(d_{rd})^{\alpha}}$$

where p is the system total transmit power and is split among the source and relay nodes using the factor μ where 0 < μ < 1, while α is the path loss exponent and its value is usually chosen between 2 and 6. We employed the Alamouti and Golden codewords as the STBC for the transmit diversity technique at the transmitting node because of the decoding simplicity of the former and the FRFD property of the latter. The Alamouti (**X)** and the Golden (**S)** codewords are defined as:

$$\boldsymbol{X} = \begin{bmatrix} x_i & x_{i+1} \\ -x_{i+1}{}^{*} & x_i{}^{*} \end{bmatrix},$$

$$\boldsymbol{S} = \begin{bmatrix} \mathcal{S}_1 & \mathcal{S}_2 \\ \mathcal{S}_3 & \mathcal{S}_4 \end{bmatrix} = \frac{1}{\sqrt{5}} \begin{bmatrix} \alpha(x_i + x_{i+1}\theta) & \alpha(x_{i+2} + x_{i+3}\theta) \\ j\bar{\alpha}(x_{i+2} + x_{i+3}\bar{\theta}) & \bar{\alpha}(x_i + x_{i+1}\bar{\theta}) \end{bmatrix} \quad (4.1)$$

respectively where (.)* denote conjugate operation, x_i represents the i^{th} transmitted symbol, and $\theta, \bar{\theta}, \alpha$ and $\bar{\alpha}$ are as defined in (3.18). The system and the received signals model under different N_t and N_r scenarios can be modeled as follows.

A. 1×1 Nodes

The S, R, and D nodes are assumed to be equipped with single transmitting and receiving antenna in this scenario to cover the SISO case as shown in Fig. 4.7. The S node distributes the Alamouti codeword **X** over the two communication phases during four time slots (t_i, i=1:4) as

$$\overbrace{\underbrace{x_i}_{t_1}\ \underbrace{x_{i+1}}_{t_2}}^{T_1}\ \overbrace{\underbrace{-x_{i+1}{}^{*}}_{t_3}\ \underbrace{x_i{}^{*}}_{t_4}}^{T_2}$$

i.e. this communication protocol needs 4 channel uses to send 2 symbols giving a symbol rate of 0.5 symbol per channel use (symb. pcu).

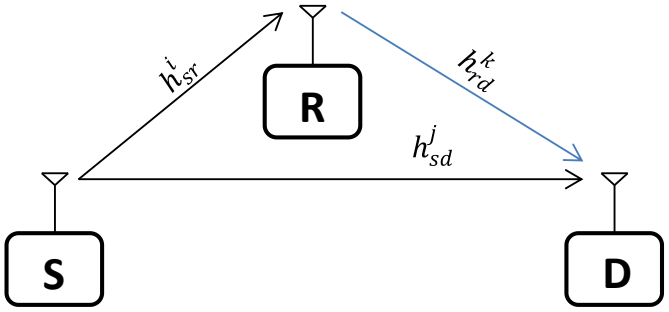

Figure 4.7: S-R-D network with 1×1 nodes.

The received signals at R and D nodes in the first two phases are

$$\begin{aligned}
&\textbf{R:} \quad \mathrm{T}_1 \begin{cases} y_r^1 = h_{sr}^1 x_1 + n_1 \\ y_r^2 = h_{sr}^2 x_2 + n_2 \end{cases} \\
&\textbf{D:} \quad \mathrm{T}_1 \begin{cases} y_d^1 = h_{sd}^1 x_1 + v_1 \\ y_d^2 = h_{sd}^2 x_2 + v_2 \end{cases} \\
&\qquad\quad \mathrm{T}_2 \begin{cases} y_d^3 = -h_{sd}^3 x_2{}^* + h_{rd}^3 \hat{x}_1 + w_1 \\ y_d^4 = h_{sd}^4 x_1{}^* + h_{rd}^4 \hat{x}_2 + w_2 \end{cases}
\end{aligned} \tag{4.2}$$

where y_r^i and y_d^j are the received signals at the time instances *i* and *j* for the R and D nodes respectively, while h_{sd}^j, h_{sr}^i and h_{rd}^k are the coefficients for channels between S and D at time *j*, S and R at time *i*, and R and D at time *k*, respectively, and n_i, v_i and w_i are AWGN and i=1,2, j=1:4 and k =3,4. Using ZF detection in the R node to detect x_i and assuming a successful detection with FDF cooperation strategy i.e. $\hat{x}_i = x_i$, we can combine the two phases signals at the D node as:

$$\begin{cases} y_{d_1}^t = (h_{sd}^1 + h_{rd}^3)\, x_1 - h_{sd}^3 x_2{}^* + \psi_1 \\ y_{d_2}^t = h_{sd}^4 x_1{}^* + (h_{sd}^2 + h_{rd}^4)\, x_2 + \psi_2 \end{cases} \tag{4.3}$$

where ψ_i is the total AWGN noise at the i^{th} phase.

B. 2×1 Nodes

In this scenario the nodes are equipped with two transmit antennas and one receive antenna as shown in Fig. 4.8, and it is assumed that R node uses the Alamouti codeword **X** in its transmission during the second phase of communication. Transmission from S and R

nodes through the four time instants frame of T_1 and T_2 is described as

$$
\begin{array}{cccccccc}
\multicolumn{8}{c}{T_1} \\
\multicolumn{4}{c}{t_1} & \multicolumn{4}{c}{t_2} \\
\multicolumn{2}{c}{S} & \multicolumn{2}{c}{R} & \multicolumn{2}{c}{S} & \multicolumn{2}{c}{R} \\
\underbrace{x_i}_{tx_1} & \underbrace{-x_{i+1}^*}_{tx_2} & \underbrace{0}_{tx_1} & \underbrace{0}_{tx_2} & \underbrace{x_{i+1}}_{tx_1} & \underbrace{x_i^*}_{tx_2} & \underbrace{0}_{tx_1} & \underbrace{0}_{tx_2} \\
\multicolumn{8}{c}{T_2} \\
\multicolumn{4}{c}{t_3} & \multicolumn{4}{c}{t_4} \\
\multicolumn{2}{c}{S} & \multicolumn{2}{c}{R} & \multicolumn{2}{c}{S} & \multicolumn{2}{c}{R} \\
\underbrace{0}_{tx_1} & \underbrace{0}_{tx_2} & \underbrace{\hat{x}_i}_{tx_1} & \underbrace{-\hat{x}_{i+1}^*}_{tx_2} & \underbrace{0}_{tx_1} & \underbrace{0}_{tx_2} & \underbrace{\hat{x}_{i+1}}_{tx_1} & \underbrace{\hat{x}_{i+1}^*}_{tx_2}
\end{array}
$$

where tx_1 and tx_2 are the 1st and 2nd transmitting antenna of S or R node. This communication protocol also needs 4 channel uses to send 2 symbols giving a symbol rate of 0.5 symb. pcu.

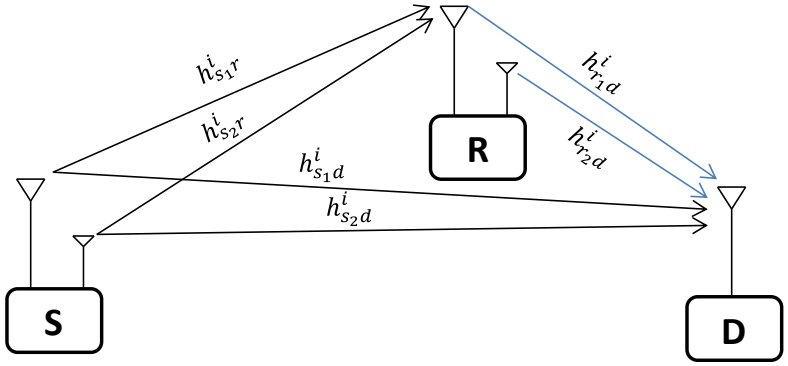

Figure 4.8: S-R-D network with 2×1 nodes.

As shown in 4.8 and assuming the sending node is transmitting a MISO 2×1 Alamouti diversity code, the relay node and the single antenna destination node receive the source signal using one antenna. This means that the relay uses only one antenna for the reception of the source data while the other antenna is idle or off. In the transmission phase, the relay uses its two antennas to transmit the 2×1 signal to the destination node in the relaying phase.

The received signals at R and D nodes in the first two phases are:

R: $$T_1 \begin{cases} y_r^1 = h_{s_1r}^1 x_1 - h_{s_2r}^1 x_2^* + n_1 \\ y_r^2 = h_{s_1r}^2 x_2 + h_{s_2r}^2 x_1^* + n_2 \end{cases}$$

$$\mathbf{D:}\qquad \mathrm{T}_1\begin{cases} y_d^1 = h_{s_1d}^1 x_1 - h_{s_2d}^1 x_2^* + v_1 \\ y_d^2 = h_{s_1d}^2 x_2 + h_{s_2d}^2 x_1^* + v_2 \end{cases}$$
$$\mathrm{T}_2\begin{cases} y_d^3 = h_{r_1d}^1 \hat{x}_1 - h_{r_2d}^1 \hat{x}_2^* + w_1 \\ y_d^4 = h_{r_1d}^2 \hat{x}_2 + h_{r_2d}^2 \hat{x}_1^* + w_2 \end{cases} \tag{4.4}$$

where $h_{s_kd}^i$, $h_{s_kr}^i$ and $h_{r_kd}^i$ are the i^{th} coefficients of the channels between the k^{th} transmitting and the receiving antenna between S and D, S and R and R and D respectively. Assuming $\hat{x}_i = x_i$, the combined two phases signals at the D node are:

$$\begin{cases} y_{d_1}^t = (h_{s_1d}^1 + h_{r_1d}) x_1 - (h_{s_2d}^1 + h_{r_2d}^1) x_2^* + \psi_1 \\ y_{d_2}^t = (h_{s_2d}^2 + h_{r_2d}^2) x_1^* + (h_{s_1d}^2 + h_{r_1d}^2) x_2 + \psi_2 \end{cases} \tag{4.5}$$

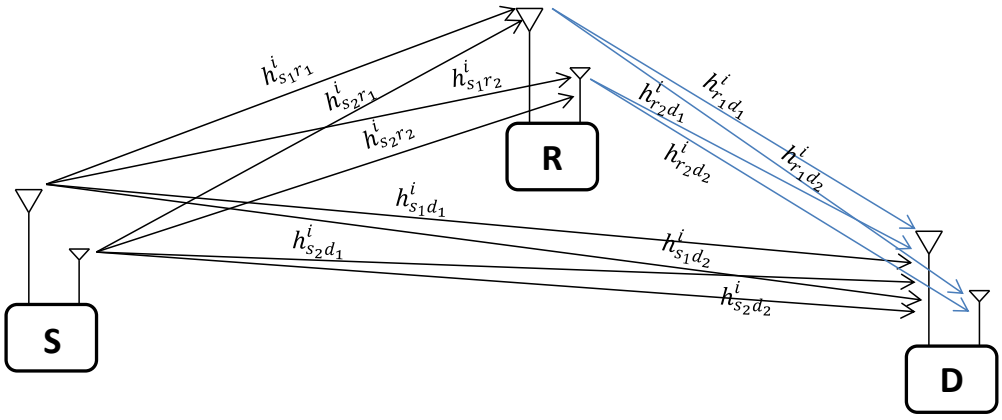

Figure 4.9: S-R-D network with 2×2 nodes.

C. 2×2 Nodes

All the network nodes are assumed to use two antennas for both transmitting and receive to each other as shown in Fig. 4.9, and the S and R nodes use the Golden codeword **S** during the transmission with the same protocol as in the 2×1 nodes scenario and by replacing each element in **X** by its equivalent in **S** e.g. replace x_i^* by $s_4 = \frac{1}{\sqrt{5}}\bar{\alpha}(x_i + x_{i+1}\bar{\theta})$ and so on. Following the same analysis in the previous scenarios, we have four received signals at each phase (instead of two in (4.2) and (4.4)) as can be transpired from Fig. 4.9 and the general form of the received signal duringT_1 at the R node is:

$$y_{rj}^i = \sum_{\substack{i=1,2 \\ j=1,2}} h_{s_1r_j}^i s_i + h_{s_2r_j}^i s_{i+2} + n_i \tag{4.6}$$

while the total received signals duringT_1 andT_2 at the D node (assuming $\hat{s}_i = s_i$) are:

$$y_{td_j}^i = \sum_{\substack{i=1,2 \\ j=1,2}} (h_{s_1 d_j}^i + h_{r_1 d_j}^i) s_i + (h_{s_2 d_j}^i + h_{r_2 d_j}^i) s_{i+2} + \psi_i \quad (4.7)$$

4.2.2 2-D AKBSD

AKBSD employing previous proposed methods, i.e. (M_1-M_4), is a solution for finding the optimum K value that best suits the varying conditions of the channel. This type of adaptation is performed over the horizontal level in the tree search to achieve the best trade-off between performance and complexity. In relay networks, another dimension of adaptation can be used within the KBSD search strategy in which a partial detection is performed to partition the detection task between the R and D nodes, this partial detection employs the adaptation over the vertical levels of the tree depending on the available resources in the R node to reduce the overhead introduced by the MIMO relay.

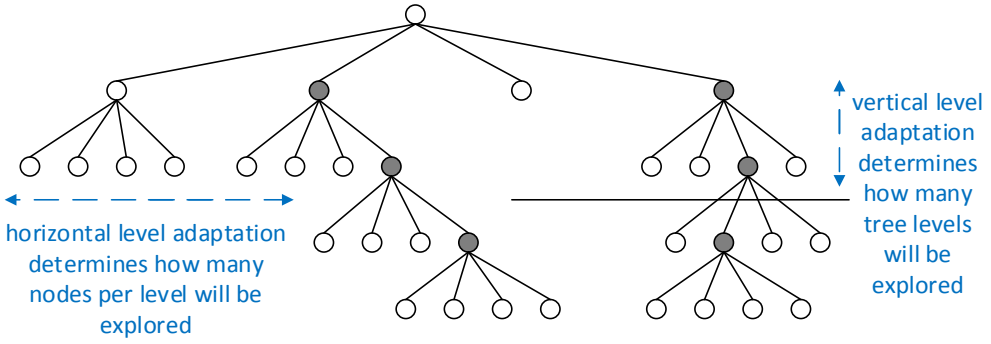

Figure 4.10: Tree structure for 2-D AKBSD shows the horizontal and vertical adaptation.

The 2-D AKBSD makes use of the two vertical and horizontal dimensions of the adaptation process in the R node to suit the dynamic operating conditions of the network. As shown in Fig. 4.10, some criteria specify how many tree levels are explored and how many nodes per level are visited while traversing the tree. While adaptation criterion in horizontal dimension can be selectivity of the channel or channel matrix analysis as measures of the channel quality i.e. selecting small or big K value depends on the quality of the channel or an

estimation of SNR value, the vertical dimension adaptation can be done based on criteria such as available resources in the relay as in [41], received signal strength or the instantaneous capacity measurement as a measure of the S-R link outage. We select the channel selectivity as a channel quality estimation method and the instantaneous capacity measurement as the adaptation criteria for the horizontal and vertical dimensions respectively. To measure the channel selectivity, we calculate the *C* parameter by (3.3). If C_i is greater than a defined threshold Γ then the channel is very frequency selective and hence the channel quality is good and vice versa. The instantaneous capacity can be used as the metric that indicate the channel state information as a measure for the S-R link quality and can be calculated as [12]:

$$C_{ap} = \log_2 det\ (\boldsymbol{I}_{N_r} + \frac{E_x}{N_t N_0} \boldsymbol{H}_{sr} \boldsymbol{H}_{sr}^H) \tag{4.8}$$

where E_x is the transmitted signal energy and N_0 is the noise power spectral density.

The 2-D AKBSD adds a pre-process part over the regular KBSD and hence it has the advantages of the KBSD, besides the advantage of being adapted based on the system dynamic conditions.

The algorithm of the 2-D AKBSD for the 2×2 scenario case is shown in Fig. 4.11. We have 4 channels between each two nodes as shown in Fig. 4.9. Working on a block of four symbols $\mathrm{x_m : x_{m+3}}, \mathrm{m} = 1{:}\,4{:}\,\mathrm{N_s}$, we calculate four $\mathrm{C_i}$ parameters, $\mathrm{i} = 1{:}\,4$, using the four instantaneous 2×2 channel coefficients and their consecutives between the different nodes, then check the obtained C values against the predefined threshold value Γ. If all the four C values are greater than Γ, then all the channels are non-frequency selective and we are in a first mode of operation where channels are assumed to be in good state and so we define a small value, $\mathrm{K_1}$, to be passed to the KBSD. While if three C values are greater than

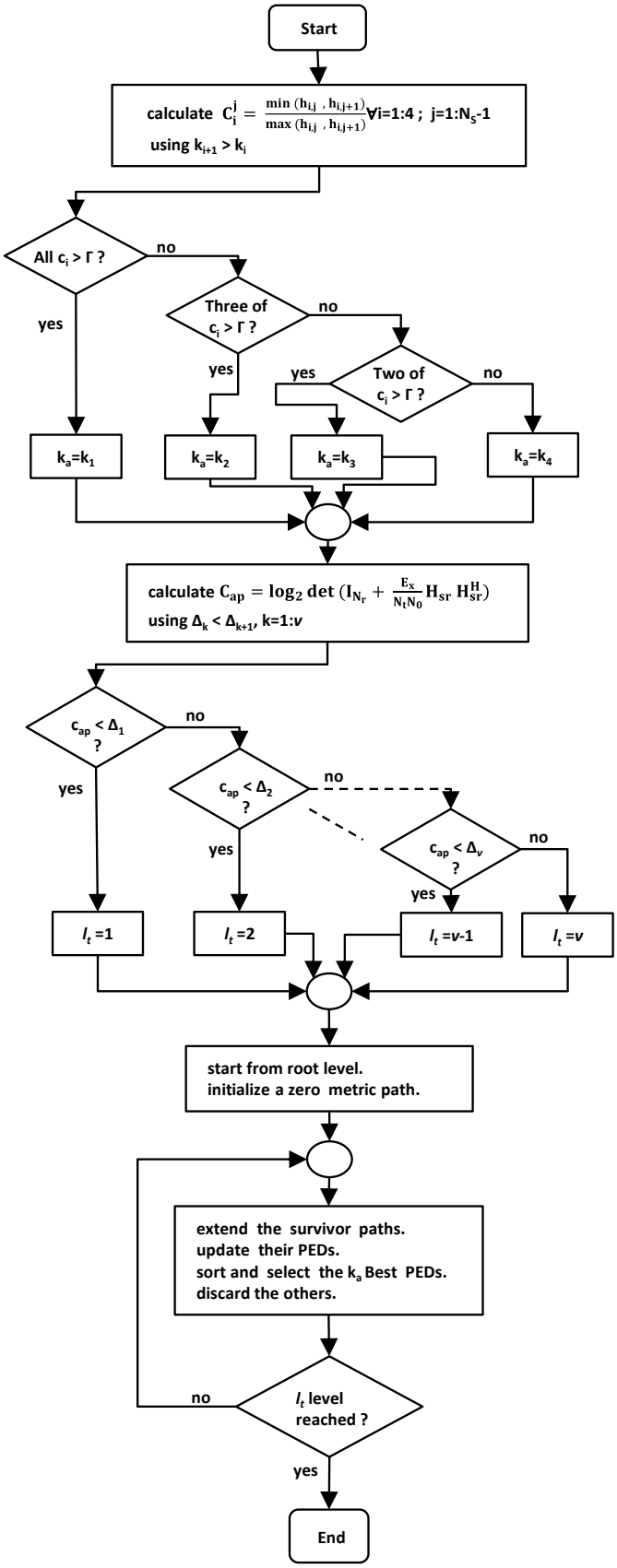

Figure 4.11: 2-D AKBSD flowchart.

the Γ, then the corresponding three channels are non-frequency selective and are in good state and a second mode of operation is activated defining a bigger value, $K_2 > K_1$and so on. This is the horizontal adaptation that determines the number of K-paths that the decoder will consider while searching the tree, in other words, here we determine how many nodes per level will be visited.

The link capacity is then calculated as a measure of the link quality using (4.8). The capacity range is divided into *v* regions (determined using numerical analysis as the case of determining the threshold value Γ) and the instantaneous capacity value is checked to know where it lies among these regions, and if it lies in the first region that's mean the capacity is low and the link quality is bad, so the relay is not sure of the received symbols correctness and hence we define a small value for the l_t that determine only one level to be explored i.e. one symbol only will be detected and relayed to the other stage to save extra computations for detection of uncertain symbols. If the instantaneous capacity value is in the second region, the relay detects two symbols and so on. This is the vertical adaptation in which we define how many levels will be explored according to the link quality between the nodes. After determining how many levels will be explored and how many nodes per level will be visited, the regular KBSD operations continue i.e. initializing a zero metric path then extend the survivor paths and calculate their PEDs, then sorting them and select the defined K-paths (number of nodes per level) and discard the others and continue until we reach the defined level before then output the obtained symbols to be relayed to the next node.

1×1 nodes detection strategy

For conventional FDF, the R node performs full detection of all the symbols using ZF then forwards those symbols to the D node during T_2 then the D node uses regular KBSD (with a sufficient K value to achieve a near ML performance) to detect the combined

transmitted signals during the two phases. On the other hand, in the case of PD, the R node performs ZF but to detect half of the transmitted symbols sent by the source and in the second phase, R transmits the detected signals to the D node which uses 2-D AKBSD with horizontal adaptation only to retrieve the original signals.

2×1 & 2×2 nodes detection strategy

For conventional FDF, both R and D nodes perform full detection of all the symbols using regular KBSD while for PD, the R node applies the 2-D AKBSD to detect part of the transmitted symbols, this part is determined based on the S-R link capacity, and in T_2, R transmits the detected part of the signals to the D node which retrieve the transmitted signals in the same manner as 1×1 node scenario.

Phase	T_1		T_2
Time Slot	t_1	t_2	t_3
Transmit Node	S	S	R
tx_1	x_i	x_{i+1}	$\hat{x}_i$
tx_2	$-x_{i+1}^*$	x_i^*	—

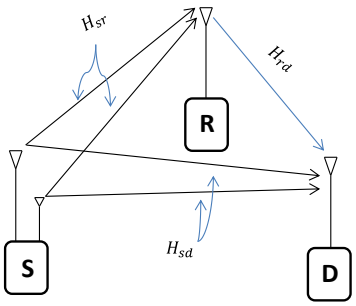

Figure 4.12: Single antenna relay in 2×1 MISO protocol.

Single antenna relay in MISO environment

A major advantage of the partial sphere detection is using a single antenna relay in a MISO transmission, using the codeword sent from the S node, R node can make horizontal adaptation and fix the vertical levels traversing to the half of the tree levels to send only half the symbols by its single antenna. This is a hybrid protocol of the 1×1 and 2×1 nodes scenarios. In this manner, we can make use of an idle single antenna device to assist in data transmission in a 2×1 MISO protocol as shown in Fig. 4.12. This raises the constraints of only involving multiple antennas relays in the transmission. Moreover, this increases the

data rate as we need only 3 channel uses instead of 4 giving symbol rate of 2/3 symb. pcu.

We suppose half-duplex communication in a 3 node wireless relay network topology with different scenarios as shown in Figs. 4.6 to 4.8. For all scenarios, we assume that the R node is in-between the S and D nodes with $d_{sd} = d_{sr} + d_{rd} = 1$, fixing $d_{sr} = 0.35$, and also we used fixed values of $\alpha = 3$, $\mu = 0.6$ and $p = 1$. We also work on 16-QAM modulation scheme and assumed that $\mathbf{H_{sd}}$, $\mathbf{H_{sr}}$ and $\mathbf{H_{rd}}$ are Rayleigh time-varying fading channels i.e. their coefficients are not constant during the transmission of the codeword elements as in the case of quasi-static channels. Monte Carlo simulations are used to calculate the BER values for different scenarios in the R and D nodes besides calculating the complexity of FDF and 2-D AKBSD or PD decoding algorithms in terms of average number of visited nodes.

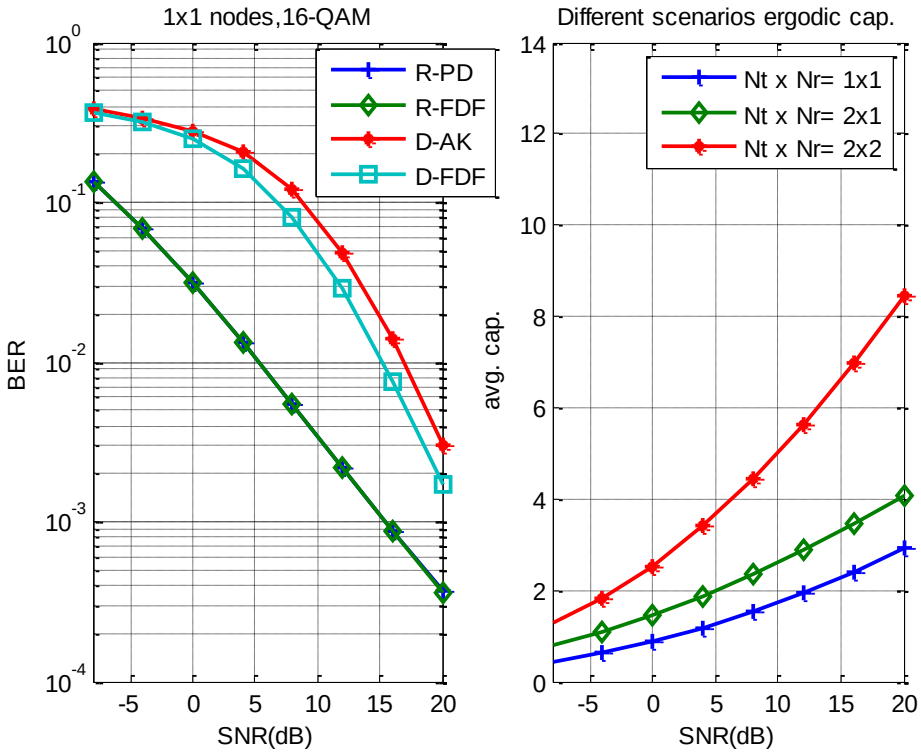

Figure 4.13: BER performance for 1×1 node for PD and FDF strategies at R and D nodes (left) and mean value of the instantaneous ergodic capacities of the S-R link for different scenarios (right).

The left part of Fig. 4.13 shows the BER performance of the 1×1 scenario for the FDF and PD detection strategies at R and D nodes. R-PD and R-FDF represent the ZF

detection of half and full symbols detection of the transmitted symbols respectively at the relay node and they give the same BER. While D-AK and D-FDF represent the detection of both partial and full detection cases using the AKBSD with horizontal adaptation only, the AK shows a near FDF performance with a loss of 1.7 dB at BER of 10^{-4}. The mean values of the instantaneous capacity for the different scenarios are plotted in the right part of Fig. 4.13 where its immediate value is used to be checked against a threshold value and as a result a suitable number of levels of the vertical adaptation is selected as illustrated in the algorithm before. The threshold values Δ and Γ are chosen based on numerical analysis and their values are Δ= 3.5 for 2×1 nodes and Δ_i= 1.5, 5 and 10 for 2×2 nodes while Γ= 0.82 for both scenarios as it doesn't depend on the number of detected symbols and hence the scenario.

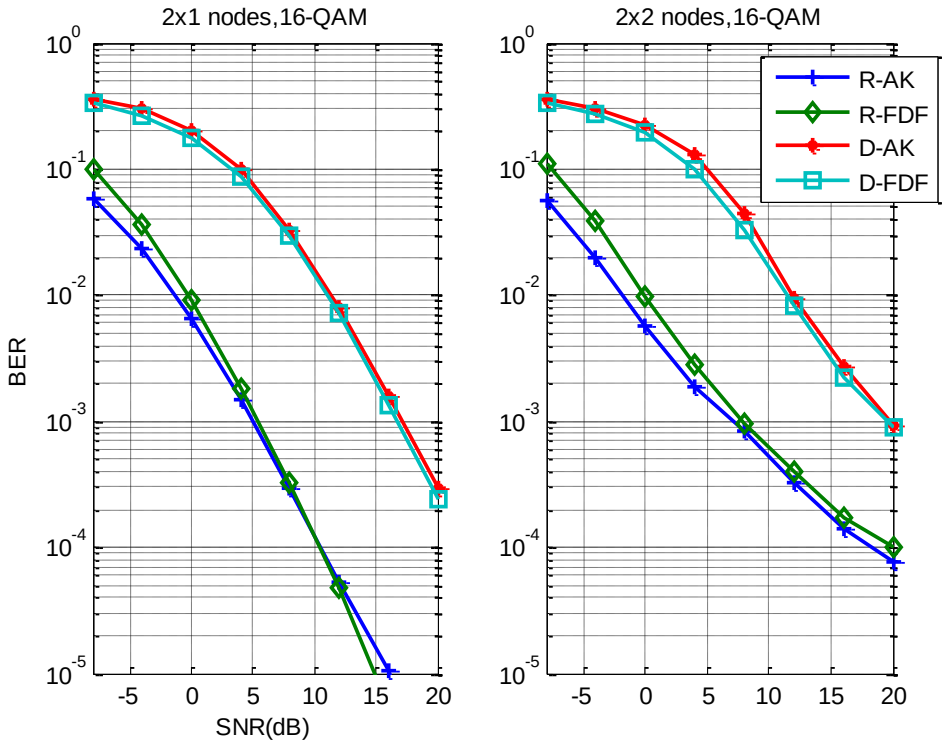

Figure 4.14: BER performance for 2×1(left) and 2×2 (right) nodes for 2DAKBSD and FDF detection strategies at R and D nodes.

Figure 4.14 shows the BER performance of the 2×1 scenario (left) and the 2×2 scenario (right) for the FDF and 2-D AKBSD detection strategies at R and D nodes. PD

using 2-D AKBSD shows a near FDF performance with a maximum loss of 0.47 and 1.2 dB all over the BER/SNR asymptotes. From Fig. 4.12 and Fig. 4.13, the worst asymptotic loss in performance for 1×1 nodes scenario is 1.8 dB while in 2×1 and 2×2 scenarios is 0.47 and 1.2 dB respectively.

Complexity of each detection strategy of FDF and 2-D AKBSD for the different scenarios is calculated in terms of average number of visited nodes for the tree based detection and in terms of execution time for ZF detection (only used in the 1×1 scenario at the relay) and is summarized with the reduction percentage in R and D nodes in table 4.2. The range of reduction is 22.2 - 24.3 % at the D node while at the R node is 24.4 - 50 % which gives a system reduction at both the R and D together of 23.3 - 40.6 %. This computation complexity reduction is in turn a power reduction with the same percentage in the network devices consumed power.

TABLE 4.2: COMPLEXITY MEASUREMENT

$N_t \times N_r$	FDF	2-D AKBSD			
	(R & D nodes)	R node	% reduction	D node	% reduction
1×1	(0.1e-6) & 37	(0.5e-7)	50 %	28	24.3 %
2×1	37	27.97	24.4 %	28.8	22.2 %
2×2	458	194.61	57.5 %	349	23.8 %

4.2.2 Hybrid Partial and Full Detection Protocol for Multi-Hop networks

In this section, we propose a new hybrid protocol, Hybrid Partial and Full Detection (HPFD), for multi-hop wireless networks that makes use of both full and partial detection strategies to solve the problem of the incremental loss of performance per hop with low computational decoding method. The full detection strategy employs the AKBSD with adaptation in the horizontal dimension while the partial detection strategy employs the 2-D

AKBSD, with the adaptation on the two dimensions of the tree, to take the benefits of not losing much performance while achieving low complexity at the relay nodes and the destination node as well.

We consider *n+2* nodes wireless network, as shown in Fig. 4.15, with S node that cooperates with *n* relay nodes assisting in data transmission to D node and each node is equipped with N_t=*2* and N_r=*2*. The transmission of each stage is assumed to be executed over two phases T_1 and T_2. We assume half-duplex communication i.e. nodes can only transmit or receive at the same instance. We also consider a Rayleigh time-varying fading channel. We assume also that the channels between each linked nodes are known in the corresponding receiving node.

We employ the Golden codeword as STBC for the transmit diversity technique at the transmitting node to make use of its FRFD property. N_s data symbols $x_i \in \mathbb{C}, i = 1{:}N_s$ are sent using the Golden codeword (**S)** defined in (4.1). For simplicity and ease of analysis, a case study of 4-hops network is discussed in the following section.

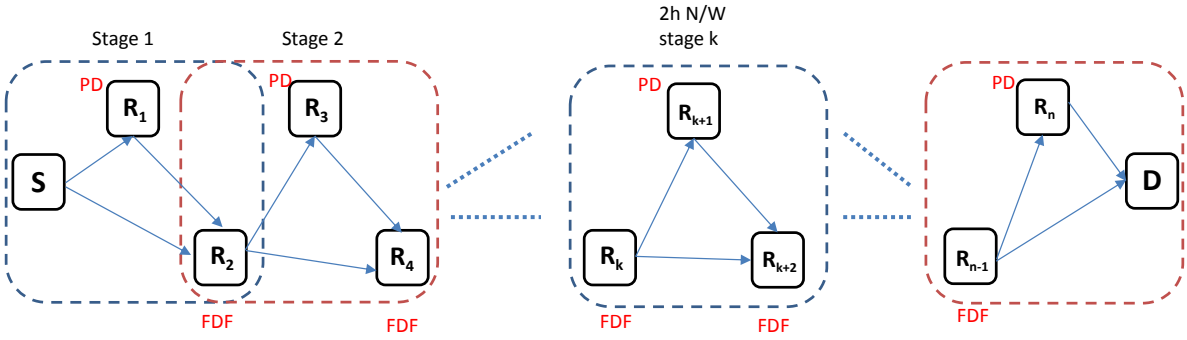

Figure 4.15: n+1 hop wireless relay network.

4-hops network case study

We consider a 4-hops, 5 nodes wireless network with a single source, single destination and 3 relay nodes. We divide the network into two stages; the first one consists of 3 nodes, namely S, R_1 and R_2 while the second stage consists of the R_2, R_3 and D nodes as

shown in Fig. 4.16. The transmitting nodes distribute the Golden codeword **S** over the four communication phases T_1, T_2, T_3 and T_4 as

$$
\begin{array}{c}
T_1 \\
\overbrace{\underbrace{s_1}_{tx_1}\ \underbrace{s_2}_{tx_2}}^{S}\ \overbrace{\underbrace{0}_{tx_1}\ \underbrace{0}_{tx_2}}^{R_1}\ \overbrace{\underbrace{s_3}_{tx_1}\ \underbrace{s_4}_{tx_2}}^{S}\ \overbrace{\underbrace{0}_{tx_1}\ \underbrace{0}_{tx_2}}^{R_1} \\
T_2 \\
\overbrace{\underbrace{0}_{tx_1}\ \underbrace{0}_{tx_2}}^{S}\ \overbrace{\underbrace{\hat{s}_1}_{tx_1}\ \underbrace{\hat{s}_2}_{tx_2}}^{R_1}\ \overbrace{\underbrace{0}_{tx_1}\ \underbrace{0}_{tx_2}}^{S}\ \overbrace{\underbrace{\hat{s}_3}_{tx_1}\ \underbrace{\hat{s}_4}_{tx_2}}^{R_1} \\
T_3 \\
\overbrace{\underbrace{\hat{\hat{s}}_1}_{tx_1}\ \underbrace{\hat{\hat{s}}_2}_{tx_2}}^{R_2}\ \overbrace{\underbrace{0}_{tx_1}\ \underbrace{0}_{tx_2}}^{R_3}\ \overbrace{\underbrace{\hat{\hat{s}}_3}_{tx_1}\ \underbrace{\hat{\hat{s}}_4}_{tx_2}}^{R_2}\ \overbrace{\underbrace{0}_{tx_1}\ \underbrace{0}_{tx_2}}^{R_3} \\
T_4 \\
\overbrace{\underbrace{0}_{tx_1}\ \underbrace{0}_{tx_2}}^{R_2}\ \overbrace{\underbrace{\hat{\hat{\hat{s}}}_1}_{tx_1}\ \underbrace{\hat{\hat{\hat{s}}}_2}_{tx_2}}^{R_3}\ \overbrace{\underbrace{0}_{tx_1}\ \underbrace{0}_{tx_2}}^{R_2}\ \overbrace{\underbrace{\hat{\hat{\hat{s}}}_3}_{tx_1}\ \underbrace{\hat{\hat{\hat{s}}}_4}_{tx_2}}^{R_3}.
\end{array}
$$

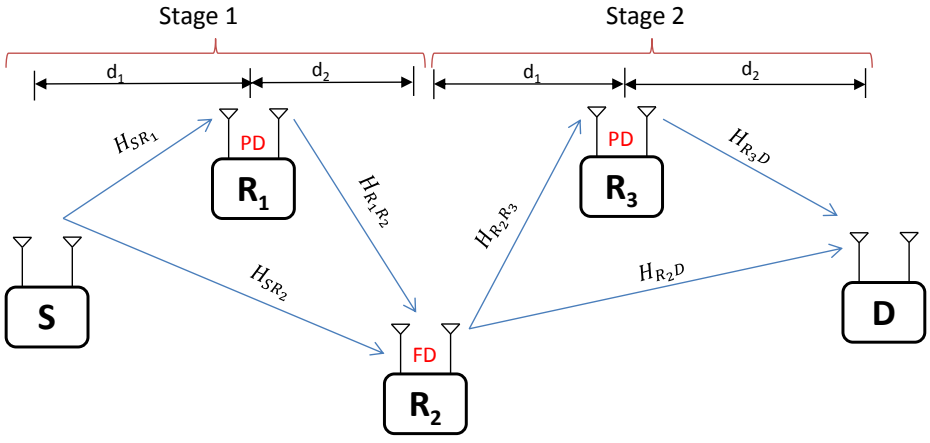

Figure 4.16: 4-hops wireless relay network with 2×2 nodes.

The general channels used between the nodes in each phase are 2×2 channels and denoted as

T_1: H_{SR_1} and H_{SR_2}

T_2: $H_{R_1R_2}$

T_3: $H_{R_2R_3}$ and H_{R_2D}

T_4: H_{R_3D}

and the detailed channels between the nodes in the first stage are shown in Fig. 4.17, where $h^i_{s_j r_{kj}}$ is the channel coefficient between the j^{th} transmit antenna of the S node and the j^{th} receive antenna of the k^{th} relay at time instant i while $h^i_{r_{kj} r_{k+1\,j}}$ is the channel coefficient between the j^{th} transmit and receive antennas of the corresponding k^{th} relay at time instant i and j=1,2.

The received signals at R_1 node in the first phase are:

$$T_1 \begin{cases} y^1_{r1} = h^1_{s_1 r_{11}} s_1 + h^1_{s_2 r_{11}} s_3 + n_1 \\ y^1_{r2} = h^1_{s_1 r_{12}} s_1 + h^1_{s_2 r_{12}} s_3 + n_2 \\ y^2_{r1} = h^2_{s_1 r_{11}} s_2 + h^2_{s_2 r_{11}} s_4 + n_3 \\ y^2_{r2} = h^2_{s_1 r_{12}} s_2 + h^2_{s_2 r_{12}} s_4 + n_4 \end{cases} \tag{4.9}$$

where y^i_{rj} is the received signal component at the j^{th} receiving antenna of R_1 at a time instant i, the $h^i_{s_j r_{kj}}$ is as defined before and n_i is AWGN and i and j=1,2.

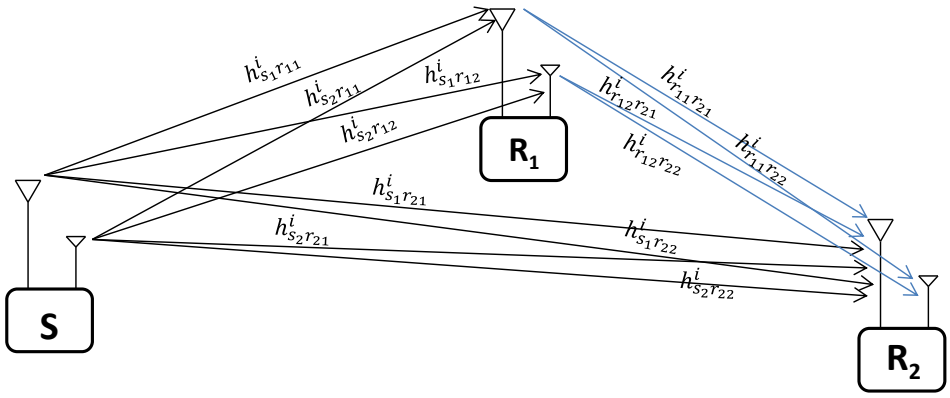

Figure 4.17: Channels between the nodes in the 1st stage

The general form of the received signal duringT_1 at the R_1 node is:

$$y^i_{rj} = \sum_{\substack{i=1,2 \\ j=1,2}} h^i_{s_1 r_{1j}} s_i + h^i_{s_2 r_{1j}} s_{i+2} + n_i \tag{4.10}$$

while the total received signals duringT_1 andT_2 at the R_2 node (assuming $\hat{s}_i = s_i$) are:

$$y^i_{tr_j} = \sum_{\substack{i=1,2 \\ j=1,2}} (h^i_{s_1 r_{2j}} + h^i_{r_{11} r_{2j}}) s_i + (h^i_{s_2 r_{2j}} + h^i_{r_{12} r_{2j}}) s_{i+2} + \psi_i \tag{4.11}$$

where ψ_i is the total AWGN noise at the i^{th} phase.

For the second stage, the received signal during T_3 at the R_3 node (assuming $\hat{\hat{s}}_i = \hat{s}_i$) is:

$$y_{rj}^{i+2} = \sum_{\substack{i=1,2 \\ j=1,2}} h_{r_{21}r_{3j}}^{i+2} s_i + h_{r_{22}r_{3j}}^{i+2} s_{i+2} + n_i \quad (4.12)$$

while the total received signals duringT_3 andT_4 at the D node (assuming $\hat{\hat{s}}_i = \hat{\hat{s}}_i$) are:

$$y_{tr_j}^{i+2} = \sum_{\substack{i=1,2 \\ j=1,2}} (h_{r_{21}d_j}^{i+2} + h_{r_{31}d_j}^{i+2}) s_i + (h_{r_{22}d_j}^{i+2} + h_{r_{32}d_j}^{i+2}) s_{i+2} + \psi_i \quad (4.13)$$

In each stage, the first node (S in stage 1 and R_2 in stage 2) sends the data to the other nodes in two time slots within a communication phase T. The two intermediate relays (R_1 in stage 1and R_3 in stage 2) performs PD and relays the detected symbols to the next nodes in the next communication phase. Finally, the nodes (R_2 in stage 1and D in stage 2) perform full detection to restore the transmitted data. The nodes perform PD using a 2-D AKBSD which adapts the number of traversed levels through the tree as well as the number of visited nodes per each level.

We assume that the R nodes that perform PD is in-between the two extreme nodes of each stage with $d_1 + d_2 = 1$ as in Fig. 4.16, using fixed $d_1 = 0.35$, and also we calculate the SNRs at the first stage nodes (similarly in the second stages) receiving antennas as [41]

$$SNR_{sr_1} = \frac{\mu p}{(d_1)^\alpha}, SNR_{sr_2} = \frac{\mu p}{(d_1+d_2)^\alpha}, SNR_{r_1 r_2} = \frac{(1-\mu)p}{(d_2)^\alpha}$$

We consider the 16-QAM modulation scheme and assumed that the channels between each two nodes are Rayleigh time-varying fading channels. Monte Carlo simulations are used to calculate the BER values in the D node for a FDF protocol between all the nodes and the HPFD protocol besides calculating the complexity of FDF, AKBSD and 2-D AKBSD decoding algorithms in terms of the average number of visited nodes.

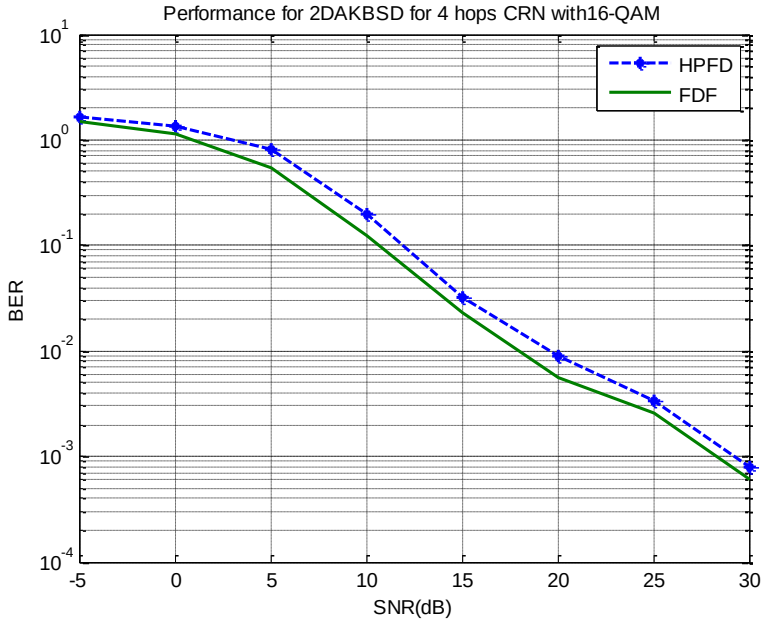

Figure 4.18: BER performance for the two protocols using 16-QAM.

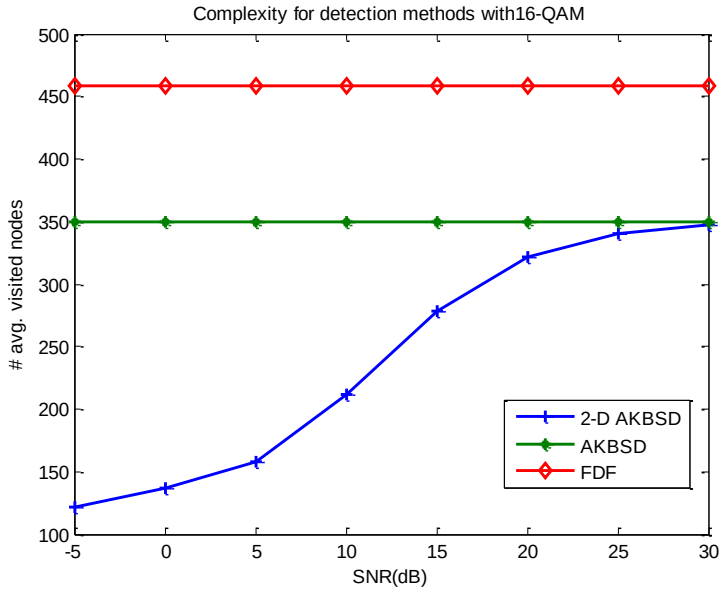

Figure 4.19: Complexity measurement for the different detection methods.

The mean values of the instantaneous capacity are used to be checked against a threshold value and as a result a suitable number of levels of the vertical adaptation is selected. The threshold values Δ and Γ were chosen based on numerical analysis and their values are Δ_i= 1.5, 5 and 10 while Γ= 0.82. Figure 4.18 shows the BER performance of the two protocols, the hybrid HPFD protocol and the conventional FDF one. The worst

performance of the HPFD protocol is 1.8 dB behind the FDF protocol among all the BER asymptotes.

Figure 4.19 shows the complexity measurement in terms of average number of visited nodes for the three decoding methods used in the FDF and HPFD protocols, the first one is AKBSD where we use only horizontal adaptation over the tree and used in the destination or the nodes which perform FD i.e. R_2 and D in the 4-hop network. The second is 2-D AKBSD which perform double adaptation on the tree and used in the relay nodes which perform partial detection i.e. R_1 and R_3 in the 4-hop network. The last method is FDF where fixed number of K (chosen to give a maximum likelihood performance) is used in a regular KBSD in the FDF protocol. The HPFD protocol gives a 57.5% complexity reduction in the relay nodes that perform PD and 23.9% reduction in the nodes that perform FD. The overall network decoding complexity reduction is 40.7% over the regular FDF protocol; this computational reduction in turn reduces the consumed power by the network nodes which makes the FDF a suitable protocol in dense networks and devices with limited power resources.

4.3 Summary

In this chapter, we illustrated the application of the AKBSD in cooperative networks i.e. CoMP application then proposed 2-D AKBSD that makes partial detection in the relay nodes in relay networks and that's give a considerable complexity reduction in the relay nodes as well as the destination nodes. Also, we proposed a HPFD protocol that is applicable in multi-hop networks. In the next chapter, we show the hardware implementation of the ACU unit via FPGA and ASIP platforms.

This page intentionally left blank.

CHAPTER: 5

IMPLEMENTATION OF THE

ADAPTIVE CONTROL UNIT

The implementation of sphere decoders has been discussed in several publications such as [55]-[58]. The proposed system doesn't modify the core implementation of the regular KBSD algorithm but rather adds an ACU unit to be responsible for the choice between the KBSD and the ZF operation as described in the general decoder block diagram shown in Fig. 5.1. Implementing the ACU unit is dependent on the adaptation algorithm (M1-M4). We choose to implement the ACU unit that employs the M3 method. Similarly, other methods can be easily implemented in the same way. In this chapter, we provide the ACU implementation via FPGA and ASIP platforms.

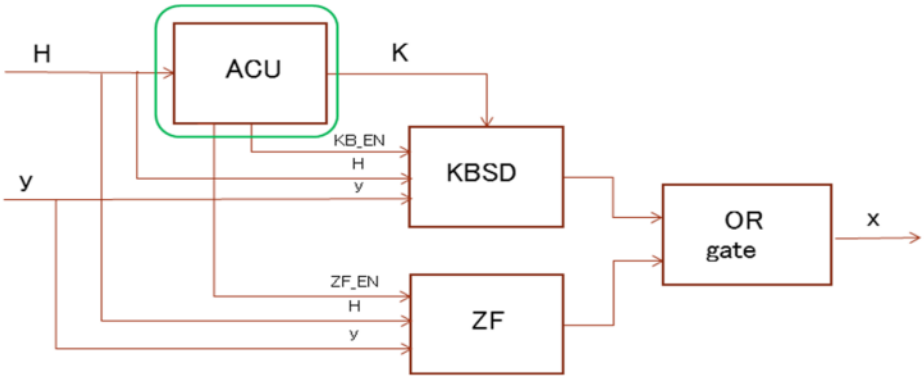

Figure 5.1: General decoder block diagram.

5.1 VHDL Implementation

In Fig. 5.1, the ACU unit block is the control block that decides which decoder will be used in the decoding process. Depending on the information passed to it i.e. the channel matrix (H), it estimates the channel quality through one of the above described methods (M_1

–M_4) then selects between the KBSD block and the ZF block by sending an enable signal to one of them while disabling the other one.

Following the adaptive method M_3 described in chapter 3, we divide the ACU block into three sub-blocks as shown in the Register To Logic (RTL) schematic of Fig. 5.2; first calculate the absolute values of the four channel coefficients in (2.11) using "B1_ABS" block then rearrange the two consecutive channel responses and divide them to get the ratios C_1 and C_2 (see (3.3)) using "B2_MinMax" block and finally the C_1 and C_2 values are checked versus the threshold value Γ to estimate the selectivity of the channel and decide which mode will be activated.

If the first mode of operation is selected then the ACU enables the ZF block using the "ZF_EN" signal and for power saving disables the KBSD block using "KB_EN" signal while in the other modes the opposite operations occur to disable the ZF block and enable the KBSD to decode according to the suitable K_1 or K_2 that sent to it by the "K" signal. The ACU operation is tested using "ISim" tool embedded in ISE Design Suite 14.1 by Xilinx® for a target FPGA "xc3s500e-5fg320" Spartan-3E device and a sample of the test bench waveforms that is generated by the Xilinx® design tool is shown in Fig. 5.2.

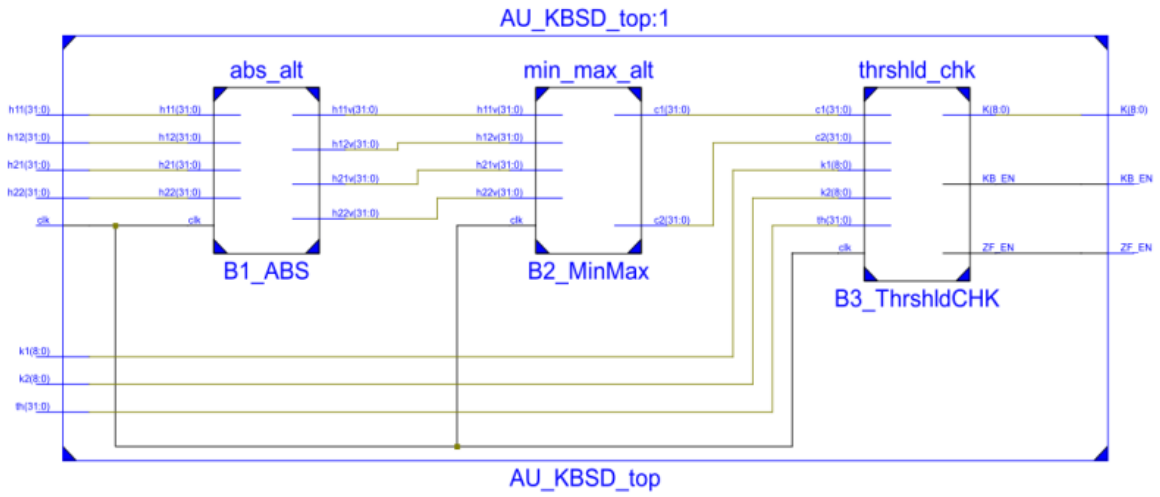

Figure 5.2: ACU RTL Schematic.

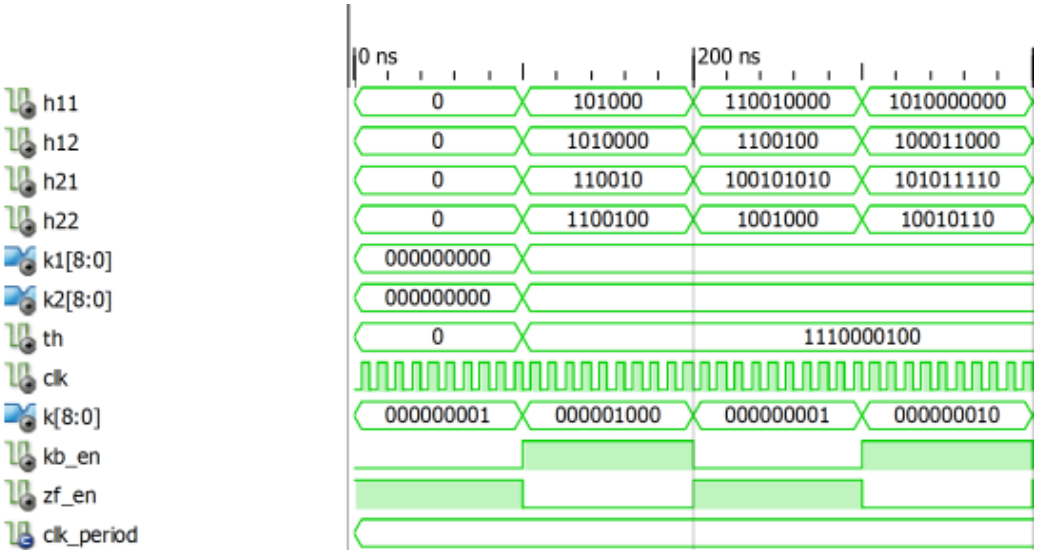

Figure 5.3: ISim test waveforms.

TABLE 5.1: SYNTHESIS REPORT SUMMARY

Device xc3s500e-5fg320	***Used***	***Available***	***Utilization***
Slice Logic Utilization			
# LUTs	*1176*	*9312*	*12%*
# Occupied Slices	*627*	*4656*	*13%*
# Slice Registers	*0*	*4656*	*0%*
Specific Feature Utilization			
# MULT18X18SIOs	*4*	*20*	*20%*
Cell Usage *(used to calculate overhead)*			
# BELS =2537	*# IOBuffers =189*	*# MULTS =4*	

To calculate the overhead of the ACU, an estimated area in Kilo Gate Equivalence (KGE) is roughly calculated according to the obtained synthesis report (summarized in

table 5.1) as:

Estimated Area=

[number of BELS gates] + [number of IO buffers]+[number of MULTs] (5.1)

where the number of BELS gates includes the number of multiplexers, inverters and Look Up Tables (LUT) gates. The estimated area equals 12.305 KGE.

The number of gates used in the different LUTs employed in that fully combinational design are obtained using the equivalent schematics of the different LUTs (LUT2:4) which are shown in Fig. 5.4 noting that LUT1 is just a 1×1 buffer gate.

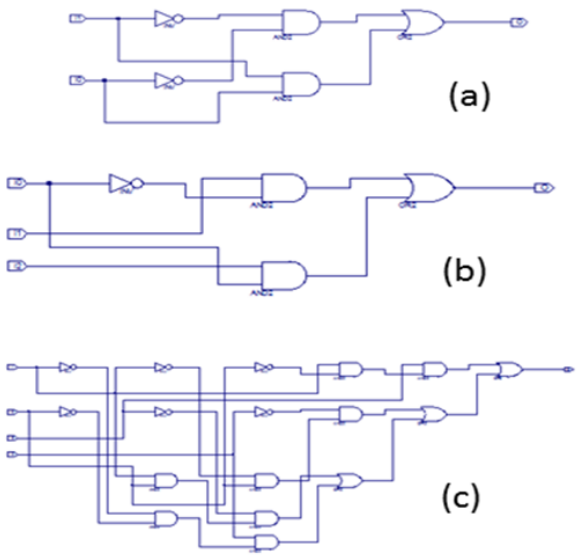

Figure 5.4: LUTs equivalent schematics of (a) LUT2[2×1] (b) LUT3[3×1] (c) LUT4[4×1].

Comparing the overhead with different KBSD implementations reported in [55] and [56] (worst case is 1790 KGE and best case is 71 KGE for different K-values), we get a small overhead of about 0.6~15% over the worst/best case area. The ACU alternates between different K-values KBSD and hence it consumes different power values with the average power below that of the KBSD using the K_2 value and hence a power saving is

automatically obtained by using the ACU.

5.2 ASIP Implementation

Application Specific Instruction Set Processor (ASIP processor) is an optimized processor designed for a special task, it can be considered as a mid-way between the software and hardware design as it combines the design of the instruction set as well as the hardware for a specific application. Since the ASIP design is customized for certain tasks, it has the optimum trade-off between performance, flexibility and power dissipation over other platforms as shown in Fig. 5. 5[57][58].

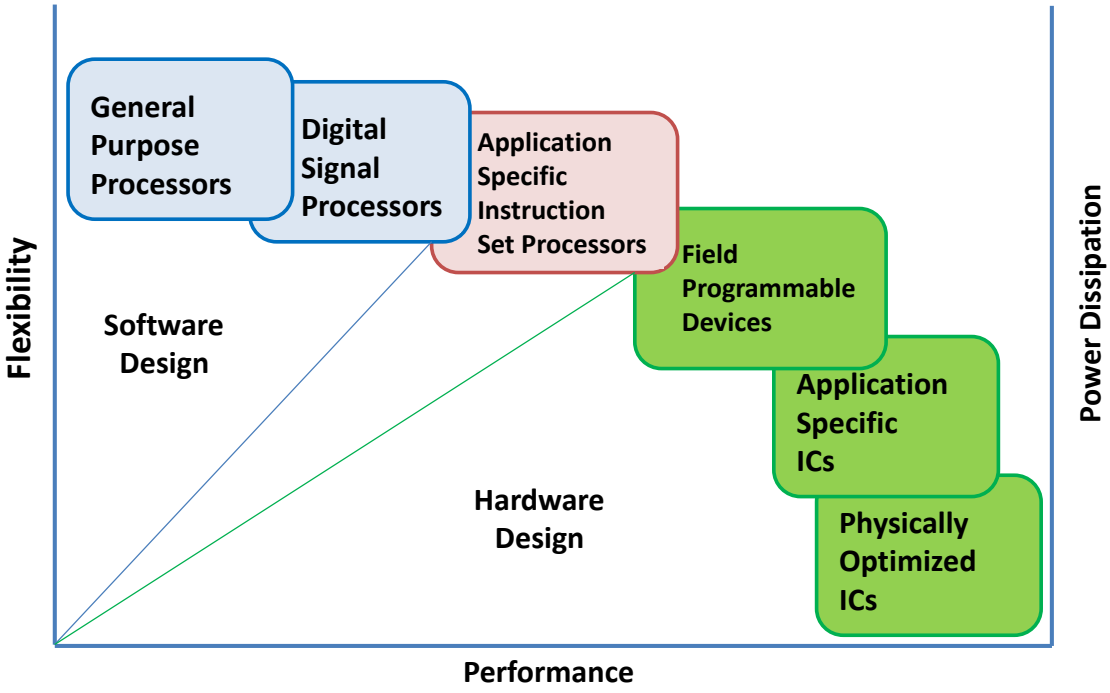

Figure 5.5: Flexibility-Power- Performance trade-off of different software and hardware implementation platforms [58].

We choose to utilize the ASIP platform for our ACU implementation to be able to switch between different standards when using the AKBSD. For example, AKBSD is applicable for both the DVB-T2 and DVB-NGH standards which differ in the number of

transmitting and/or receiving antennas, modulation techniques, space time codewords … etc.

ASIP design can be performed by completely describing it via Architecture Description Language (ADL) or obtaining it after software programming of an existing processor or using a so called Transport Triggered Architecture (TTA) [58].

In our design, we used the "Asip Meister®" ADL tool [59] to model the ACU unit on ASIP. The tool has the advantage of early estimation of resources such as area, power and delay in an early stage of design. The design stages are:

- Setting the processor specifications.
- Declare the resources.
- Set the storage/memory specifications.
- Define the processor interface and instruction types and format.
- Estimate the processor design performance.
- Generate Assembler file.
- Design the instruction micro operation.
- Generate the HDL and compiler.
- Verification and Implementation of the processor model.

The high level architecture of the AKBSD is shown in Fig. 5.6, different variables e.g. channel matrix, K and threshold values, …etc are stored in the memory from the previous blocks in the receiver. U#1, the ACU, calculates the adaptive K value, *Ka*, and outputs it with the enable signals of the ZF and KBSD blocks. U#2 performs QR decomposition and outputs the *q* and *r* values, while U#3 calculates the PEDs and performs the sorting operations. It should be noticed that U#2 and U#3 represent together the hard coding part of the KBSD while adding U#4, that outputs the LLR values of the transmitted signal, is necessary for the implementation of soft decoding such as the KB-LSD.

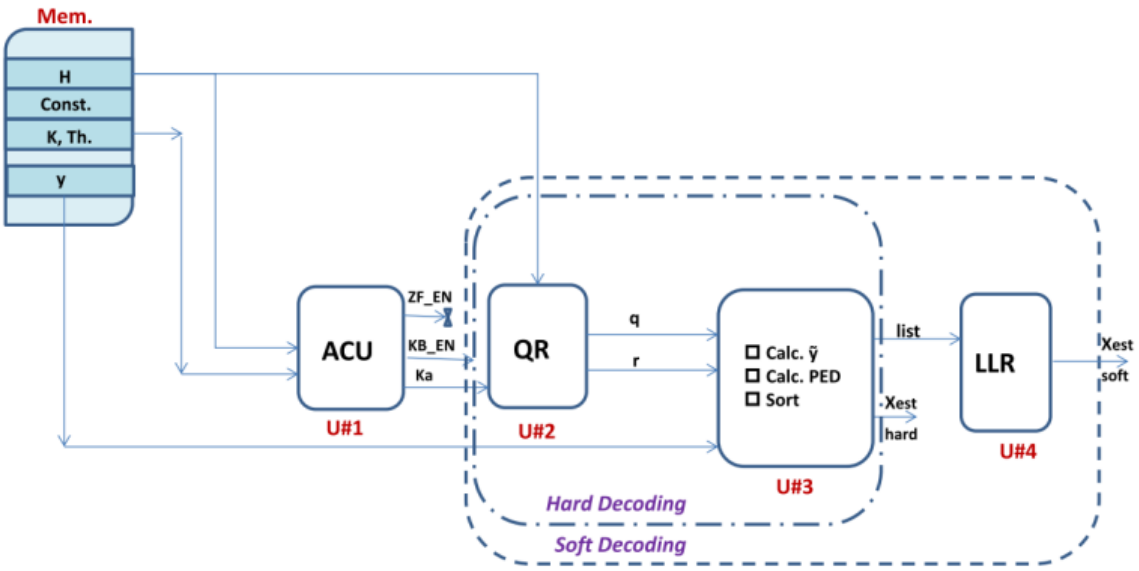

Figure 5.6: High level architecture of the AKBSD.

Table 5.2: Architecture Parameters of the B-STD32

Parameter	Type
Basic Architecture	*RISC*
Memory Architecture	*Harvard*
Instruction length	*32*
Data length	*32*
Addressing	*Byte address*
Byte order	*Big Indian*
Register Type/Number	*GPR/32*
# pipeline stages	*4*

We modeled the ACU unit only here (named U#1) while U#2, U#3 and U#4 are somehow implemented via different architectures in recent publications, e.g. in [60]-[65]. The task performed by the ACU was described in Section 5.1. We designed two main instructions that can perform the operation of the ACU and build on one of the Brownie

processors family named Brownie STD 32-bit processor (B-STD32) [66] designed by "Asip Meister® " tool. The ACU inherits the features of the B-STD32 architecture which is shown in table 5.2.

The two instructions related to the ACU behavior (named GENC and GENKA) are of the Register and Register (RR) instruction type, as shown in Fig. 5.7, which are used to perform an operation by using two source registers (rs1, rs2) and write back the result to the register (rd) and (func) is a sub-opcode[2] of RR type and the lower 6 bits are an opcode and fixed to "000001" in the case of RR type. The GENC and GENKA instruction formats, code allocation, mnemonic format and its usage with the AKBSD parameters are described in Fig. 5.8.

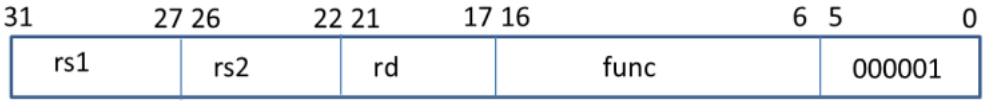

Figure 5.7: RR instruction format.

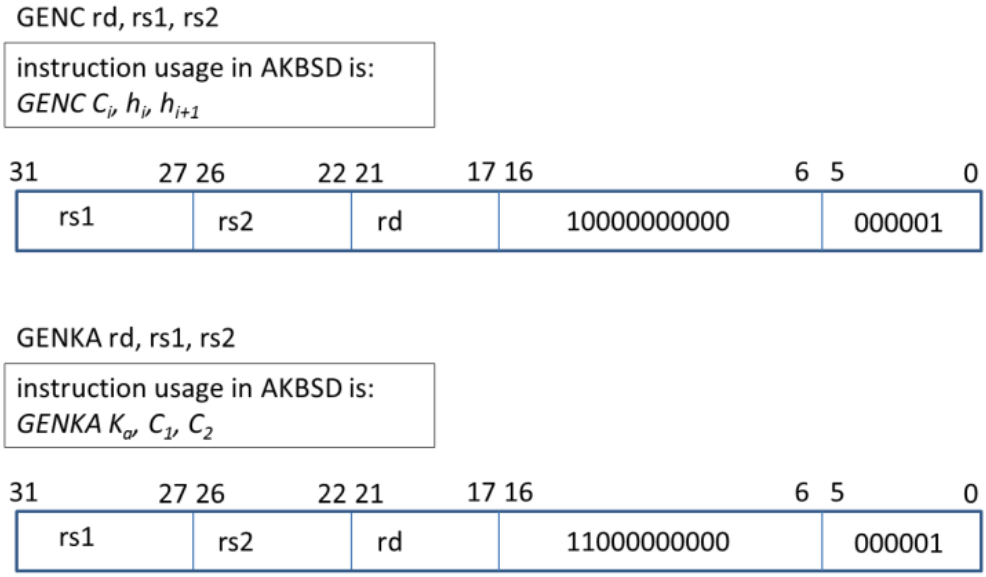

Figure 5.8: GENC and GENKA instructions format and mnemonic.

[2]*opcode is the part of the machine language instruction which indicates the operation to be performed by the processor unit.*

The estimated architecture level performance of the ACU is calculated, as shown in table 5.3 and reported by the "Asip Meister® " tool , and it gives almost neither power addition nor delay while the area overhead was typically increased by 0.8 % over the B-STD32 and consumes around only 330 extra gates. Sample of the assembly code that can be used to implement the ACU unit is shown in Fig. 5.9 in which we load the channel response values from the data memory and then calculate the C_1 and C_2 values to generate the adaptive K-value (K_a) that will be passed to the KBSD if it is greater than 0, i.e. $K_a > 0$, or the ZF decoder will be activated as the instantaneous decoder if the calculated $K_a=0$.

Table 5.3: Architecture Level Estimation

Parameter	B-STD32	B-STD32 + ACU	Overhead %
Area [gates]	*40055*	*40384*	*0.8 %*
Delay [ns]	*32.78*	*32.78*	*0 %*
Power [uW/MHZ]	*1299*	*1299*	*0 %*

```
LW %GPR22,0(%GPR16);load values of h11 in register GPR22 from the
;data memory with address equals value of GPR16 + offset
LW %GPR23,0(%GPR17);load values of h12
GENC %GPR24,%GPR22,%GPR23 ;calculate c1

LW %GPR22,0(%GPR18);load values of h21
LW %GPR23,0(%GPR19);load values of h22
GENC %GPR25,%GPR22,%GPR23 ;calculate c2

GENKA %GPR26,%GPR24,%GPR25 ;generate Ka

BRZ%GPR26,#0x0FFE0700 ;if Ka==0 jump to enable the ZF decoder
```

Figure 5.9: Sample of assembly code for the ACU unit implementation.

Since the ASIP implementation for the ACU consumes almost no extra power when added to other units and since power saving is automatically obtained by using the ACU, it is now clear that the ACU saves the power in regular KBSD, but at the expense of small increase in the area as shown in tables 5.1 and 5.3.

5.3 Summary

In this chapter, we covered the hardware implementation of the ACU unit of the AKBSD employing M3 adaptation method via the FPGA and ASIP platforms and showed that the ACU consumes almost no power nor delay but on the other hand adds small area to the decoder implementation area. In the next chapter, we conclude the work done through this thesis and show the future work that can be done to extend this work.

CHAPTER: 6

CONCLUSIONS AND FUTURE WORK

This chapter is dedicated to summarize the work done through this thesis and to illustrate the tasks that can be performed as a future work for further research.

6.1 Conclusions

The thesis contributions can be summarized in the following points:

- We proposed employing a modified sphere decoder, namely AKBSD, which relies on adapting the number of paths in the search of the KBSD according to the operating environment especially the channel quality.
- We offer to adaptively estimate a suitable number of K-paths through an adaptive unit, i.e. ACU, depending on specific criteria such as: channel quality estimation, channel matrix analysis and SNR estimation, and to search only these number of branches to save more processing operations while traversing the tree.
- The achieved reduction in the decoder complexity makes it more suitable for hardware implementations.
- This type of adaptation is performed over the horizontal level in the tree to achieve the best trade-off between performance and complexity.
- In cooperative networks, another dimension of adaptation is partial detection over the vertical levels of the tree can be utilized to reduce the overhead introduced in the MIMO relay.
- Therefore, we proposed a new 2-D AKBSD that makes use of the two vertical

(number of traversed levels) and horizontal (number of visited nodes per level) dimensions of the adaptation process in the R node to suit the dynamic conditions of the network.

- We proposed a new hybrid partial and full detection protocol for multi-hop networks that greatly reduce the decoding complexity especially in the nodes that perform partial detection task.
- As a step of the decoder implementation, we also presented a hardware implementation and an ASIP model for the ACU unit.

6.2 Future Work

The future work directions are shown in the following points:

- In this work, we did not implement a channel estimator block in the receiver side assuming perfect channel knowledge and depending on previous blocks in the receiver structure; hence a study that includes the channel estimation task will exactly characterize the whole system performance.
- 3-D Space Time Space (STS) [67] offers an efficient scheme to cope with equal and unequal received powers in Single Frequency Network (SFN) scenarios whatever the receiver position, using the AKBSD for the decoding of the 3-D STS codes is expected to reduce its high decoding complexity.
- Implement the whole decoder blocks via ASIP to be fully applicable in hardware implementations and make use of the reduced power consumption property of the ASIP.

PUBLICATION LIST

Published:

1. A.A.A. El-Banna, M. Elsabrouty, "CIR-based Adaptive K-Best Sphere Decoder for DVB-T2," 1st international workshop on modeling, measurements and optimization of video performance over wireless networks -- In conjunction with 11th Wiopt, Tsukuba Science City, Japan, May 2013.
2. A.A.A. El-Banna, M. Elsabrouty, A. Abdelrahman, "VHDL Implementation of Adaptive Control Unit in CIR-based Adaptive K-Best Sphere Decoder for DVB-T2," 12th Edition of IEEE Faible Tension Faible Consommation, Paris, France, June 2013.
3. A.A.A. El-Banna, M. Elsabrouty, A. Abdelrahman, "Low Complexity Adaptive K-Best Sphere Decoder for 2x1 MISO DVB-T2," 10th International Symposium on Wireless Communication Systems, Ilmenau, Germany, August 2013.
4. A.A.A. El-Banna, A. Emran, M. Elsabrouty, A. Abdelrahman, "Adaptive Iterative Decoding of MISO-BICM for DVB-T2," 32nd IEEE International Conference on Consumer Electronics, ICCE Las Veges, USA, January 2014.
5. A.A.A. El-Banna, M. Elsabrouty, A. Abdelrahman, and Seiichi Sampei, "Low Complexity Adaptive Detection of Distributed SFBC in Open-Loop CoMP," the 19th IEEE Symposium on Computers and Communications, ISCC Madeira, Portugal, June 2014.

Under Publication (to be submitted)**:**

6. A.A.A. El-Banna, M. Elsabrouty, and Seiichi Sampei, "Adaptive K-Best Sphere Decoder for DVB systems," IEEE Transactions on Consumer Electronics.
7. A.A.A. El-Banna, M. Elsabrouty, and Seiichi Sampei, "2-D Adaptive K-Best Sphere Detection for Cooperative Relay Networks," IEEE Wireless Communications Letters.

8. A.A.A. El-Banna, M. Elsabrouty, and Seiichi Sampei, "Hybrid Partial and Full Detection Protocol for Multi-Hop Cooperative Relay Networks," Comex letter, IEICE, 2014.

REFERENCES

[1] R. Prasad, *Future Trends and Challenges for ICT Standardization*, 1st ed., chapter 3: River Publishers, 2010.

[2] J. Mietzner. (2014, May 20). *Multiple-Antenna Systems* [online]. Available: http://www.ece.ubc.ca/~janm/Lectures/lecture_mimo.pdf

[3] DVB Project. (2014, Jan. 27). *DVB Standards* [Online]. Available: http://www.dvb.org/standards

[4] K. Okubo, A. Chang-Jun, T. Omori, and K.-Y. Hashimoto, "Enhancement of cell-edge throughput performance with CoMP transmission using QO-STBC scheme," in *Proc. IEEE 2nd Global Conf. on Consum. Electron.,* Oct. 2013.

[5] Y. Liu, Y. Li, D. Li, and H. Zhang, "Space-time coding for time and frequency asynchronous CoMP transmissions," in *Proc. IEEE Wireless Commun. and Networking Conf.*, Apr. 2013.

[6] J. Wang *et al.*, "Multi-cell collaborative transmission combining closed-loop and open-loop techniques," in *Proc. IEEE Veh. Tech. Conf.,* Sep. 2011.

[7] S. Chae, and D. I. Kim, "Antenna selected space-time block code coordinated multi-cell transmission," in *Proc. the 21st Annual IEEE Int. Symp. on Personal, Indoor and Mobile Radio Commun.,* Sep. 2010.

[8] S. Han, "SNR-dependent radius control sphere detection for MIMO systems and relay networks," *trans. on emerging telecom. tech.,* 2013.

[9] Y. Kim, B. Cho, and J. Kim, "Wireless communications: trend and Technical issues from MIMO-OFDM system, advanced trends in wireless communications," InTech, 2011.

[10] Han-Kui Chang *et. al.*, "Multiple antenna techniques, recent advances in wireless communications and networks," InTech, 2011.

[11] A. Huebner et al., "On Cyclic Delay Diversity in OFDM Based Transmission Schemes," 7th *Int. OFDM Workshop,* Germany, Nov. 2002.

[12] Y. Cho et. Al., *MIMO-OFDM wireless communications with MATLAB,* chapters 10 and 11, John Wiley & Sons, 2010.

[13] V. Tarokh, H. Jafarkhani, and A. R. Calderbank, "Space–time block codes from orthogonal designs," *IEEE Trans. Inform. Theory*, vol. 45, pp. 1456–1467, July 1999.

[14] Ran Gozali. (2014, Jun. 18). *A tutorial on space time coding and MIMO channel* [online]. Available: https://www.rocq.inria.fr/secret/C2/Transparents/Boutros.pdf

[15] S. Alamouti, "A simple transmit diversity technique for wireless communications,"

IEEE J. Sel. Areas Commun., vol. 16, no. 8, pp. 1451 – 1458, Oct.1998.

[16] 3GPP, "Evolved universal terrestrial radio access (E-UTRA); further advancements for E-UTRA physical layer aspects (release 9)," TR 36.814, V9.0.0, Tech. Rep., Mar. 2010.

[17] IEEE 802.16e-2005 and IEEE 802.16-2004/Cor 1-2005 (Amendment and Corrigendum to IEEE Std 802.16-2004), ―IEEE Standard for Local and Metropolitan Area Networks Part 16: Air Interface for Fixed and Mobile Broadband Wireless Access Systems Amendment 2:Physical and Medium Access Control Layers for Combined Fixed and Mobile Operation in Licensed Bands and Corrigendum 1,2006, pp. 1–822.

[18] G. J. Foschini, "Layered space–time architecture for wireless communication in fading environments when using multiple antennas," *Bell Labs Tech. J.*, vol. 1, no. 2, pp. 41–59, Autumn 1996.

[19] J. Choi, "Capacity/throughput optimization for H-BLAST with SC receiver over MIMO channels," *IEEE Trans. on Wireless Channels*, vol. 7, pp. 1016– 1024, March 2008.

[20] N. Prasad and M. K. Varanasi, "D-BLAST lattice codes for MIMO block Rayleigh fading channels", in Proc. *40th Annual Allerton Conf. on Comm. Control, and Comput.*, Monticello, IL, Oct., 2002.

[21] P. Wolniansky, G. Foschini, G. Golden, and R. Valenzuela, "V-BLAST: An architecture for realizing very high data rates over the rich scattering wireless channel," in Proc. *ISSSE*, Sept. 1998.

[22] R. de Francisco, M. Kountouris, D. T. M. Slock, and D. Gesbert, "Orthogonal linear beamforming in MIMO broadcast channels," in Proc. *IEEE Wireless Commun. and Networking Conf.* , Hong Kong, Mar. 2007.

[23]J Benesty, J Chen & Y Huang, Conventional Beamforming Techniques, *Microphone Array Signal Processing*, Berlin, Germany: Springer,2008, pp. 39 - 64.

[24]C. P. Schnorr and M. Euchner, "Lattice basis reduction: Improved practical algorithms and solving subset sum problems," *Math. Programming*, vol. 66, no. 2, pp. 181–191, Sep. 1994.

[25] Z. Guoet, and P. Nilsson, "Algorithm and implementation of the K-Best sphere decoding for MIMO detection," *IEEE J. Sel. Areas Commun.*, vol. 24, no. 3, Mar. 2006.

[26] K. Wong, C. Tsui, R. Cheng, and W. Mow, "A VLSI architecture of a K-Best lattice decoding algorithm for MIMO channels," in Proc. *IEEE Int. Symp. on Circuits and*

Syst., May 2002.

[27] S. Han, T. Cui, and C. Tellambura, "Improved K-Best sphere detection for uncoded and coded MIMO systems", *IEEE Wireless Commun. Lett.*, vol. 1, no. 5, Oct. 2012.

[28] C. Shen, and A. M. Eltawil, "A radius adaptive K-Best decoder with early termination: algorithm and VLSI architecture," *IEEE Trans. Circuits Syst. I, Reg. Papers*, vol. 57, no. 9, 2010.

[29] J. Xiao, P. Ren, and Q. Du, "A variable breadth based adaptive tree search algorithm for MIMO systems," in *Proc. 1st IEEE Int. Conf. on Commun.in China*, Aug. 2012.

[30] B. Kim, and K.Choi, "SNR measurement free adaptive K-Best algorithm for MIMO Systems," in *Proc. IEEE Wireless Commun. and Networking Conf.*, Apr. 2008.

[31] D. L. Milliner, and J. R. Barry, "A layer-adaptive M algorithm for multiple-input multiple-output channel detection," in *Proc. IEEE 8th Workshop on Signal Process. Advances in Wireless Commun.*, Jun. 2007.

[32] C. Shen, and A. M. Eltawil, "An adaptive reduced complexity *K-Best* decoding algorithm with early termination," *in Proc. 7th IEEE Consumer Commun. and Networking Conf.*, Jan. 2010.

[33] L.G. Barbero, and J. S. Thompson, "A fixed-complexity MIMO detector based on the complex sphere decoder," in *Proc. IEEE 7th Workshop on Signal Process. Advances in Wireless Commun.*, Jul. 2006.

[34] L. Barbero and J. Thompson, "Performance analysis of a fixed-complexity sphere decoder in high-dimensional MIMO systems," in *Proc. IEEE Int. Conf. on Acoust., Speech and Signal Process.*, May 2006.

[35] Joseph Boccuzzi, *Signal Processing for Wireless Communication*, 1st ed., the McGraw-Hill Companies, Inc., 2008.

[36] ETSI, "Digital Video Broadcasting (DVB); Implementation guidelines for a second generation digital terrestrial television broadcasting system (DVB-T2) DVB Document A133," Feb. 2012.

[37] ETSI, "Frame structure channel coding and modulation for a second generation digital terrestrial television broadcasting system (DVB-T2) DVB Document A122," Jun. 2008.

[38] I. Sobrón, M. Mendicute, and J. Altuna, "Full-rate full-diversity space-frequency block coding for digital TV broadcasting," in *Proc. 18th EURASIP European Signal Process. Conf.*, Aug. 2010.

[39] D. Sayed, M. Elsabrouty, A. Shalsh, "Improved synchronization, channel estimation, and simplified LDPC decoding for the physical layer of the DVB-T2 receiver," *EURASIP J. on Wireless Commun. and Networking*, Mar. 2013

[40] L. Vangelista *et al.*, "Key Technologies for Next-Generation Terrestrial Digital Television Standard DVB-T2,"*IEEE Commun. Mag.*, pp146-153, Oct. 2009.

[41] K. K. Amiri, M. Wu, J. R. Cavallaro, and J. Lilleberg, "Cooperative partial detection using MIMO relays," *IEEE Trans. Comm.*, vol. 12, no. 2, pp. 5039-5049, Oct.2011.

[42] M. Myllyla; P. Silvola; M. Juntti; J.R. Cavallaro, "Comparison of Two Novel List Sphere Detector Algorithms for MIMO-OFDM Systems, " *Personal, Indoor and Mobile Radio Commun., 2006 IEEE 17th Int. Symposium on* , vol., no., pp.1,5, 11-14 Sep. 2006.

[43] B. Hochwald and S. ten Brink, "Achieving near-capacity on a multiple-antenna channel," *IEEE Trans. Commun.*, vol. 51, no. 3, pp. 389–399, Mar. 2003.

[44] M. Damen, A. Tewfik, and J. Belflore, "A construction of a space-time code based on the theory of numbers," *IEEE Trans. on Information Theory*, vol.48, no. 3, pp. 753–760, Mar. 2002.

[45] ETSI, "Digital Video Broadcasting (DVB); Next Generation broadcasting system to Handheld, physical layer specification (DVB-NGH). DVB Document A160," Nov. 2012.

[46] S. Bashir, M. Naeem, A. A. Khan, and S. I. Shah, "An application of univariate marginal distribution algorithm in MIMO communication systems," *Int. J. of Commun. systems*, vol. 23, no. 1, pages 109-124, Jan. 2010.

[47] 3GPP, "Technical specification group radio access network; coordinated multi-point operation for LTE physical layer aspects (release 11)," TR 36.819, V11.1.0, Tech. Rep., Dec. 2011.

[48] R. Vaze, and R. W. H. Jr, "Cascaded orthogonal space–time block codes for wireless multi-hop relay networks," *EURASIP J. on Wireless Commun. and Networking*, 2013.

[49] A. Sendonaris, E. Erkip, and B. Aazhang, "User cooperation diversity. part I and II," *IEEE Trans. Comm.*, vol. 51, no. 11, pp. 1927–1948, Nov. 2003.

[50] P. A. Anghel, G. Leu, and M. Kaveh, "Multi-user space-time coding in cooperative networks," in *Proc. Int. Conf. on Acoust., Speech and Signal Process.*, 2003.

[51] S. S. Ikki, and M. H. Ahmed, "Performance analysis of adaptive decode-and-forward cooperative diversity networks with best-relay selection," *IEEE Trans. Comm.*, vol. 58, no. 1, pp. 68–72, Jan. 2010.

[52] A. Nosratinia, and A. Hedayat, "Cooperative Communication in wireless networks," *IEEE Comm. Mag.*, Oct. 2004.

[53] A. Bansal, M. Bhatnagar and A. Hjørungnes, "Decoding and performance bound of demodulate-and-forward based distributed Alamouti STBC," *IEEE Trans. Comm.*, vol. 12, no. 2, pp. 702–713, Feb. 2013.

[54] C. Hucher, G. R-B Othman, and J-C. Belfiore, "AF and DF protocols based on Alamouti ST code," in *Proc. IEEE Int. Symp.on Inform. Theory*, Jun. 2007.

[55] S. Mondal, A. Eltawil, C. Shen, and K. Salama, "Design and Implementation of a Sort Free K-Best sphere decoder," *IEEE Trans. Very Large Scale Integr. (VLSI) Syst.*, Oct. 2010.

[56] B. Weu, and G. Masera, "A Novel VLSI architecture of fixed-complexity sphere decoder," in *Proc.13th Euromicro Conf. of Digital Syst. Design: Architectures, Methods and Tools*, Sep. 2010.

[57] P. Salmela, "Implementations of baseband functions for digital receivers," Ph.D. dissertation, Tampere University of Technology, Aug. 2009.

[58] M. T.Gamba, "Algorithms and architectures for the detection of MIMO signals," Ph.D. dissertation, Bretagne University, 2011.

[59] ASIP Meister user manual," by ASIP Solutions Inc., Jul. 2008.

[60] J. Antikainen *et al.*, "Application-specific instruction set processor implementation of list sphere detector," in *Proc. Conf. on Signals, Syst. and Comput.*, 2007.

[61] J. Antikainen et al., "Fine-grained application-specific instruction set processor design for the K-Best list sphere detector algorithm," in *Proc. Int. Conf. on Embedded Comput. Syst.: Architectures, Modeling, and Simulation*, 2008.

[62] M. Myllyla, M. Juntti, and J. Cavallaro, "Architecture design and implementation of the increasing radius – list sphere detector algorithm," *in Proc. IEEE Int. Conf. on Acoust., Speech and Signal Process.,* 2009.

[63] P. Salmela, "Implementations of baseband functions for digital receivers," Ph.D. dissertation, Tampere University of Technology, Aug. 2009.

[64] Z. Wang, A. Erdogan, and T. Arslan, "A parallel hybrid merge-select sorting scheme for K-Best LSD MIMO decoder on a dynamically reconfigurable processor," in *Proc. IEEE 21st Int. Symp. on Personal Indoor and Mobile Radio Commun.,* 2010.

[65] M. T.Gamba, "Algorithms and architectures for the detection of MIMO signals," Ph.D. dissertation, Bretagne University, 2011.

[66] "Brownie STD 32, reference manual," ASIP Solutions Inc., 2008.

[67] Y. Nasser *et. al.*, "Efficient 3D Space Time Space Block Code for Future Terrestrial Digital TV," in Proc. *IEEE 9th Workshop on Signal Process. Advances in Wireless Commun.,* 2008.

This page intentionally left blank.

ملخص

إن الإتصال عن طريق الهوائيات المتعددة (MIMO) يعتبر تكنولوجيا جاذبه فى تطبيقات الإتصالات اللاسلكيه. حيث إن إستخدام الهوائيات المتعددة قد ساعد فى تطور العديد من أنظمة الإتصالات اللاسلكية مثل الجيل الرابع للأنظمه الخلويه وتكنولوجيا البث الأرضى الرقمى. كما تعتبرالهوائيات المتعددة الظاهرية موضوع بحث نشط فى مجال الشبكات الخلوية والتعاونية.

وفى هذه الرسالة ، نتناول بالبحث مشكلتى إنتقائية التردد والوقت فى كل من ترميز التردد والوقت على الترتيب. فعامة يعتمد الفك البسيط لترميز التردد والوقت على فرضية أن القناة ثابتة على مدى الرموز المتتابعه المكونه لتقنية التنوع. ولكن فى حالة عدم تحقق هذه الفرضية ، ونعنى هنا حالات القنوات المتغيرة ، فإنه يجب تطبيق عمليات فك ترميز أكثر تعقيداً مثل فك الترميز الأكثر تشابها أو فك الترميز الكروى.

إن فك الترميز الكروى بأفضل عدد مسارات (KBSD) هو نظام فك ترميز قليل التعقيد و ثابت الإنتاجية ؛ ومع ذلك فإن أدائه يعتمد بشكل كبير على قيمة المعامل K والتي تحدد عدد العقد التى سيتم زيارتها أثناء إجتيازشجرة البحث. ومن هنا ، فإننا نقدم توظيف العديد من التعديلات على فك الترميز الكروى لتهيئة عدد المسارات المستخدمه فى البحث فى جهاز فك الترميز الكروى بأفضل عدد مسارات (KBSD). حيث إن هذه الخوارزميات المطورة تُقدِّرعدد مناسب من المسارات من خلال وحدة التحكم التكيفي (ACU)، إعتماداً على بعض المعاييرالمرتبطه بجودة القناة مثل : تحليل مصفوفة القناة ، تقدير نوعية القناة و تقدير نسبة طاقة الإشارة إلى الضوضاء.

إن التسوية الجيدة بين تعقيد جهاز فك الترميز وأدائه والناتجة عن تهيئة عدد المسارات يجعله أكثر ملاءمة للتطبيقات العمليه له ، و تنفيذ هذا النوع من التكيف يعتبرعلى المستوى الأفقي في شجرة البحث وذلك لتحقيق أفضل مفاضلة بين الأداء و التعقيد. بينما في الشبكات التعاونية ، هناك بعداً آخر من التكيف يمكن استخدامه فى الكشف الجزئي على المستويات العمودية للشجرة وذلك للحد من الإضافات التي أدخلت في جهاز التتابع. لذلك فقد إقترحنا جهاز فك الترميز الكروى المكيف (2-D AKBSD) ثنائى الأبعاد الجديد والذى يستفيد من إستخدام بُعدَى عملية التكيف ، العمودي (عدد المستويات التى يتم اجتيازها) والأفقي (عدد العقد التى يتم زيارتها فى كل مستوى) في جهاز التتابع لتتناسب مع الظروف المتغيرة للشبكة . كما تم عرض بروتوكول جديد للكشف الكلى والجزئى يمكن إستخدامه فى الشبكات متعددة القفزات. وأخيرا كخطوة لتنفيذ جهاز فك الترميزعملياً، فقد قمنا بتنفيذه باستخدام لغة وصف الأجهزه للشرائح المتكاملة عالية الكثافه (VHDL) بالإضافه الى تنفيذ معالج ضبط التعليمات المحدده بالتطبيق (ASIP) لوحدة التحكم التكيفي (ACU).

فك الترميز الكروى المكيف بأفضل عدد مسارات لأنظمة بث الفيديو الرقمى والشبكات التعاونية

مقدمة من

أحمد عبدالعزيز بدوى البنا

للحصول على درجة

دكتوراه فى الفلسفة

فى

هندسة الإلكترونيات والإتصالات

لجنة الإشراف	الجامعة	التوقيع
أ.م.د. / عادل عبد الرحمن	الجامعه المصريه اليابانيه للعلوم والتكنولوجيا- مصر	.....
أ.م.د. / مها الصبروتى	الجامعه المصريه اليابانيه للعلوم والتكنولوجيا- مصر	.....
د. / محمد فرج	جامعة الأسكندرية - مصر	.....
أ.د. / سيتشى سامباى	جامعه اوساكا - اليابان	.....

لجنة المناقشة والحكم على الرسالة	الجامعة	موافقون
أ.د. / حسام شلبى	الجامعه المصريه اليابانيه للعلوم والتكنولوجيا - مصر	.....
أ.م.د. / اوسامو موتا	جامعه كيوشو - اليابان	.....
أ.م.د. / عادل عبد الرحمن	الجامعه المصريه اليابانيه للعلوم والتكنولوجيا - مصر	.....
أ.م.د. / مها الصبروتى	الجامعه المصريه اليابانيه للعلوم والتكنولوجيا - مصر	.....

نائب رئيس الجامعة للتعليم والشئون الكاديمية

أ.د. أحمد عبد المنعم ابو إسماعيل

This page intentionally left blank.

فك الترميز الكروى المكيف بأفضل عدد مسارات لأنظمة بث الفيديو الرقمى والشبكات التعاونية

رسالة علمية

مقدمة إلى كلية الدراسات العليا

فى هندسة الإلكترونيات والإتصالات والحاسبات

الجامعة المصرية اليابانية للعلوم والتكنولوجيا

كإستيفاء جزئي لمتطلبات الحصول على درجة

دكتوراه فى الفلسفة

فى

هندسة الإلكترونيات والإتصالات

مقدمة من

أحمد عبدالعزيز بدوى البنا

سبتمبر ٢٠١٤